Panu Karjalainen

**Vehicle Nanoparticle Emissions under Transient Driving
Conditions**

Tampere 2014

Panu Karjalainen

Vehicle Nanoparticle Emissions under Transient Driving Conditions

Thesis for the degree of Doctor of Science in Technology to be presented with due permission for public examination and criticism in Sähkötalo Building, Auditorium S2, at Tampere University of Technology, on the 21st of November 2014, at 12 noon.

Doctoral candidate: Panu Karjalainen, M.Sc.
Aerosol Physics Laboratory
Department of Physics
Tampere University of Technology

Supervisors: Jorma Keskinen, prof.
Aerosol Physics Laboratory
Department of Physics
Tampere University of Technology

Topi Rönkkö, adjunct prof.
Aerosol Physics Laboratory
Department of Physics
Tampere University of Technology

Pre-examiners: Veli-Matti Kerminen, prof.
Division of Atmospheric Sciences
Department of Physics
University of Helsinki

Zhi Ning, assistant prof.
School of Energy and Environment
City University of Hong Kong

Opponents: Tuukka Petäjä, prof.
Division of Atmospheric Sciences
Department of Physics
University of Helsinki

Barouch Giechaskiel, Ph.D.
Sustainable Transport Unit
Institute for Energy and Transport
Joint Research Centre (JRC)
European Commission

Abstract

Real-world driving consist mostly of transients, where the engine parameters are constantly changing. In emission regulation this has been partially considered by including transient driving cycles in emission standards. However, specific particle emissions data for detailed driving conditions have remained limited. This thesis covers results of transient exhaust particle emissions, including both diesel and gasoline engines. The experiments were performed in laboratories and on the road. The focus was always on the real-world particle emissions.

During transient cycles both heavy-duty (HD) diesel engines and light-duty (LD) gasoline vehicles produced elevated soot particle concentrations during accelerations. For instance, in on-road experiment of a LD gasoline vehicle, the exhaust plume particle concentrations at steady speeds were at clean ambient levels, but during accelerations concentrations were 10–50 times the background level. For gasoline vehicles the soot particle size distributions were bi-modal in nature. Currently neither LD gasoline nor nonroad HD diesel engines necessarily need to employ particle filtration in the exhaust system in order to meet the demands of the relevant legislation.

Sulfur originating in the fuel or lubricant oil can be stored inside catalysts, and later be released, forming semivolatile nucleation mode (NM) particles when temperature rises. This behavior was detected for LD and HD engines in the engine laboratory, for a HD vehicle on the road and in a simplified measurement setup in an aerosol laboratory. The aerosol laboratory test indicated that the NM formation does not necessarily require hydrocarbons or sulfated hydrocarbons; particles are electrically neutral and evaporate when they undergo thermal treatment. While sulfur is released from the catalysts, the HD road engine study indicated that the increased NM particle emission is not explained by the concentration of gaseous sulfuric acid. The sulfur storage and release depends greatly on the driving history, also due to this NM particle emissions seem plausible, even with low sulfur fuels. With catalytic particle filters, the amount of soot is reduced, promoting semivolatile NM particle emissions.

An unexpected observation was made that some engines produce nanoparticles containing lubricant oil derived metals during driving while not fueled. Exhaust particles were observed during engine braking events for a HD truck and LD gasoline vehicles. For the truck and gasoline vehicles, the engine braking related particles contributed up to 20–30% and 3–30% of the total number emissions, respectively. These particle emissions can be a reality for all vehicle types not using particle filtration, including the latest technology vehicles. In particle filters, engine braking related particles can affect the ash accumulation and transport mechanisms.

Preface

This thesis has been written based on research at the Aerosol Physics Laboratory of the Department of Physics at Tampere University of Technology during the years 2010–2014. I am grateful to my supervisors professor Jorma Keskinen and Doc. Topi Rönkkö for giving me the job as a research assistant in 2007 and for keeping me busy of work in an innovative research environment ever since.

The experimental research of this type is definitely team work. It has been my privilege to work with so many people during the years. I want to thank my roommate Anssi Arffman for everything related to work, but especially for everything related to all the other things. I owe my gratitude to Dr. Juha Heikkilä for introduction and guidance to emission-related particle measurements. I wish to thank also Dr. Jaakko Yli-Ojanperä for guidance and numerous discussions. I want to thank all the members of the emission group in the Aerosol Physics Laboratory. I see that when the people change, some things always stay the same but some fresh and totally new ideas are brought to the table.

Finally, I thank my father and brother Niko for all their support. Paula, thanks for sharing my life everyday and for the motivation to finish this thesis. My two daughters bring true meaning to life. They have kept me fairly busy while finalizing this thesis.

Articles included in this thesis

Paper 1.   Panu Karjalainen, Topi Rönkkö, Tero Lähde, Antti Rostedt, Jorma Keskinen, Sanna Saarikoski, Minna Aurela, Risto Hillamo, Aleksi Malinen, Liisa Pirjola and Arno Amberla. Reduction of Heavy-Duty Diesel Exhaust Particle Number and Mass at Low Exhaust Temperature Driving by the DOC and the SCR. *SAE International Journal of Fuels and Lubricants*, 2012, 5(3), doi: 10.4271/2012-01-1664.

Paper 2.   Panu Karjalainen, Topi Rönkkö, Liisa Pirjola, Juha Heikkilä, Matti Happonen, Frank Arnold, Dieter Rothe, Piotr Bielaczyc and Jorma Keskinen. Sulfur Driven Nucleation Mode Formation in Diesel Exhaust under Transient Driving Conditions. *Environmental Science & Technology*, 2014, 48, 2336–2343, doi: 10.1021/es405009g.

Paper 3.   Topi Rönkkö, Liisa Pirjola, Leonidas Ntziachristos, Juha Heikkilä, Panu Karjalainen, Risto Hillamo and Jorma Keskinen. Vehicle Engines Produce Exhaust Nanoparticles Even When Not Fueled. *Environmental Science & Technology*, 2014, 48, 2043–2050, doi: 10.1021/es405687m.

Paper 4.   Panu Karjalainen, Liisa Pirjola, Juha Heikkilä, Tero Lähde, Theodoros Tzamkiozis, Leonidas Ntziachristos, Jorma Keskinen and Topi Rönkkö. Exhaust particles of modern gasoline vehicles: A laboratory and an on-road study. *Atmospheric Environment*, 2014, 97, 262–270, doi: 10.1016/j.atmosenv.2014.08.025.

Author's contribution to the publications

Paper 1. I planned the experiments together with Tero Lähde and Topi Rönkkö. Further, I was responsible for running the experiments. I did most of the data analysis, as well as the writing for the paper. The ACSM data analysis was done by Sanna Saarikoski of Finnish Meteorological Institute.

Paper 2. I was involved with three of the four experiments described in this paper. I performed the aerosol laboratory experiments alone, had a leading role in light-duty passenger car engine experiments and participated in the heavy-duty truck on-road measurements. I did most of the data analysis and the writing for the paper.

Paper 3. I participated in all the experiments described in this paper. I assisted Topi Rönkkö in writing the manuscript and provided data analysis and figures for the paper. I had a supporting role in revising the manuscript and responding to reviewer comments.

Paper 4. I did all the data analysis, drew the figures and wrote most of this paper. I participated in both the on-road and laboratory experiments.

Symbols and abbreviations

D_a	aerodynamic diameter
D_p	particle diameter
N	particle number concentration ($1/cm^3$)
ACSM	aerosol chemical speciation monitor
ATS	aftertreatment system
BC	black carbon
CIMS	chemical ionization mass spectrometer
CO	carbon monoxide
CPC	condensation particle counter
DED	double ejector diluter
DOC	diesel oxidation catalyst
DPF	diesel particulate filter
DR	dilution ratio
EEPS	engine exhaust particle sizer
ELPI	electrical low pressure impactor
ESC	European Stationary Cycle
EUDC	Extra-Urban Driving Cycle (of the NEDC)
FSC	fuel sulfur content
FTIR	Fourier transform infrared spectroscopy
GDI	gasoline direct injection
GMD	geometric mean diameter
GSA	gaseous sulfuric acid
HC	hydrocarbons
HD	heavy-duty
LD	light-duty
MAAP	multi-angle absorption spectrometer
MS	mass spectra
Nano-SMPS	scanning mobility particle sizer (nano, TSI model 3085)
NEDC	New European Driving Cycle
NH_3	ammonia
NM	nucleation mode
NO_x	total of mono-nitrogen oxides NO and NO_2
OBD	on-board diagnostics
pDPF	partial diesel particulate filter
PFI	port fuel injection

PM	particulate matter (mass)
PM_{10}	particulate matter (mass, smaller than 10 µm)
$PM_{2.5}$	particulate matter (mass, smaller than 2.5 µm)
PN	particulate number (PMP protocol, $D_p > 23$ nm)
ppmw	parts per million (weight)
PTD	porous tube diluter
RH	relative humidity
SCR	selective catalytic reduction
SIDI	spark-ignited direct injection
SM	soot mode
SMPS	scanning mobility particle sizer (long, TSI model 3071)
SO_2	sulfur dioxide
SO_3	sulfur trioxide
SOA	secondary organic aerosol
SOF	soluble organic fraction
TCTC	Transient Cold Test Cycle
TD	thermodenuder
TEM	transmission electron microscopy
THC	total hydrocarbons
TWC	three-way catalytic converter
UCPC	ultrafine condensation particle counter
UDC	Urban Driving Cycle (of the NEDC)

Contents

Chapter 1

Introduction

Probably the worst air quality catastrophe in history took place in London in the winter of 1952, when still air and a great deal of pollution sources were present. A dense fog that lasted four days was reported to have caused 4000 excess deaths. Deaths, mostly caused by respiratory and cardiovascular complications (Logan, 1953), drew attention to urban air quality and pollution control. A set of particle samples collected from the time before the Clean Air Act of 1956, and analyzed with modern day equipment (Whittaker et al., 2004), revealed that most of the particle were soot, smaller than 1 µm in size and consisted of primary particles in size range of 10–50 nm. Also, high quantities of the metals Fe, Pb, Cu, Mn, V and As were detected in the samples. The combustion of sulfur-rich coal has been blamed for causing the highest concentrations and most severe air quality problems. Later, the famous six-city study of Dockery et al. (1993) performed in the U.S. associated the increased mortality with a combination of high PM together with high sulfur dioxide (SO_2) concentrations.

Today, a large set of regulations and continuous air quality monitoring has lead to better air quality in many cities worldwide. The conditions are still quite different between developed and developing countries. As an example, in Beijing, the average concentration of particle mass below 2.5 µm ($PM_{2.5}$) during 2011 was 65 µg/m^3 (Wang et al., 2013), whereas in European cities the annual averages have usually been below 25 µg/m^3 (Putaud et al., 2010).

A big contributor to urban PM concentrations and air quality problems is traffic. In urban areas, the highest particle concentrations have been measured at locations of dense traffic: on highways, on roads (Pirjola et al., 2006; Kittelson et al., 2000) and in street canyons (Wehner et al., 2002; Ketzel et al., 2003; Longley et al., 2003). Traffic-related emissions such as particulate matter (PM), total hydrocarbons (THC), carbon monoxide (CO) and nitrogen oxides (NO_x) have been regulated in almost every country (Dieselnet, 2014). Sulfur compound emissions have been regulated by setting the maximum value for the fuel sulfur content (FSC) which is presented in units of mg (S) per kg (fuel), ppmw. Today, the FSC in some parts of China or Brazil (for example) can be of a magnitude 100 times higher than in Europe (Dieselnet, 2014).

The tightest emission regulations have been typically set in Europe, North America, Japan and South Korea in terms of vehicular PM. From the particle emission point of

view also the particulate number (PN) emission of nonvolatile particles has been regulated from the Euro 5 emission level for light-duty (LD) diesel vehicles. This emission limit is also coming for gasoline direct injection (GDI) (a.k.a. spark-ignited direct injection, SIDI) passenger cars and heavy-duty (HD) road diesel vehicles. This nonvolatile particle regulation is only limited to particles roughly greater than 23 nm in diameter. This artificial size limit, however, is not based on the harmfulness of the exhaust particles. By this method the nonvolatile particles smaller than 23 nm, or semivolatile particles at any size are not counted. As we will learn more in the context of this thesis, the existence of both of these particle types is plausible, and the real-world particle emissions can be quite different compared to the regulated PN.

The adverse health effects of particles are usually associated with the concentrations of $PM_{2.5}$ or PM_{10} in the ambient air but the health risks are also linked with the concentrations of black carbon (BC) (Janssen et al., 2011) and nanoparticles (Oberdörster et al., 2005). Vehicles affect urban particle concentrations by the emissions of primary and secondary particles where the particle number concentrations (both nonvolatile and semivolatile) are relatively high. Primary particle emissions are nonvolatile particles that are formed in the engine but also semivolatile particles that are potentially formed in the exhaust dilution process into the atmosphere. Secondary aerosol from the exhaust is formed in the atmosphere through the oxidation processes of semivolatile organics (Robinson et al., 2007) by generating new particles with nucleation or growing existing particles with condensation. Practically all of these particles containing the complex mixtures of exhaust pollutants (Maricq, 2007) are inhalable and present in the urban air. Usually, some metals or specific semivolatile organics are considered the hazardous material in the exhaust related particles. So far, there is lack of particle number data for epidemiological studies whereas there is a great deal of ambient PM data available.

Diesel exhaust particles have been studied more than gasoline exhaust particles since for decades the diesel engine generated much more visible smoke and higher $PM_{2.5}$ emissions. Technological advancements for cleaner combustion, e.g. by increasing the fuel injection pressure (Lähde et al., 2011), have led to smaller diesel soot emissions. The PN limit, where applied, has practically forced the usage of effective particle filters, which has more or less solved the soot emission issue. The exhaust particle number concentrations of gasoline vehicles have typically been lower than diesel exhaust particle concentrations without a particle filter (Mathis et al., 2005). However, the general need to enhance the fuel economy has led to the use of direct fuel-injection techniques also in gasoline vehicles (Alkidas, 2007). This change has increased particle emissions from gasoline vehicles (Aakko and Nylund, 2003; Mohr et al., 2006; Braisher et al., 2010). As in diesel exhaust, the particle number emitted by GDI vehicles is dominated by ultrafine particles, the particle size distribution is often bi-modal (Barone et al., 2012; Sementa et al., 2012; Sgro et al., 2012; Maricq et al., 1999a), and the particles consist mainly of elemental carbon. In general, GDI technology is replacing port fuel injection (PFI) technology as the major fuel injection strategy and

solution for gasoline engines. Estimations project that in North America, GDI vehicles will cover up to 60% of the light-duty vehicle fleet by 2016 (CARB, 2010).

To simplify the engine exhaust measurements, particle emission studies have usually been performed so that engine speed and torque have been kept constant for a sufficient time so that also exhaust temperatures have reached their steady-state values. Then physical and chemical properties of exhaust particles have been reported for a set of different engine loads and speeds with different fuels, lubricants or aftertreatment systems (ATSs). In fact, real-world driving does include steady state phases, but most of all it consists transients, where the engine load and speed change frequently. In addition to technological parameters, changing driving conditions also affect particle emissions. In emissions regulations this has been partially considered by including transient driving cycles in emission standards. As a result, the number of exhaust studies focusing on emissions under transient conditions has now increased (Giakoumis et al., 2012). However, specific data for detailed driving conditions have remained limited because of the difficulties in the measurement and data analysis, as well as the fact that the regulated quantity is the particulate mass or number integrated over the test cycle. Particle emissions under transient driving conditions are discussed further in this thesis and in all the enclosed articles (**Papers 1–4**).

1.1   Aim and scope

This thesis aims to provide new information of exhaust particles under transient driving conditions needed in the scientific community and in future legislative work. Generally dedicated particle studies in the past have been done under steady-state conditions where the speed and torque of the engine have been kept constant for a while, and the results only imply what the particle emissions are under ideal conditions. Transients in driving, such as changes in engine torque and speed are, however, ordinary and dominant phenomena. These transients are often included in test protocols, but the actual emissions are determined by taking an average over the whole test cycle or part of it.

This thesis covers experiments where the effect of transient conditions in engine-out emissions or tailpipe emissions are studied. The effect of exhaust aftertreatment technologies in real-world particle emissions is also studied. In total 7 different vehicles/engines are studied covering a large set of various vehicle technologies but is statistically a small sample size. In the studies, particle number concentrations and emissions are analyzed, as well as particle size distributions. Studies also include analyses of particle morphology, chemical composition and volatility characteristics.

The main focus of the work is in the formation of the smallest exhaust particles. Between different cases, the particle size (or number) can be similar but the particle compositions and formation mechanisms can be completely different. In order to achieve deeper understanding, the instantaneous particle emissions must be linked to the simultaneous driving conditions, driving history and vehicle technologies used.

The main objectives of this work are to find answers to questions relating to exhaust particle emissions:

- What are the exhaust particle emissions under transient driving conditions, by size and number?

- How do transients affect the characteristics of exhaust particles?

- What are the real-world particle emissions of diesel and gasoline engines equipped with modern technology exhaust aftertreatment?

1.2   Terminology used in this thesis

Here I want to point out some important things related to the terminology used in this thesis and the papers included. Used abbreviations are listed in the chapter "Symbols and abbreviations" at beginning of the thesis.

Particle volatility is described so that exhaust particles are either *semivolatile* or *nonvolatile*. These definitions can be understood so that exhaust components that are in the particle phase in the hot exhaust gas inside the tailpipe are nonvolatile. The components that are in the gas phase inside the tailpipe but later condense onto existing particles or form new particles in the cooling dilution are semivolatile. When the diluted exhaust sample is passed through the thermodenuder (TD) operating at 265 °C, the particles downstream are understood to be nonvolatile. When a porous tube diluter (PTD) is normally used, the particle size distributions consist of both nonvolatile and semivolatile particle fractions. When a double ejector diluter (DED), where the first ejector is heated to 250 °C, is used the existing particles are also considered to be nonvolatile.

Nucleation and soot particles are divided in terms of formation mechanisms into two distinctive particle modes. Generally *nucleation mode* (NM) particles are formed in a cooling dilution process, but they can posses a nonvolatile core depending on the engine, driving conditions and the ATS. *Soot mode* (SM) particles are formed during the combustion process inside the cylinders of an engine. Soot particles are fractal-like nonvolatile particles that consist of carbonaceous primary spheres in the hot exhaust. During the cooling and dilution process semivolatile material (e.g. sulfuric acid, hydrocarbons) can also condense on these particles. Often the SM containing semivolatiles is called *accumulation mode* when measured after the cooling dilution or in the atmosphere.

Chapter 2

Exhaust particles

The exhaust gas of internal combustion engines consists of gaseous and particle phase components. The balance between these two phases depends on chemical compositions, concentrations and temperatures. Condensable gases include most often organics and sulphates (Kittelson, 1998; Schneider et al., 2005), where the actual molecular compositions can be numerous. The number of different organic species is in the order of hundreds or thousands (Rogge et al., 1993) while sulfur related nucleation (or condensation) is traditionally associated with gaseous sulfuric acid (GSA).

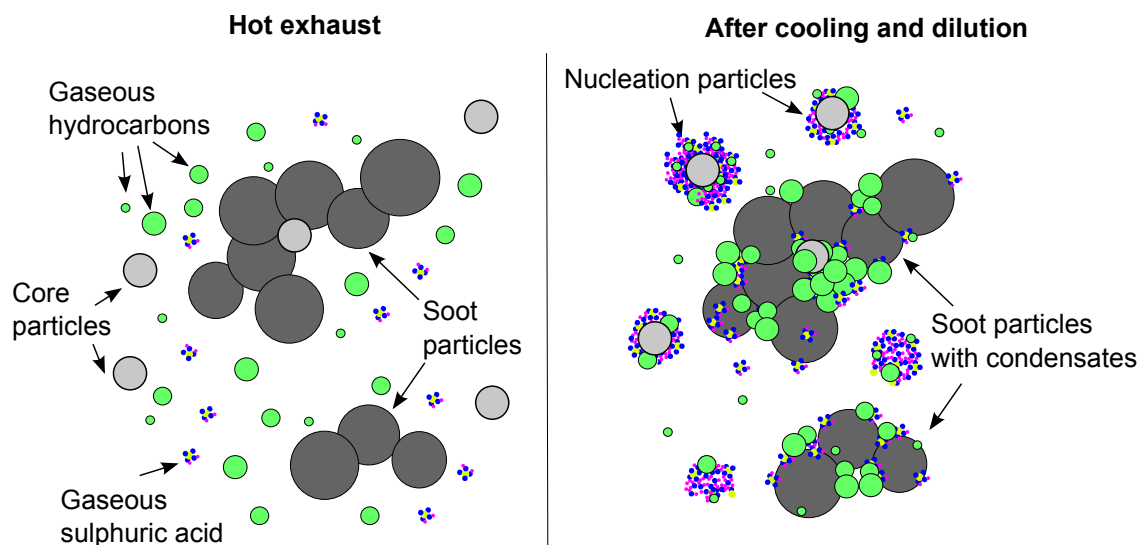## 2.1 Division into nucleation and soot particles

Figure 2.1: Gaseous and particle phase components in hot exhaust gas and in the diluted exhaust under ambient conditions.

Nucleation and soot particles are divided in terms of formation mechanisms into two distinctive particle modes (Kittelson, 1998). Nucleation mode (NM) particles can be semivolatile,

and can posses a nonvolatile core depending on the engine, driving conditions and the aftertreatment system (ATS) (Rönkkö et al., 2007; Filippo and Maricq, 2008; Lähde et al., 2009). Traditionally the NM is reported to be formed in a cooling dilution process of various hydrocarbons and GSA. In the absence of core particles, the NM formation is considered to be sulfur driven. Soot particles are formed during the combustion process inside the combustion chambers. Soot particles are fractal shaped nonvolatile particles in the exhaust system that consist of primary spheres. During the cooling dilution process of exhaust gas to ambient air, semivolatile material (e.g. GSA, organics) condenses on soot, making the particles larger. Also the effective density of highly agglomerated large particles will increase when the particles become more spherical (Ristimäki et al., 2007; Olfert et al., 2007). During this condensation process the mobility diameter of a particle does not necessarily increase, whereas the aerodynamic diameter does. Figure 2.1 is a graphical illustration of the gaseous and particle phase components in hot exhaust gas and in the diluted exhaust under ambient conditions based on the literature cited above.

The nonvolatile core particles are generally smaller than 10 nm, whereas NM particles are generally smaller than 40 nm. The soot mode (SM) mean diameter is generally in the size range of 20–100 nm, which means that SM particles can overlap with NM particles in a particle size distribution on some occasions. Often the SM is called *accumulation mode* when including condensates and measured in urban air.

Examples of particle number size distributions for a light-duty diesel engine without an ATS, a heavy-duty (HD) diesel engine without an ATS, and an LD GDI car with a three-way catalytic converter (TWC) are shown in Figure 2.2. Datas were retrieved from the experiments of **Papers 1, 2 and 4**. Figure 2.2 shows a clear difference between soot particle concentration levels between LD engines with gasoline and diesel technologies, that is, the SM concentration in the case of the diesel engine was ∼25 times higher than that of the GDI engine. For the modern HD nonroad engine, the SM concentrations were closer to the concentration levels of the GDI. The particle size distribution of the GDI engine was bi-modal where both modes are considered to be soot with a difference that the smaller mode is primary particles and the larger mode consists of soot agglomerates. With all the engines/vehicle there were also other particle modes present. With the FSC of 340 ppmw, there was a sulfur driven nucleation mode at a high load, which was not the case when the FSC was low (6 ppmw). In the case of the nonroad HD engine there were NMs present both at a medium load and high load. Size distributions measured through the TD in this case indicated that there were also nonvolatile core particles. Seemingly these core particles grew to a larger size as seen especially in the size distribution corresponding to high engine load.

So called *coarse mode* particles are reported constantly in the literature, especially in the case of old engines and aftertreatment technologies. These particles are larger than 1 μm in diameter, and do not practically affect the particle number. Instead, they can affect PM emissions. These particles are considered to be accumulated particle material on the surfaces of the exhaust systems. When a high level of PM is accumulated on the walls, some
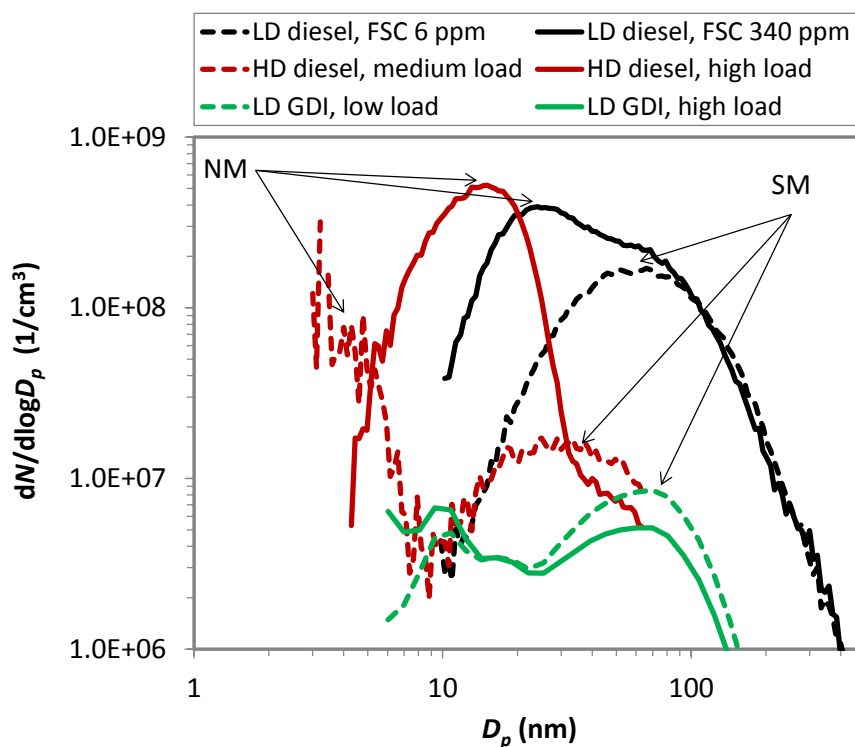
Figure 2.2: Examples of exhaust particle size distribution of a HD diesel engine without an aftertreatment system (ATS) (**Paper 1**), a LD diesel engine without an ATS (study of **Paper 2**) and a LD GDI vehicle with a TWC (**Paper 4**). The sampling was conveyed with a PTD without the TD so semivolatile components can also be partially present. $dN/dlogD_p$ is normalized particle number concentration and D_p mobility particle size.

of the PM can be released due to vibration, heat and exhaust flow forces in the form of flake-like particles. Since the focus here is in the exhaust particle number and properties of the sub-500 nm particles, the coarse particle mode is not studied and covered within this thesis.

2.2   Engine-out emissions

Engine-out particle emissions are either measured at the end of the tailpipe or after the exhaust manifold before any ATS. These particle emissions are not really directly any tailpipe emissions of modern engines since practically all vehicles are now equipped with some form of ATS in developed countries. Determining the engine-out emissions is in fact also the way to study the physical (size, morphology, number, mass) and chemical characteristics of particles originating from the engine. These particles are partially real-world emissions when no particle filtration is used. These particles also affect the accumulation of PM inside the

diesel particulate filter (DPF) and thus the regeneration frequency (Lapuerta et al., 2012) and operating life of DPF devices (Sappok et al., 2009).

In the case of an LD diesel engine the nonvolatile engine-out particle size distributions are typically plainly soot. Only during low load conditions such as idle, a nonvolatile NM has been observed (Filippo and Maricq, 2008). In the case of HD diesel engines, engine-out particle size distributions are quite often bi-modal consisting of soot and core particles (Rönkkö et al., 2007; Lähde et al., 2009). When measured with a cooling dilution (such as a PTD), particle growth due to condensation of the organics is effective (Vaaraslahti et al., 2004). In the case of GDI vehicles, engine-out particle size distributions have been reported to be bi-modal (Barone et al., 2012; Maricq et al., 1999b).

2.3   Effect of exhaust aftertreatment on exhaust particles

Diesel aftertreatment devices can be categorized into three groups: oxidation catalysts, particle filters and reduction catalysts. The purpose of devices in each group is quite different. Diesel oxidation catalysts (DOCs) efficiently oxidize gaseous hydrocarbons (HC) and CO that come out of the engine. However, the effect of the DOC on PM emissions is small. Diesel particulate filters (DPFs) are effective in collecting the nonvolatile particle fraction that is formed inside the engine's cylinders. The collection efficiency (or reduction efficiency) of nonvolatile soot particles in a DPF can be over 99%. A partial diesel particulate filter (pDPF) is a system with an open channel structure cabable of reducing 30–70% of soot particles and practically all the non-volatile cores. Selective catalytic reduction (SCR) devices are installed on vehicles in order to reduce NO_x concentrations, however, the SCR systems may have some effects on particle emissions as well. The three-way catalytic converter (TWC) is the catalyst solution for gasoline engines that has a high efficiency in gaseous pollutant reduction. Table 2.1 summarizes the typical performance of various exhaust ATSs.

2.3.1   Diesel oxidation catalyst

Diesel oxidation catalysts are installed on vehicles in order to remove gaseous pollutants: CO and HC. The CO and HC removal is based on the oxidation reaction on the surfaces of the DOC. The DOC washcoat is loaded with a noble metal catalyst (platinum, palladium) that reduces the thermal energy needed for the oxidation reaction, where either O_2 or NO_2 serves as the oxidant. Operating ideally, the oxidation reaction products are CO_2 and H_2O for HC, and CO_2 for CO. The DOC also reduces the semivolatile fraction of PM that often consists of HC. Typically, the effect of the DOC on nonvolatile soot mode particle mass or number is small. Johnson and Kittelson (1996) modeled a nonvolatile soot number reduction of ∼5% for a DOC structure. Vaaraslahti et al. (2006) reported a PM decrease caused by a

Table 2.1: General picture of the effects of exhaust aftertreatment systems (ATSs) on particles. Also common pros and cons related to costs and exhaust particles are listed.

ATS	Purpose to reduce	Soot reduction	Nucleation mode possibility	Pros	Cons
No ATS			Nonvolatile & semivolatile	Maintenance free, costs nothing	Emissions
DOC	CO & HC	$< 10\%$	Nonvolatile & semivolatile	Maintenance free, low pressure drop, gaseous pollutant reduction	Low reduction of PM
DPF	Soot	$> 95\%$	Semivolatile	PM & PN reduction	Active regeneration, high pressure drop, fuel penalty
pDPF	Soot	30–70%	Semivolatile	Maintenance free, soot reduction vs. DOC, NM core removal, low pressure drop	Soot reduction vs. DPF
SCR	NO_x		Semivolatile & maybe nonvolatile	High NO_x reduction, optimal engine parameters can be used	Active control, urea consumption
TWC	HC, CO & NO_x	$< 10\%$	Semivolatile & nonvolatile	High gaseous pollutant reduction	Low particle reduction

DOC to be 6–27% depending on the engine load, so that higher PM reduction was observed during at low load and mostly caused by the reduction in soluble organic fraction (SOF).

In real-world emissions, the DOC affects the emitted particle size distribution of the vehicle. With a DOC, the amount of condensing or nucleating HC is reduced. When the FSC is high enough, oxidative aftertreatment can cause the formation of NM particles when the exhaust temperature is at a sufficient level. The requirements for existence of the NM are in general as follows: (1) high enough fuel sulfur content, (2) active catalyst and (3) high exhaust temperature (Herner et al., 2011). The sulfur driven nucleation formation is explained by the oxidation of SO_2 within the oxidation catalyst to SO_3, which later forms GSA (Arnold et al., 2012). The sulfur driven nucleation mode particles are formed, according to current knowledge, via sulfuric acid-water nucleation when the exhaust gas is cooled and diluted in the presence of ambient air. Note that there are no number regulations limiting these semivolatile particles, however, these particles (also condensed matter on soot) accumulate onto the PM emissions where the particles of diluted exhaust are collected on a membrane or fiber filter and the filter is subsequently weighted. The semivolatile fraction can also adsorb onto these filters from the gas phase and cause an artifact in the result (Chase et al., 2004; Högström et al., 2012). In the mass size distribution, the effect of semivolatile nucleation mode is minor, but in the particle number size distribution these particles can be dominant. The amount of exhaust particles originating from sulfur depends heavily on the driving mode and the driving history of the vehicle. At low temperatures sulfur is stored inside the catalyst, and when the temperature is increased, sulfur is released from the aftertreatment device (e.g. Maricq et al. (2002), Rönkkö et al. (2006), Giechaskiel et al. (2007), **Paper 1**).

2.3.2 Diesel particle filters

Diesel particulate filters are typically ceramic wall-flow filters that are used currently in both LD and HD diesel applications. The exhaust gas flow channels are partially blocked and flow is forced through porous filter walls. The collection efficiency (or reduction efficiency) of nonvolatile soot particles in a DPF can be over 99%, or even over 99.9% (Vaaraslahti et al., 2004; Bergmann et al., 2009; Herner et al., 2011; Mohr et al., 2006) depending partially on the filter PM loading. The reduction of soot particles is more effective with a loaded filter than with a clean filter (Mohr et al., 2006; Mamakos et al., 2011). The trapped particulate material (mostly soot) causes the pressure drop over the filter to rise and the filters must be regenerated occasionally. Some DPFs can be regenerated continuously by installing a DOC in front of the DPF, thereby generating NO_2 which can oxidize soot at typical exhaust gas temperature levels. Otherwise, DPFs need an excess heating system for active regeneration such as electrical heating or engine internal or external fuel after-injection. In HD diesel engines only the fuel injection regenaration method is commonly used. Increased NM particle emissions have been reported during active DPF regeneration events (Mamakos et al., 2011).

Partial diesel particulate filters (a.k.a. open channel filters) are based on deep filtration,

and the structure is open, unlike in a wall-flow DPF. These pDPFs consist of curved open channels that are surrounded by a metallic mesh grid or fiber structure (Lehtoranta et al., 2007). Similar catalysts are used in pDPFs as in DOCs, often with lower precious metal contents. Partial filters do not require active regeneration procedure — instead they are regenerated passively by NO_2 and O_2 when the exhaust gas temperature is at a sufficient level. The system is practically maintenance-free, which enables convenient retrofitting onto existing vehicles. The nonvolatile particle reduction efficiency of the pDPF is generally somewhere around 50%, depending on the particle size, exhaust velocity, exhaust temperature and filter structure (e.g. size, design). Also the engine size has an effect on the number collection efficiency; in HD applications the number reduction has been observed to be 50–70% (Heikkilä et al., 2009; Karjalainen et al., 2010) but in an LD application the total reduction efficiencies during low and medium loads were 30–40% and ∼50%, respectively (Bielaczyc et al., 2012). The possible particle collection mechanisms within the pDPF structure are diffusion, inertial impaction and interception; however, due to the difficult geometry and soot loading-dependent flow pattern, the particle collection phenomena within the pDPF structure are not completely understood.

The nonvolatile particle reduction efficiency of the pDPF depends strongly on the particle size, such that the reduction efficiency curve has a minimum near particle diameters of ∼100 nm. The problem in general is that around 100 nm particle sizes, the soot particle concentrations are high (see e.g. Figure 2.2). Especially important is that the core particle mode almost vanishes in a pDPF. Altogether, these filters are very efficient in removing the sub-10 nm particles (∼99%) by thermal diffusion (Heikkilä et al., 2009; Karjalainen et al., 2010). This way the open channel filters are able to prevent the nucleation mode emission: the nonvolatile mode itself is removed and the NM formation does not take place if the condensable vapor concentrations are low. Otherwise, without the pDPF, the core particles could be able to grow by condensable vapors during the dilution and cooling process. However, with a high sulfur level fuel (340 ppmw) and high enough exhaust temperature (over 350 °C), the sulfur driven nucleation has been observed in the DOC & pDPF application (Bielaczyc et al., 2012).

Wall-flow type DPFs were not used in the studies of this thesis, but pDPFs were applied in the studies of **Paper 2**.

2.3.3   Selective catalytic reduction

The Selective catalytic reduction (SCR) method is used to reduce NO_x emissions that are formed in the high temperature combustion within the engine combustion chamber. For instance, the increase in fuel injection pressure causes the soot particle size to drop and decreases the PM emission while more NO_x and core particles are formed during the combustion of diesel fuel (Lähde et al., 2011). The NO_x emission is addressed frequently by an SCR-system that is installed in the tailpipe. NO_x is reduced in a selective catalyst using ammonia as the reductant. Ammonia is generated by hydrolysis of urea solution which is

injected into the hot exhaust gas. However, the efficiency of the SCR depends on various parameters, such as urea injection placement and operational parameters, the SCR catalyst and exhaust gas temperatures (Johnson, 2009). Overall, the SCR allows a diesel engine to be run at maximum efficiency, emitting high amounts of engine-out NO_x (Mollenhauer and Tschoeke, 2010). At the same time, with high fuel injection pressure, soot particle mass is reduced (Lähde et al., 2011). However, the SCR system can be a potential source of new exhaust particles if ammonia is able to penetrate the system (Lemmetty et al., 2007) or by other means. In some cases, an oxidative "slip catalyst" is installed at the back end of the SCR to oxidize excess ammonia.

The SCR's effect on emission related particles is not yet well known, but there are a few studies concerning the topic (Thiruvengadam et al., 2011; Herner et al., 2011, 2009; Krahl et al., 2007; Hu et al., 2009). Both Thiruvengadam et al. (2011) and Herner et al. (2011) measured particles with a DPF & SCR aftertreatment in a HD diesel application. Thiruvengadam et al. (2011) found out that after the SCR NM concentrations were over an order of magnitude larger than with an aftertreatment that consisted solely of a DPF. The higher the exhaust temperature was, the higher the NM particle concentrations were. Under the threshold temperature of 380 °C, there was no significant amount of NM particles. Results of Herner et al. (2009) confirm that after the DPF & SCR, a large quantity of small particles ($D_p < 20$ nm) can be observed. Comparing different ATSs installed on test vehicles, the total particle number emission rate was the largest at steady cruise (50 m/h = 80.5 km/h) mode. At the same time the amount of particles larger than 20 nm was the smallest. During a reasonably cold test cycle, the particle emission rate was smaller than during cruise, since the exhaust temperature was significantly lower. Concluding, both studies indicate an increase of NM particle number emissions when the SCR system is used and the exhaust temperature is high. The formation is explained by the oxidative potential of the SCR system, by increasing the oxidation of SO_2 to SO_3, therefore, promoting the formation of sulfur driven nucleation mode. This is in correlation with the study of Hu et al. (2009), however, they also observed that a vanadium-based SCR system emitted considerable amounts of vanadium in the nanoparticle size range. This can also cause an increase in the NM particle emissions. Particle emissions with an SCR aftertreatment over a low exhaust temperature transient test cycle were studied in **Paper 1**.

2.3.4 Three-way catalytic converter

Three-way catalytic converters have been used since late 1980s in gasoline operated vehicles in order to reduce NO_x and oxidize CO and HC (Eastwood, 2008). This is possible since gasoline engines operate typically under stoichiometric combustion conditions and therefore there is practically no oxygen in the exhaust entering the TWC. At the first stage, NO_x is reduced to O_2 and N_2. Later at the second stage, CO is oxidized to CO_2 and HC are oxidized to H_2O and CO_2. The TWC itself is not a solution to remove the non-volatile PN & total PM emissions of gasoline vehicles. In the studies of **Papers 3 & 4** TWCs were used in all

three gasoline vehicles.

2.4 Transient conditions

From the particle emissions point of view, transient phenomena can be understood as situations whenever there are changes in particle concentrations. These changes in particle emissions are often related to the fast changes in engine operation, such as changes in torque or speed. In turbocharged engines, the turbocharger lag is often blamed for the increased soot or smoke concentrations during accelerations (Rakopoulos and Giakoumis, 2009; Rakopoulos et al., 2010). The increased amount of PM is explained by the fact that the fuel injection rapidly follows the change in demand but there is a delay in turbocharger activation. Thus the fuel consumption increases rapidly but the increase in the intake air mass flow is slower. This generates high local fuel to air ratios, and hence a higher amount of soot can be formed.

Exhaust particle concentration changes can be also caused by slower processes like slow changes at temperatures at various locations. There is a relatively slow change in temperatures during engine warmup after a cold start of a vehicle. It requires minutes for engine and lubricant oil to heat up in order to reach optimal fuel evaporation, and thus, optimal efficiency. Temperature changes inside the ATS are usually lagged due to the thermal capacity of the ATS. Hence, it requires sufficient time for the ATS to reach steady-state temperature profile or to follow the changes in engine operation.

In general, it has been observed that during transient cycles, the particle size distributions can be bi-modal (Wang et al., 2006), and the highest particle emissions occur during heavy acceleration when the engine is heavily loaded (Wang et al., 2006; Maricq et al., 1999b,c). Transient driving conditions can affect both NM and SM particles (Liu et al., 2007). Increased emissions of nucleation particles, affected by FSC and exhaust dilution and thus proposed to be formed by sulfuric compounds, has been observed at deceleration as well. As with steady state tests, the particle emissions during transient cycles has been observed to be affected by vehicle technologies like exhaust aftertreatment (Wang et al., 2006) and fuel type (Wang et al., 2006; Liu et al., 2007; Rakopoulos et al., 2010; Giakoumis et al., 2012). Particle emissions under transient driving conditions are discussed further within this thesis and all the enclosed articles (**Papers 1–4**).

Chapter 3

Experimental procedures

This thesis consists of experiments performed in the engine and aerosol laboratories (**Papers 1–4**) and on the road (**Papers 2–4**). The main focus is on the number and characteristics of the exhaust particles. The instrumentation used consisted mostly of fast on-line particle and gas analyzers which is very important since most of the studies were performed under transient conditions where particle emissions alter rapidly. Together with the fast instruments, transmission electron microscopy (TEM) analyses were performed in **Papers 3 and 4**.

3.1   Engines and vehicles

3.1.1   Diesel engines and vehicle

All the tested diesel engines/vehicle with the information of test routines are briefly described in Table 3.1.

Heavy-duty diesel engines

Two heavy-duty diesel engines were used in the studies of this thesis: a nonroad engine (Diesel 1) in **Paper 1** and a road engine (Diesel 2) in **Paper 3**.

In **Paper 1**, the test engine (Diesel 1) was a HD Stage 3b emission level 6-cylinder nonroad diesel with the rated power of 200 kW. The engine was equipped with an aftertreatment system (ATS) consisting of a DOC and an SCR system which is also the ATS of the corresponding serial production version. An especially designed Transient Cold Test Cycle (TCTC) was driven in the experiments. Details of a single TCTC are shown in Figure 3.1. This cycle was designed so that the exhaust temperature stays at a low level and the urea injection is only partially active. These low exhaust temperatures are representative of low load conditions during wintertime which is a very typical use of this engine type and ATS. The fuel used met the EN590 quality standard (Dieselnet, 2014).

In **Paper 3**, tests were run with a HD 6-cylinder 10.6 l diesel road engine (Diesel 2) capable to produce maximum power of 324 kW at 1900 min^{-1} and maximum torque of

Table 3.1: Short summary of properties of the tested diesel engines/vehicle and the test routines.

Vehicle	Diesel 1	Diesel 2	Diesel 3	Diesel 4
Studied in	**Paper 1**	**Paper 2**	**Paper 2**	**Papers 2–3**
Type	HD nonroad	HD road	LD	HD road
Emission level	Stage 3b	Euro IV	Euro 4	Euro II
Displacement (l)	6.6	10.6	1.9	11.7
Fuel sulfur content	< 10 ppmw	< 10 ppmw	6, 65 & 340 ppmw	< 10 ppmw
Aftertreatment system	DOC & SCR	DOC & pDPF	DOC & pDPF	No ATS / DOC & pDPF
Tested in	Engine dyno	Engine dyno	Engine dyno	On-road
Test routine	TCTC	Steadys	Steadys	Real route

2100 Nm at 1000–1400 min^{-1}. This engine type reaches the Euro IV emission level when equipped with a DOC & pDPF. The driving operation consisted of selected driving modes of the 13-step European stationary cycle (ESC) (Dieselnet, 2014) in order to measure particle emissions under both low and high load conditions. The fuel used met the EN590 fuel quality standard.

Light-duty diesel engine

In **Paper 2**, LD diesel engine tests were performed with a 4-cylinder 1.9 l common rail diesel engine (Diesel 3) on an engine dynamometer. This engine type meets Euro 4 emission levels when equipped with a DOC. Synthetic 5W-30 lubricant oil was used in the engine. Three different sulfur level diesel fuels were used containing 6 ppmw, 65 ppmw and 340 ppmw of sulfur. The exhaust aftertreatment was a combination of a diesel oxidation catalyst (DOC) and a partial diesel particulate filter (pDPF) (diameters 127 mm, mesh lengths 74.5 mm and 150 mm and Pt-loadings 40 g/ft^3 and 10 g/ft^3, respectively). Three identical DOC+pDPF devices were used, one for each fuel.

Tests with each fuel were run in two driving modes. The duration of the first (low load) mode (engine speed 1350 rpm, engine torque 52 Nm) was 48 hours. The second (medium load) mode (3000 rpm, 125 Nm) was operated for an hour. While the exhaust gas temperature before the DOC was lower than 250 °C during the first mode, during the second mode it was increased up to 380 °C with all the fuels. Thus from the viewpoint of the pDPF functioning, the first mode represents driving conditions where soot particles are
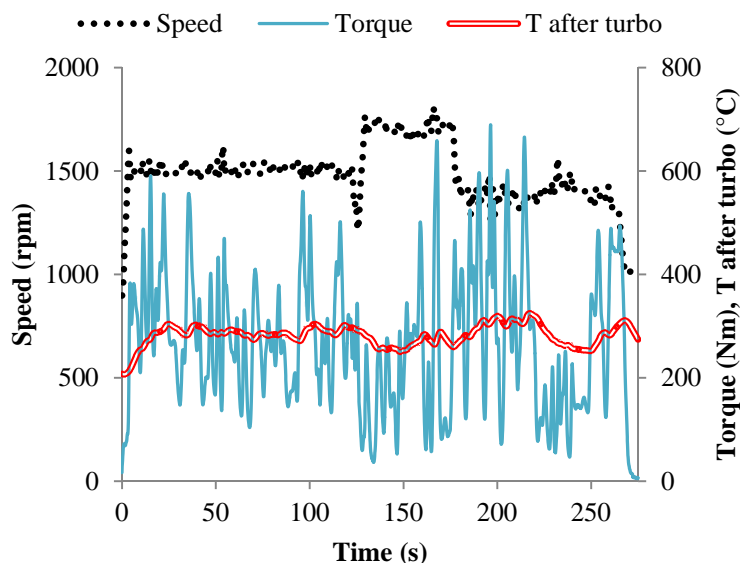
Figure 3.1: Transient cold test cycle (**Paper 1**) speed, torque and temperature profiles for the test engine (Diesel 1).

collected onto the pDPF's surfaces but the oxidation of the collected soot is at minimum. During the second driving mode the collected soot is oxidized: in other terms, the pDPF is regenerated.

Heavy-duty diesel truck

Real-world measurement of the emissions of a HD diesel truck (Diesel 4) was performed under real driving conditions on the normal transportation route of the truck. Experiments were performed on highway 4 between Jyväskylä and Oulu, Finland. The truck transported cargo with typical payloads, hence, from the truck's point of view the measurements represented real-world operation. Due to the continuously changing driving conditions, the data of certain driving parameters (engine speed, engine torque, pedal position, exhaust temperature, and pressure) were collected with a time resolution of 1 s. The location and speed of the vehicle were measured and saved using the GPS.

The truck (emission level Euro II without an ATS, mileage 800 000 km) used diesel fuel meeting the fuel standard EN590 and having a FSC of less than 10 ppmw. The lubricant oil was high quality SAE 10W-40 suitable for long oil change intervals, which met the requirements of the truck manufacturer. The truck was not equipped with an exhaust ATS in **Paper 3**, whereas in **Paper 2** there was a retrofit ATS consisting of a DOC and a pDPF. Particle concentrations of the exhaust plume were measured by chasing the truck with its trailer in a mobile laboratory. The distance between truck and laboratory vehicle was kept at 12 ± 2 m. An aerosol sample taken directly from the exhaust plume had a 1.6 s exhaust

residence time in the atmosphere at a speed of 80 km/h. This time is considered sufficient for aerosol processes to achieve a relatively stable condition (Keskinen and Rönkkö, 2010). During the measurement, ambient air temperature and relative humidity (RH) were 5–15 °C and 57–92%, respectively.

Studies were conducted on Highway 4 in Finland between the cities of Oulu and Jyväskylä where one test run was approximately 350 km long. Near Jyväskylä, the test consisted mainly of uphill and downhill driving while near Oulu, the route was relatively flat. The vehicle speed was near 80 km/h during most of the measurement time. The engine load varied greatly, depending mainly on the altitude profile; during uphill driving, the engine torque was typically at maximum and during downhill driving, it was zero, meaning engine braking conditions. In total, more than 30% of the time, the engine was at maximum or minimum torque. Here "torque" refers to the torque produced by the engine; negative torque caused by the inertia of the truck was not measured. In order to minimize the effects of other traffic on the results, the measurements were performed in the late evening and night. Thus, the number of oncoming vehicles averaged only 28 per hour during the 4.5 h test of which 46% were HD and 54% LD vehicles.

3.1.2   Gasoline vehicles

All the tested gasoline vehicles with the information of test routines are briefly described in Table 3.2.

Table 3.2: Short summary of properties of the tested gasoline vehicles and the test routines.

Vehicle	GDI 1	GDI 2	GDI 3
Studied in	**Paper 3**	**Papers 3-4**	**Paper 4**
Year	2011	2011	2012
Aftertreatment system	TWC	TWC	TWC
Displacement (l)	2.0	1.8	1.8
Injection system	GDI (Stratified)	GDI (Stratified)	GDI (Stratified) & PFI
Tested in	Chassis dyno	Chassis dyno	On-road
Test routine	NEDC, constant loads	NEDC	Accelerations and decelerations

In **Paper 3** the test vehicle, named GDI 1 here, was a new gasoline direct injection (GDI) passenger car (model year 2011, displacement 2.0 l), equipped with a TWC to control CO, HC and NO$_x$ emissions. On the basis of the on-board diagnostics (OBD) data, the vehicle ran in stoichiometric mode at all operating ranges except directly after starting. The fuel was gasoline with ethanol content below 10%. Experiments were conducted during the New European driving cycle (NEDC) (Dieselnet, 2014) consisting of accelerations, short steady state driving conditions, decelerations (conducted by engine braking) and idling conditions. All of the measurements were performed with a warmed-up engine so that at least one NEDC cycle was driven just before the tests reported here. Exhaust aerosol was sampled from two different locations of the exhaust pipe: in the engine bay right after the exhaust manifold and after the whole exhaust pipe (including the TWC) and an exhaust transfer line.

In **Papers 3 & 4**, the test vehicle (GDI 2) was a modern gasoline fueled passenger car made in 2011 and it was driven on a single roll chassis dynamometer. The GDI engine of the test vehicle (1.8 l displacement) was turbocharged and used fuel stratified injection technology below 3000 rpm. The engine was controlled to operate globally at stoichiometric oxygen concentration but there are local lean and rich sections in the combustion chamber. The exhaust aftertreatment was performed by means of an original TWC. The engine was run with low sulfur (< 10 ppmw) 95-octane gasoline-ethanol blend fuel where the ethanol concentration was below 10%. The lubricant oil (viscosity grade 5W-30) contained phosphorus, sulfur, calcium and zinc, 900 ppmw, 2780 ppmw, 3200 ppmw and ppmw, respectively. The experimental routine consisted of test cycles and steady engine load points. Before the test series, the vehicle was warmed up during an NEDC. During this warm-up run the emissions were also measured. The NEDC cycle was repeated in total eight times. Steady-state test points were driven at the wheel speed of 80 km/h in 5th gear so that the chassis roll brake was controlled in order to achieve wheel powers of 5 kW, 10 kW and 20 kW.

The engine (1.8 l displacement) of the test vehicle (GDI 3) in **Paper 4** was turbocharged and also used fuel stratified injection technology. However, compared to GDIs 2 & 3 this engine was newer generation including both GDI and PFI injection systems. Under low load conditions, only the PFI injector is used. This engine also operated under global stoichiometric combustion conditions. The fuel and lubricant were from exactly the same batches as in the laboratory experiments of GDI 2. Due to technological differences compared to GDI 1 & 2, lower particle emissions were expected from GDI 3. On-road tests were performed in Alastaro (Finland) in a low-traffic flat road section far away from any town. Thus, the background particle were low and typical for rural background (∼2000–3000 1/cm^3). Before the test series, the test vehicle was driven ∼200 km at typical highway/freeway speeds of 80–120 km/h. The experiments were performed under sunny and dry conditions (temperature 23–24 °C, wind speed 1–2 m/s, RH 40–60%). Test runs consisted of constant speed chases and controlled acceleration & deceleration routines. The acceleration and deceleration routines were run in first gear (20–50–20 km/h), in second gear (30–70–30 km/h and 30–90–30 km/h) and in third gear (30–70–30 km/h). The deceleration was caused only by

engine braking so that the accelerator pedal was lifted, and vehicle was kept rolling at its natural pace. The test vehicle was chased with the mobile laboratory. Similarly as in the chasing experiments on the HD truck, the distance between the car and the van was kept at around 12 m, although during accelerations and decelerations the constant distance was difficult to maintain exactly.

3.1.3   Aerosol laboratory simulation

At the aerosol laboratory experiment in **Paper 2**, sulfur related particle formation and gas phase oxidation of SO_2 were measured before and after a small scale catalyzed pDPF. This pDPF device was scaled so that the flow velocities were comparable to a real-world application as in Karjalainen et al. (2010). More details of the pDPF can be found in the experimental section of **Paper 2**.

Experiments were performed using different mixtures of SO_2 and filtered air ($\sim$5% RH at 25 °C), passing this mixture through heaters and the small scale pDPF. In the pDPF SO_2 is oxidized to SO_3, which can form GSA in the presence of water. The SO_2–SO_3 conversion was calculated by from SO_2 concentrations upstream and downstream of the pDPF. The test was conducted at a temperature range of 238–412 °C and over the SO_2 concentration range of 1.8–61.4 ppm. If SO_2 is assumed to originate solely from the pure combustion of the fuel, then 1.8 ppm corresponds to FSC = 32 ppmw and 61.4 ppm corresponds to FSC = 1100 ppmw. To study the role of storage and release of sulfur compounds in an oxidative catalyst, there was first a low temperature phase which enabled sulfur compound storage and then the test gas temperature was increased to decompose and desorb the accumulated sulfur species. In this experiment, an SO_2–air mixture (50 ppm of SO_2) was passed through the pDPF at 240 °C at first in order to simulate the adsorption conditions of sulfur compounds. The sulfur storage into the sampling and dilution system was prevented during this storage phase by flushing the PTD with filtered instrument air. After one hour, the SO_2 feed was shut down, the sample flow was taken through the PTD and the temperature of the air flowing through the pDPF was increased to 370 °C.

3.2   Laboratory experiments

The laboratory experiments can be categorized as follows: experiments in engine dynamometers, on a chassis dynamometer and in an aerosol research laboratory (Figure 3.2). The exhaust gas sample was conveyed from three locations of the exhaust systems at the engine dynamometers (Figure 3.2a): before aftertreatment, after a DOC and after an SCR or a pDPF. At the chassis dynamometer (Figure 3.2b) the exhaust sample of tested passenger cars was conveyed either before a TWC, or from a transfer line after the whole exhaust system. At the aerosol laboratory (Figure 3.2c), sulfur related particle formation and gas phase oxidation of SO_2 were studied measuring SO_2 concentrations before and after a small-scale
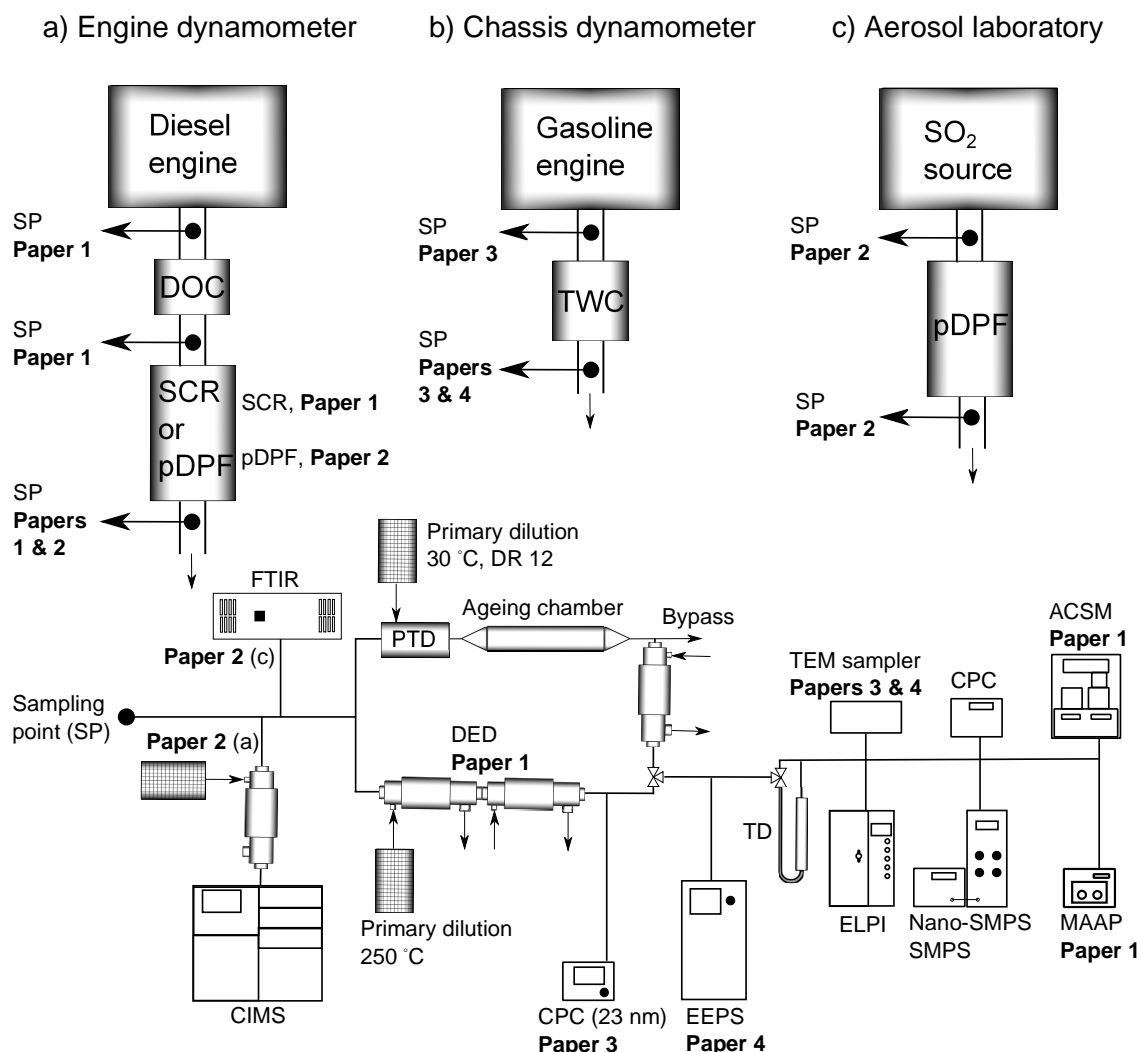
catalyzed pDPF.

Figure 3.2: Experimental setups in laboratory studies of **Papers 1–4**.

The raw exhaust dilution was performed with a partial sampling and dilution system. A porous tube diluter (PTD) (Ntziachristos et al., 2004) was used as a primary diluter where the dilution ratio (DR) and dilution air temperature were always set to 12 and 30 °C, respectively. This dilution method with chosen dilution parameters has been observed to mimic the primary real-world nucleation mode (NM) formation process (Rönkkö et al., 2006; Keskinen and Rönkkö, 2010). Overall the formation of NM particles is sensitive to the choice of sampling parameters (Mathis et al., 2004), and partitioning of semivolatile organics between particle phase and gas phase depends on the total DR used (Lipsky and Robinson, 2006). The exhaust originating secondary NM particle formation in the atmosphere (Robin-

son et al., 2007) is a different process and cannot be studied with this setup.

There was an another primary dilution option in **Paper 1** to use a double ejector diluter (DED), where the primary dilution air was heated to 250 °C. The secondary dilution was always performed with an ejector diluter (Dekati Diluter, DR ∼8). Occasionally the diluted exhaust was passed through a thermodenuder (TD) (Rönkkö et al., 2011) at 265 °C to study the volatility of particles. The nonvolatile particle loss correction for the TD was calculated according to the particle loss curve presented in Heikkilä et al. (2009). The TD treatment was used in all **Papers 1–4**. The DR correction was calculated based on the CO_2 concentrations measured in raw exhaust, after the primary dilution and after the secondary dilution. For nonvolatile particles the DR correction gives the particle concentrations of raw exhaust, and for semivolatile particles, the result is the formation potential of new particles in standard cubic centimeter of raw exhaust. Only in **Paper 2**, a Fourier transform infrared spectroscopy (FTIR) (Gasmet Technologies, 2014) analyzer without additional dilution was applied in the aerosol laboratory experiment, also in the engine dynamometer experiment, a chemical ionization mass spectrometer (CIMS) (Speidel et al., 2007) was applied downstream of a heated ejector (250 °C).

The particle size distributions were measured with a scanning mobility particle sizer with a long DMA (SMPS) (Wang and Flagan, 1990), a scanning mobility particle sizer with a nano DMA (Nano-SMPS) (Chen et al., 1998), an electrical low pressure impactor (ELPI) (Keskinen et al., 1992) and in **Paper 4** an engine exhaust particle sizer (EEPS) (Johnson et al., 2004). The ELPI was equipped with an extra stage (17 nm $< D_a <$ 28 nm) (Yli-Ojanperä et al., 2010) and a filter stage (7 nm $< D_a <$ 17 nm) (Marjamäki et al., 2002), both increasing the nanoparticle size resolution of the instrument. SMPSs were used when the engines operated under steady-state driving conditions, whereas the ELPI and EEPS were also used under transient conditions with a time resolution of 1 Hz. The particle number concentrations were measured with a condensation particle counter (CPC) (Agarwal and Sem, 1980). Most often an ultrafine condensation particle counter (UCPC) (Stolzenburg and McMurry, 1991) with a cut-point of 2.5 nm was used. In **Paper 3** also a CPC with a cut-point of 23 nm was utilized in order to estimate the nonvolatile PN emissions. Naturally, particle number concentrations were also measured with the ELPI and EEPS. Thus, there was a possibility to study particles that were below the detection limit of the ELPI or the EEPS but were detected by the UCPC. In **Paper 1**, the real-time black carbon (BC) concentration and chemical composition of particles were measured with a multi-angle absorption spectrometer (MAAP) (Petzold and Schönlinner, 2004) and an aerosol chemical speciation monitor (ACSM) (Ng et al., 2011), respectively. The sampling line lengths and flow rates were kept similar between the different experiments, hence only a minor differences in particle diffusion losses were expected.

Additional and more specific information of the experimental routines in each study are reported in the experimental sections of **Papers 1–4** and in the supporting information of **Papers 2–3**.

3.3   On-road chase experiments

The on-road experiments in **Papers 2–4** were performed by chasing test vehicles with a mobile laboratory: Helsinki Metropolia University of Applied Sciences' (Pirjola et al., 2004, 2006; Rönkkö et al., 2006) "Sniffer" van. This mobile laboratory van can be used in stationary and mobile air quality monitoring and in the chase studies of individual vehicles by the laboratory van. Both HD and LD vehicles' emissions can be measured on the road as long as the test vehicle velocity is below ∼90 km/h.
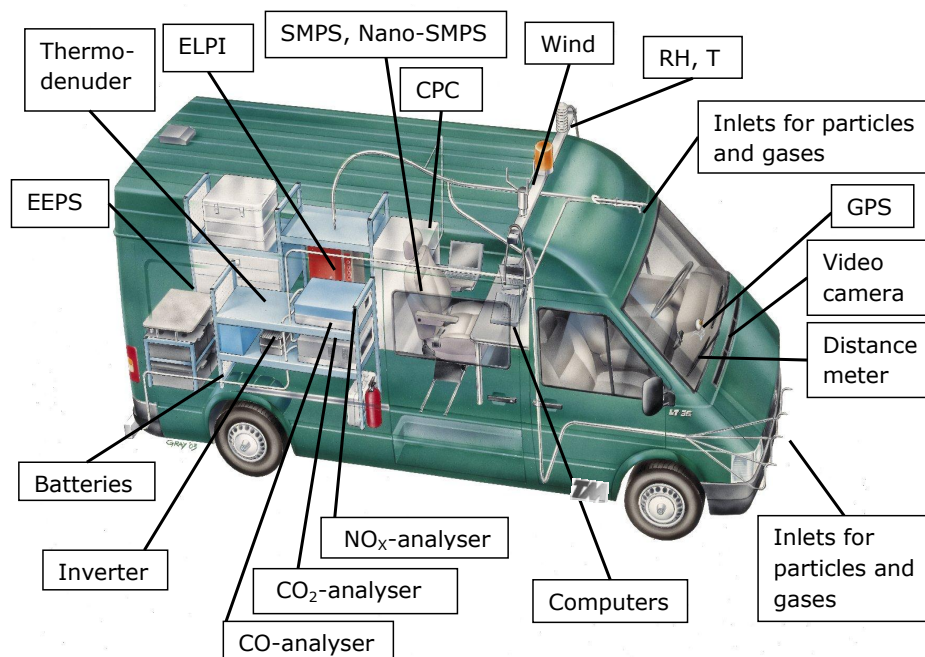

Figure 3.3: Instrumentation in the "Sniffer" mobile laboratory. An EEPS was used only in **Paper 4** whereas SMPSs were used in **Papers 2–3**.

A schematic representation of the instrumentation and assembly in the mobile laboratory is represented in Figure 3.3. The probe to sample the exhaust plume aerosol located in the front bumper of the laboratory vehicle, about 0.5 m from ground level. Real-time particle studies were measured with same instruments used in the laboratory experiments (e.g. ELPIs, SMPSs, CPCs, an EEPS). In front of a UCPC, a passive aerosol diluter (with DR of ∼13), was used in order to dilute the particle concentrations to suitable levels for the instrument. In addition to particle measurements, gaseous NO_x, CO, and CO_2 and relative wind speed and direction, temperature, and RH were also measured. A GPS unit was used to save the velocity and position of the laboratory vehicle.

Chapter 4

Results and discussion

4.1 Overview of the results

Mainly, the physical properties and emissions of the exhaust particles were studied in this thesis and the articles enclosed. Soot particle emissions were detected during combustion of fuel (as expected), but the soot mode (SM) properties were technology-dependent. As an example, soot particle number size distributions (in arbitrary units) are shown in Figure 4.1 for LD diesel (Diesel 3) and gasoline (GDI 2) engines.

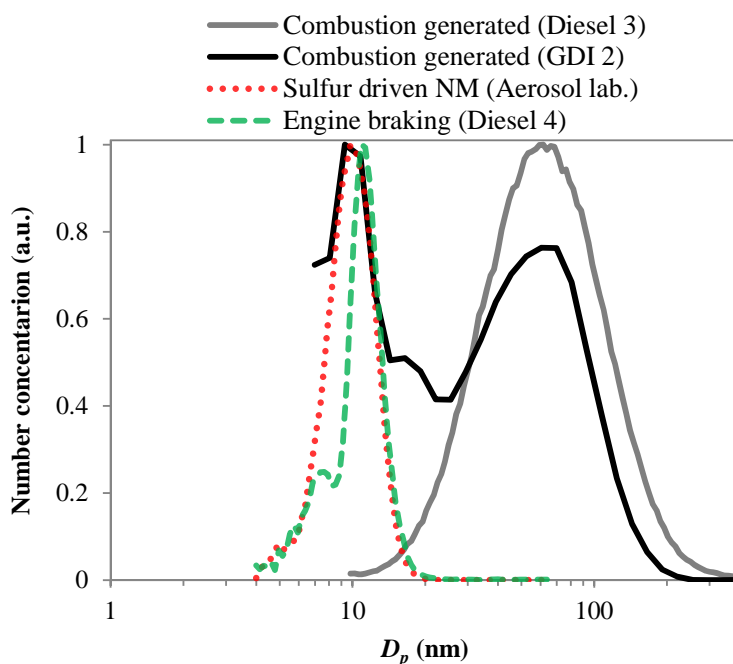Figure 4.1: Example of particle number size distributions (concentrations in arbitrary units (a.u.)) measured during different experiments.

The main focus in this thesis is however in smaller exhaust particles than typical diesel soot. The particle mode with a GMD of $\sim$10 nm was measured for example, during combustion of fuel for GDI 2, in the aerosol laboratory experiment during the release of sulfur,

and under engine braking conditions for a HD diesel truck (Diesel 4) on the road (Figure 4.1). In all these cases, the particle compositions and formation mechanisms are completely different indicating that the particle size (or number) does not reveal everything. For deeper understanding, the instantaneous particle emissions must be linked to the simultaneous driving conditions, the driving history and the vehicle technologies (aftertreatment system, fuel, engine type) used.

This chapter presents and discusses the main results of transient related particle emissions and phenomena. The results are covered in the following order: (1) particle emissions while fuel is combusted, (2) sulfur driven nucleation mode (NM) particles and (3) particles under engine braking conditions.

4.2 Particle emissions during combustion of fuel

4.2.1 Heavy-duty diesel engine

In the papers included in this thesis the particle emissions of a HD engine and the emission reduction by exhaust aftertreatment were studied in **Paper 1**.

Figure 4.2 (left side) shows the total particle number concentrations during two example TCTCs for the nonroad diesel studied in **Paper 1**. The upper part (Figure 4.2a) shows the concentrations measured after the DED system, Figure 4.2b the concentrations after the PTD system without the TD. Concentrations were measured using an UCPC and thus they cover the exhaust particles larger than $\sim$2.5 nm in diameter.

Three results can be observed. At first, with all the aftertreament systems (ATSs), the exhaust particle number concentration varied strongly. This variation was caused mainly by rapid changes in engine torque during a TCTC. The variation was highly repeatable, resulting in practically identical concentration from a cycle to another. Secondly, it can be seen that the choice of the sampling system affected the particle concentrations greatly. In the PTD system, the semivolatile NM formation and condensation of semivolatile compounds on existing nonvolatile particles is possible, but in the DED system these processes have been practically suppressed. Thus based on the results in Figure 4.2, the exhaust particle number concentration depends on the gas-to-particle conversion processes of semivolatile compounds in the exhaust dilution and cooling. Thirdly, it can be noticed that the ATS had an extremely large impact on exhaust particle number concentration, almost two orders of magnitude when measured after the PTD sampling system. The effects were reductive, so that both the DOC and the SCR decreased the concentrations. In addition, it can be seen that the DOC and the SCR reduced both the nonvolatile particle concentrations (DED dilution, Figure 4.2a) and total particle concentrations and the effects were qualitatively similar throughout the cycle. It can also be seen that the exhaust aftertreatment affected the variation of particle concentrations, both absolute values (seen on the left) and relative values (showed as standard deviation error bars on the right). Combining these three results,
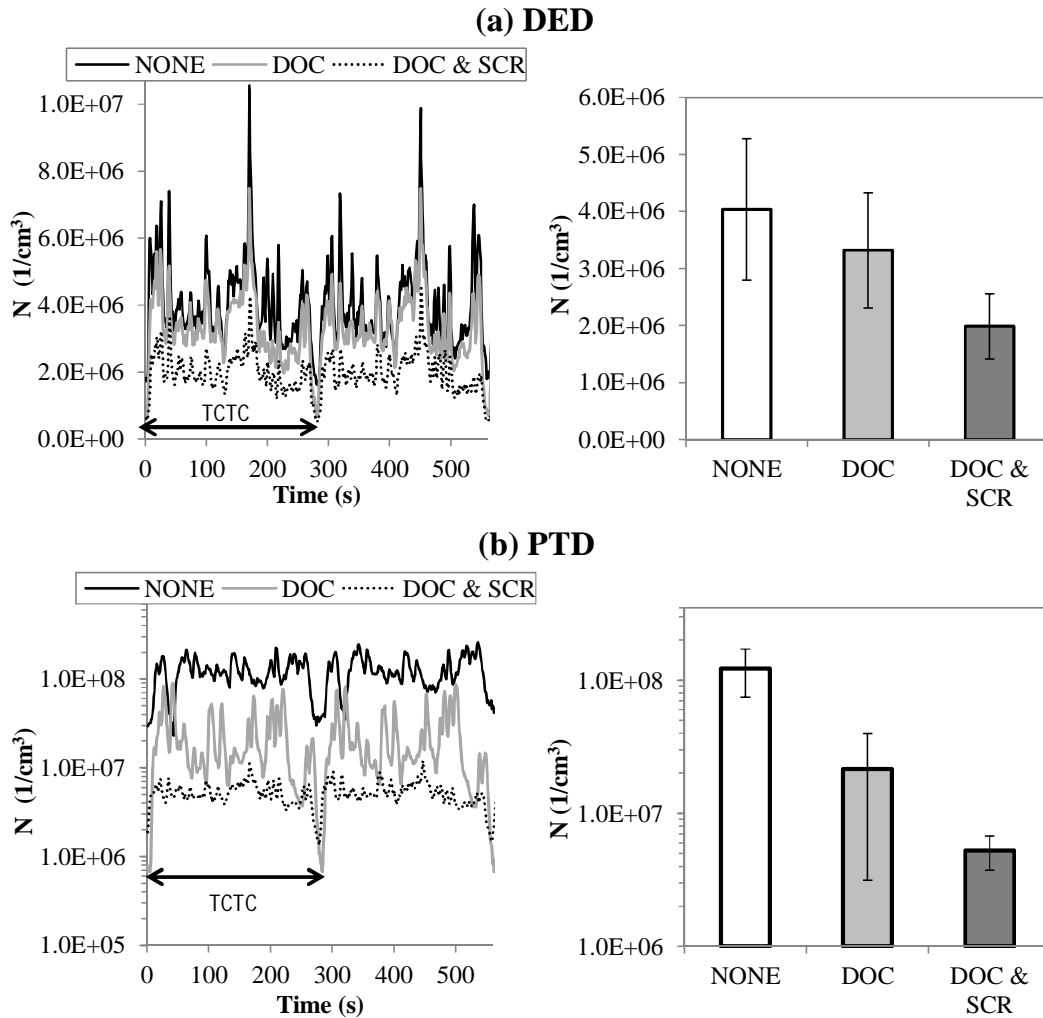
Figure 4.2: Total particle number concentration variations over the TCTC (left) and concentration averages over the TCTC (right) with two sampling methods: (a) nonvolatile particles (DED sampling) and (b) all particles (PTD sampling) (**Paper 1**). Data were measured with a UCPC with a 2.5 nm cut-point.

it seems that both the DOC and the SCR affect the semivolatile exhaust compounds so that the formation of new particles, or condensation on very small core particles, during the exhaust cooling is reduced. However, it should be noted that semivolatile compounds can also condensate on existing particles affecting particle sizes and hence also on particle losses in the sampling line. If the condensation of semivolatile material is in an important role, such as in the case of no ATS and PTD sampling, the smallest particles grow to a greater size reducing the diffusion particle losses in the sampling system. In this size range the smaller the particle size is the greater the particle losses. Because of some uncertainties

in particle sizes, the particle number concentration measured with different sampling and dilution setups are not fully comparable.

The DR corrected particle number concentration ($1/cm^3$) averages (arithmetic mean) over the TCTC are shown on the right side of Figure 4.2. With the DED sampling and CPC (Figure 4.2a), the DOC reduced total particle number concentration/emission ($D_p > 2.5$ nm) by 17.7% and the DOC & SCR by 50.8%. The particle number reduction rates were larger with the PTD sampling (Figure 4.2b), 82.5% for the DOC and 95.7% for the DOC & SCR. The standard deviation of concentrations was significantly the largest with the PTD & DOC, ~80% of the average number concentration – otherwise the deviation was 25–40% of the average concentrations.
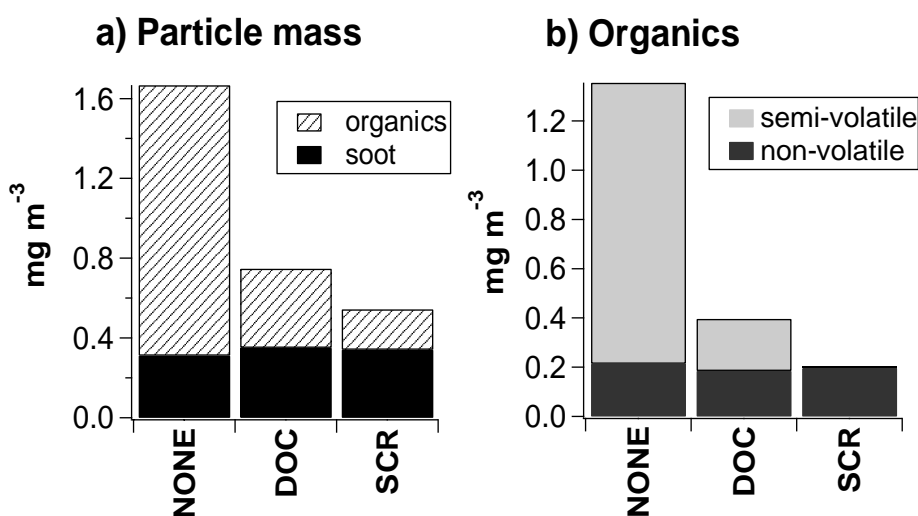

Figure 4.3: The effect of aftertreatment on the mass concentration and chemical composition (a) and the volatility of organics (b) in submicrometer particles (**Paper 1**). In (a) "organics" means total organics measured by the ACSM. In (b), "semivolatile" organics indicates the fraction that is reduced by the TD and "nonvolatile" organics the fraction that remains in the particle phase after the TD treatment.

Without exhaust aftertreatment, the exhaust particles were on average mostly composed of organics and soot, measured by the ACSM and MAAP, respectively. The mass concentration as well as the chemistry of particles changed due to the use of exhaust aftertreatment. Without aftertreatment, the fraction of organics dominated the submicrometer particle mass (81%; Figure 4.3a). Organic compounds were oxidized in the DOC and SCR so that their contribution on mass emission reduced to 53% after the DOC and 37% after the SCR. The amount of soot remained the same after the DOC and SCR. After the SCR, the concentration of total organics was 15% of that without the aftertreatment, and soot constituted a larger portion of the particle mass (63%) than organics. The concentrations of particulate inorganic components (nitrates, sulfates, ammonium and chlorides) were below the detection

limit of the instrument.

The volatility of organics was investigated by using the TD. The organics was found to be less volatile when the measurement was performed downstream of the aftertreatment devices. Without aftertreatment, most of the organics were semivolatile (84%; Figure 4.3b). After the DOC, organics consisted of nearly equal fractions of semivolatile and nonvolatile components (53% and 47%, respectively). The decrease in the total concentration of organics was caused dominantly by semivolatile components. After the DOC and SCR only a small portion (3%) of organics consisted of semivolatile compounds. After the DOC and SCR the concentrations of nonvolatile and semivolatile organics were 92% and 0.5% of those without the aftertreatment, respectively.
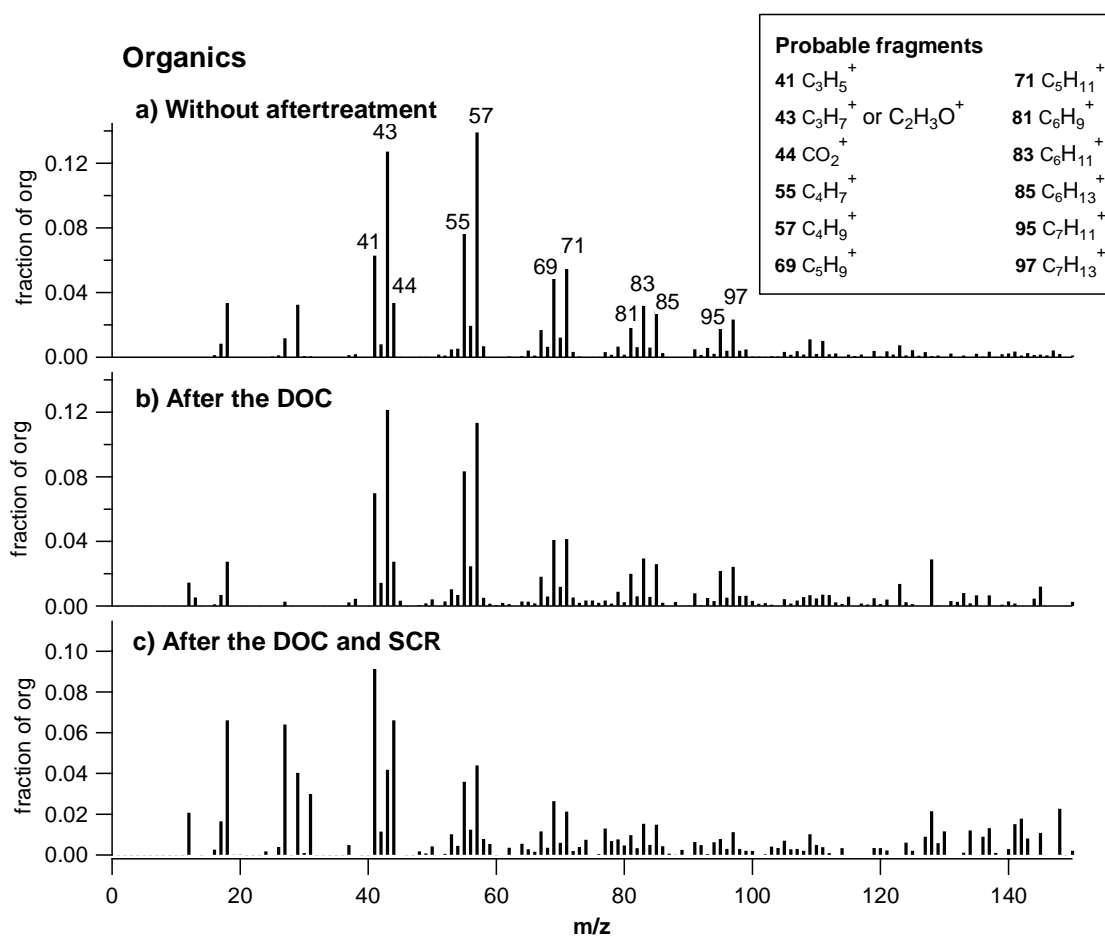

Figure 4.4: Organics mass spectra of Diesel 1 from the ACSM, average over the TCTC (**Paper 1**).

A more detailed characterization of the organic fraction in particle emissions was performed by investigating the mass spectra (MS) of organics with and without the ATSs (Figure 4.4). The MS of organics was similar without the aftertreatment and after the DOC

suggesting that the chemical composition of organics did not change significantly because of the DOC. The MS without the aftertreatment and after the DOC had the largest signal at m/z ratios of 41, 55, 57, 69 and 71, which are typical characteristics for primary vehicle emissions (Canagaratna et al., 2007). These m/z ratios are probably fragments from hydrocarbon compounds. There was also a pronounced peak at m/z 43 that could have been composed of both the hydrocarbon $C_3H_7^+$ and the oxidized component $C_2H_3O^+$. In the MS of organics, m/z 44 is mostly composed of the CO_2^+ ion. This CO_2^+ ion is formed from organic acids, which are the most oxidized chemical species in particles. The ratio of m/z 44 to the total signal of organics can be used to estimate how oxidized the organic matter is (Ng et al., 2010). In this study without exhaust aftertreatment and after the DOC, m/z of 44 had a fraction of $\sim$3% of the total organics signal. That is a very low fraction indicating that the oxidation state of organics was low, which is unexpected for the measurement downstream of the DOC. According to Ng et al. (2010), the fraction of $\sim$3% of m/z 44 corresponds to a ratio of $\sim$0.2 for oxygen to carbon atoms meaning one oxygen atom corresponds to five carbon atoms. The MS after the DOC & SCR differed from the MS without the aftertreatment and after the DOC (Figure 4.4). Organic compounds were clearly more oxidized after the DOC & SCR ($\sim$7% fraction of m/z 44). The same hydrocarbon peaks were observed in the MS after the SCR & DOC, and m/z of 41 (most likely $C_2H_5^+$) was even larger than for the MS without the aftertreatment and after the DOC. However, the total concentration of organics was very low after the DOC & SCR, and therefore the uncertainties associated with the MS are large.

4.2.2   Modern gasoline vehicles

This section focuses on the particle emissions of GDI vehicles that are associated with the combustion of fuel (**Paper 4**).

Laboratory study

Time-resolved particle emissions of the test vehicle (GDI 2) were determined from the measured exhaust particle concentrations by taking into account the simultaneous exhaust mass flow rate. Averaged temporal particle emissions (particles per second, 1/s) with standard deviations are shown in Figure 4.5 over the whole NEDC. Results for the UCPC (a), the ELPI (b) and the EEPS (c) are shown separately so that total size range for each instrument is considered. The emissions for particles larger than 23 nm in diameter (d) and the particulate mass emissions (e) are shown too, both calculated from the size distributions measured using the EEPS. Mass emission was calculated for particles in the size range of 5.6–560 nm assuming spherical particles with a density of 1 g/cm^3. Overall, the instruments showed very good repeatability between the NEDCs with an exception that the standard deviation was relatively high during the last 100 seconds of the NEDC. In general, particle emissions depended a lot on the driving condition; e.g. at the end of idle modes the concentration

level was low, in the particle size range covered by the ELPI and the EEPS even near zero if the detection limits of the instruments are taken into account, while during accelerations the particle number emission increased to high values, at the first accelerations of the NEDC even larger than 10^{12} 1/s.

Table 4.1: Total particle number emission factors (1/km) for GDI 2 during the UDC, EUDC and NEDC, measured using the UCPC, ELPI and EEPS. Emission factors for particle number above 23 nm in diameter (EEPS, $D_p > 23$ nm) and for particulate mass (EEPS, mass) were calculated from the EEPS data. TD indicates the measurement with the thermodenuder. (**Paper 4**)

Instrument	UDC	EUDC	NEDC
UCPC (1/km)	6.87E+12	1.55E+13	1.23E+13
UCPC (1/km), TD	7.33E+12	4.58E+12	5.60E+12
ELPI (1/km)	5.64E+12	7.36E+12	6.73E+12
ELPI (1/km), TD	6.84E+12	3.23E+12	4.56E+12
EEPS (1/km)	5.54E+12	1.04E+13	8.58E+12
EEPS, $D_p > 23$ nm (1/km)	3.92E+12	1.75E+12	2.55E+12
EEPS, mass (mg/km)	0.436	1.29	0.751

In addition to time-resolved emissions, the particle number (1/km) and mass (μg/km) emission factors were determined for the Urban Driving Cycle (UDC) and Extra-Urban Driving Cycle (EUDC) as well as for the whole NEDC. These can be seen in Table 4.1. When looking at the combustion generated nonvolatile particles (TD), in general, the emissions were higher during the UDC than the EUDC. In fact, the TD treatment did not affect significantly the particles during the first 1100 s of the NEDC, as can be seen from Figure 4.5. The emission of particles larger than 23 nm, obtained from the EEPS data, was higher during the UDC compared to the EUDC. The overall emission of these particles was about 2.5×10^{12} 1/km. In the perspective of the European legislation, the upcoming Euro 6 level for GDI vehicle particle number will start at 6×10^{12} 1/km and after three years will be 6×10^{11} (Dieselnet, 2014). So the emission level of the vehicle tested is somewhere between these limits. However, one must bear in mind that the official measurement protocol differs from the measurement method here.

Figure 4.6 shows the raw exhaust particle number size distributions (a) and size-segregated emissions (b). The particle size distributions were bi-modal under acceleration and steady speed conditions; the geometric mean diameter (GMD) of the smaller particle mode was ∼10 nm, while for the larger mode the GMD was ∼70 nm, according to the EEPS data.
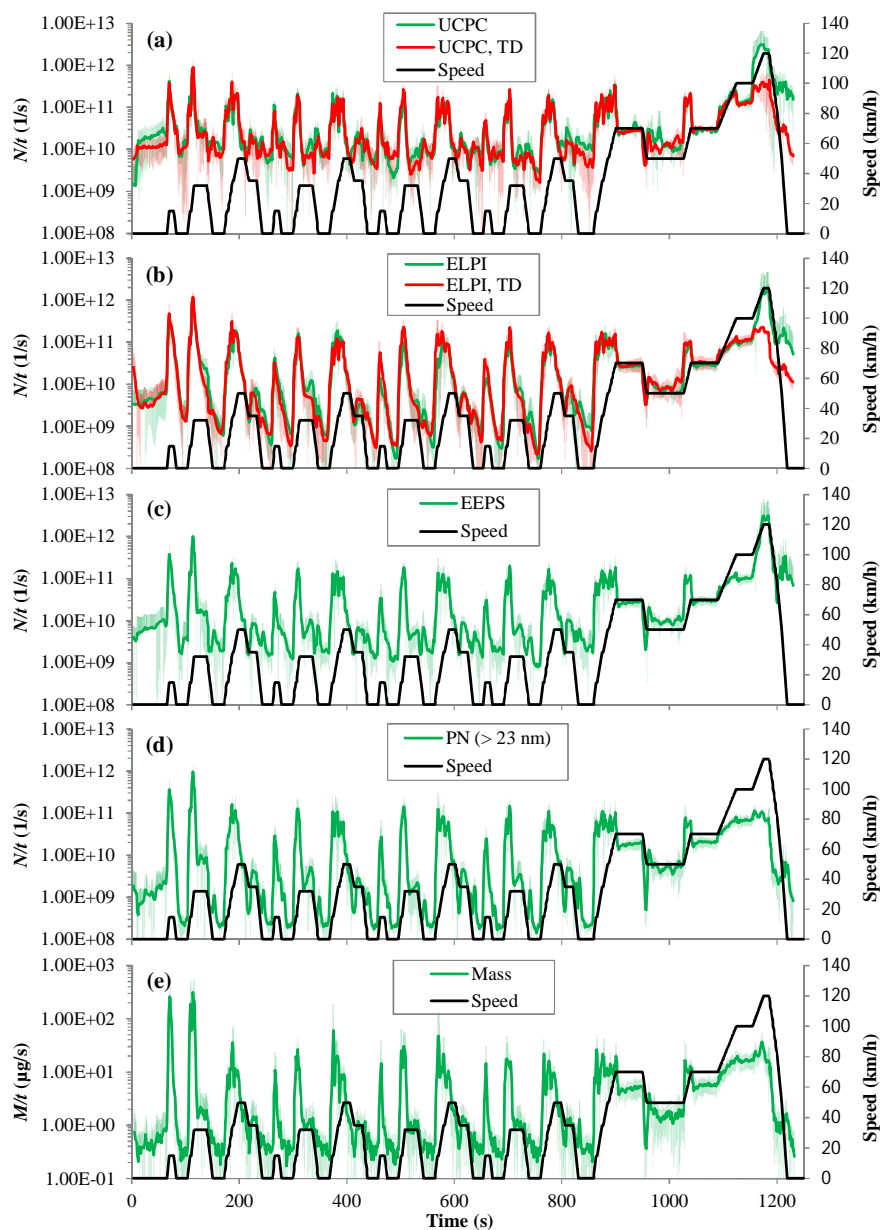
Figure 4.5: Time series of particle emissions over the NEDC cycles for (a) particle number measured with the UCPC (with & without TD), (b) number with the ELPI (with & without TD), (c) number with the EEPS (only without TD), (d) number of particles over 23 nm calculated from the size distributions measured by the EEPS and (e) particulate mass, also calculated from the EEPS data. The "shadowed" area indicates the standard deviation. (**Paper 4**)

During accelerations, i.e. when the engine was most heavily loaded, the concentrations of larger particles were typically higher than concentrations in the smaller particle mode.

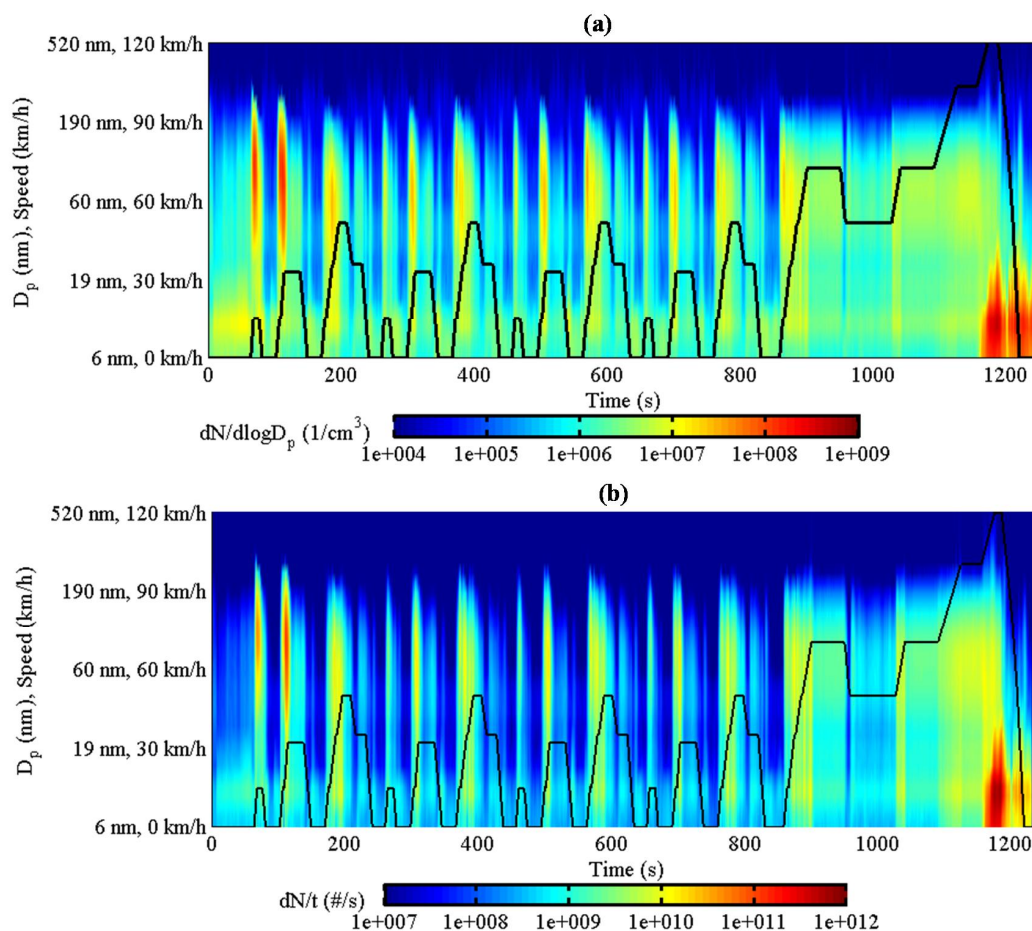Figure 4.6: Mean particle size distributions measured by the EEPS during the NEDC cycle (8 repetitions) in terms of (a) dilution ratio corrected particle concentrations (dN/dlogDp) and (b) particle emissions per second (dN/t). Black line shows the wheel speed profile. (**Paper 4**)

In order to confirm the observations from transient driving, the size distributions were also measured under steady state driving conditions (speed 80 km/h, wheel powers 5 kW, 10 kW and 20 kW), with and without the TD. These can be seen in Figure 4.7. It can be concluded that the TD treatment (at 265 °C) did not cause any significant change in the size or number of the exhaust particles in the particle size range measured by the ELPI. The TD particle loss correction (Heikkilä et al., 2009) was applied to the size distribution measured through the TD with unit density (1 g/cm^3) assumption.

On-road study

The on-road study of particle emissions of GDI 3 was conducted under conditions with very low particle concentrations in ambient air making it possible to also study a low emitting
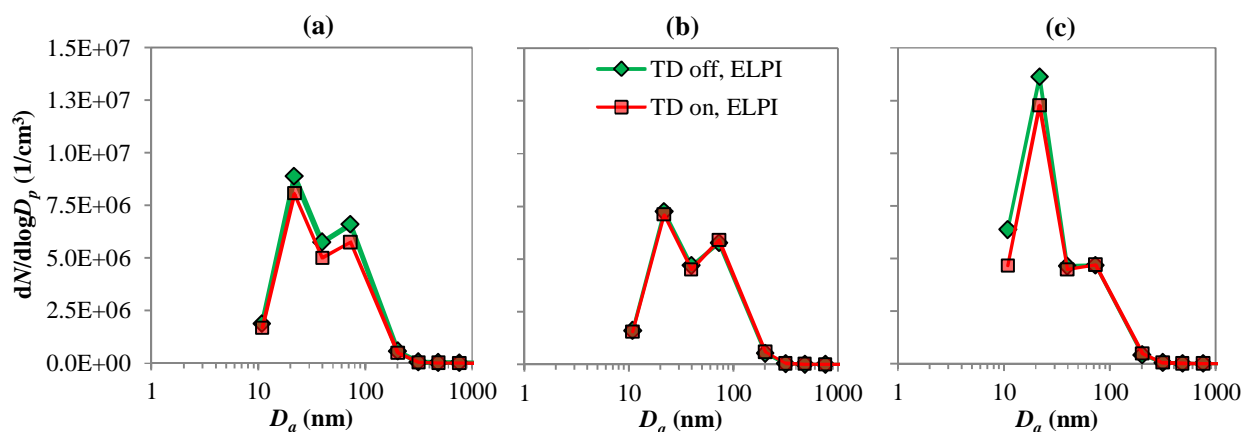
Figure 4.7: Effect of thermodenuder treatment (TD at 265 °C) on the exhaust particle size distributions measured by the ELPI at steady state driving modes: (a) 5 kW, (b) 10 kW and (c) 20 kW. (**Paper 4**).

vehicle. Measurements were made in order to see the effects of on-road driving conditions and exhaust dilution on particle emissions but also to verify the particle concentrations and characteristics in the real exhaust plume. Because of the differences in technology between GDI 1–3, an exact and quantitative comparison to the laboratory results is not meaningful or even possible. Qualitatively, results largely confirmed many findings of the laboratory study.

The on-road study consisted of steady speed (low load) tests and transient acceleration/deceleration routines. At constant speeds, the total particle concentrations in the exhaust plume were at the background concentration level ($\sim$2000–3000 $1/cm^3$) indicating extremely low concentrations of engine out soot particles. Conversely, in the transient tests the particle emissions were significant during accelerations (Figure 4.8a). The highest particle concentrations were observed during accelerations where the total number concentrations of the exhaust plume reached the level of 40000–50000 $1/cm^3$, which is about 20-fold higher compared to the background aerosol. During accelerations, the plume particle concentration closely followed the trends of CO_2 concentrations. To give a rough estimation for exhaust emission factors by estimating the dilution ratio from CO_2 concentrations of diluted sample and raw exhaust during 70 km/h constant speed and taking account the exhaust flow rates, the number emission factor was 7.7×10^{11} 1/s. Looking at the results from different accelerations in Figure 4.8b, it can be seen that the increased engine torque and lower engine speed increased the particle number concentration in the exhaust plume; when accelerating from 30 km/h to 70 km/h the concentrations were larger in 3rd gear than in 2nd gear.

During accelerations the particle size distributions were measured with the ELPI. Results of maximum concentrations of accelerations from 30 to 90 km/h are shown in Figure 4.9. Similarly as in the laboratory study, the particle number size distribution was dominated
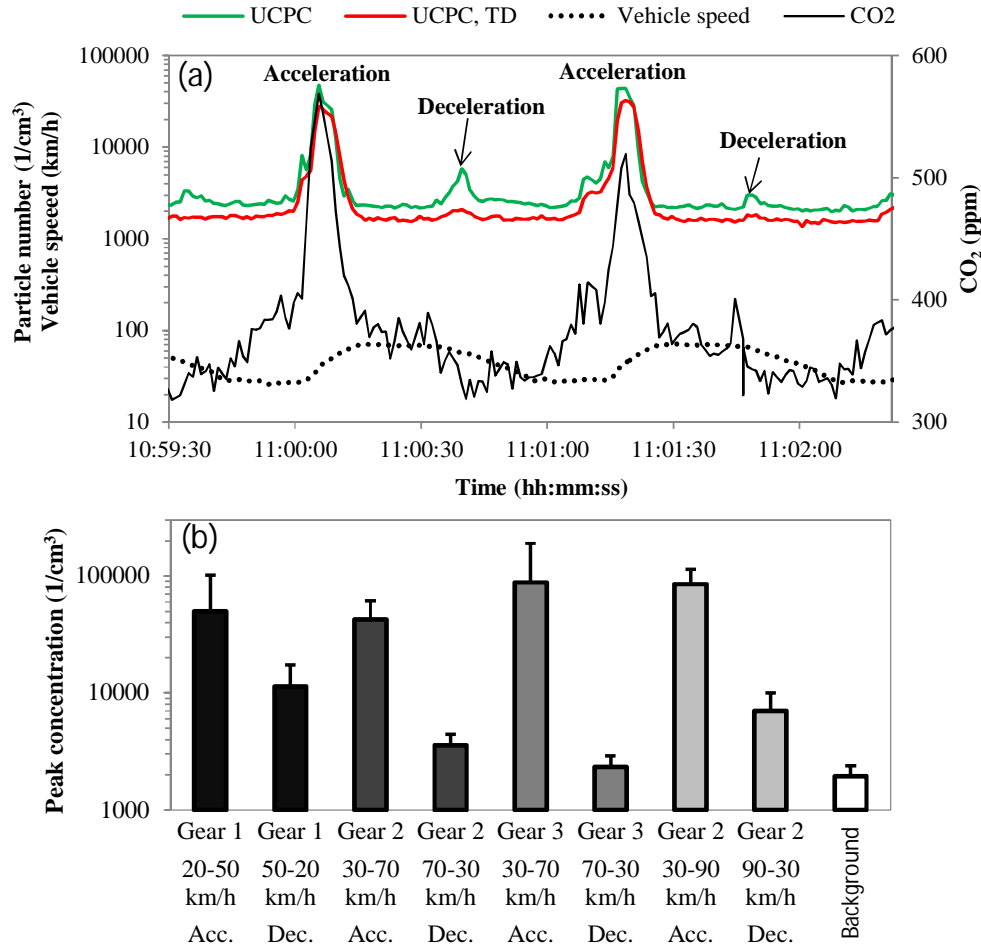
Figure 4.8: Total particle number (UCPC), nonvolatile particle number (UCPC, TD) and CO_2 concentrations in the exhaust plume of GDI 3 during the acceleration and deceleration routine between 30 km/h and 70 km/h (2nd gear) (a). Exhaust plume total particle concentrations (UCPC measurement) during accelerations and decelerations in the on-road experiment (b). Error bars indicate the standard deviation (only mean+stdev) of mean concentrations between several consecutive tests. Also, the background aerosol concentration is shown. (**Paper 4**)

by ultrafine particles. The mean size of the emitted particles was approximately 20 nm for the ELPI. In addition, the bi-modality of the particle size distributions was observed during certain acceleration; however, not as clearly as in the laboratory experiments (Figures 4.6 & 4.7).

Figure 4.9: Particle number size distributions during the repetitions of acceleration tests from 30 km/h to 90 km/h. Background aerosol size distributions were measured a few minutes after the test on the same test road. (**Paper 4**)
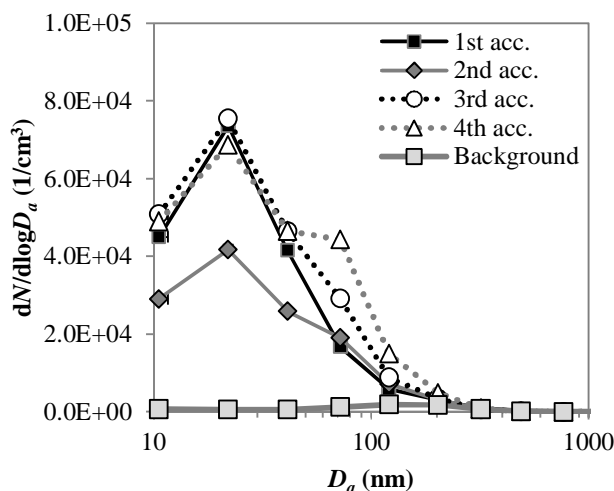
4.2.3 Discussion

The study of Diesel 1 (**Paper 1**) focused on particles during a transient test cycle. One must keep in mind that these measurements were performed mostly at low engine loading. However, the test cycle used covers a very typical scenario of the use of this commercial engine type. Currently, HD nonroad diesel engines do not need to apply particle filters mandatorily. The results indicate that the particle emission downstream of the DOC & SCR (which is also the real configuration, in real use) is mainly nonvolatile soot with low level of semivolatile components on the surface. The use of the DOC & SCR seemingly had a major advantage when NM particles are of concern. Phenomena in particle formation can differ from those of the steady state driving modes, but overall, phenomena during transient test cycle are thought to cause higher and more realistic engine-out soot and HC emissions due to non optimal combustion conditions.

Results indicate that soot particle concentrations and BC emissions were not affected by the ATS which was also the assumption before the measurements. Rather, the exhaust aftertreatment significantly affected the semivolatile particle compounds — NM particle emission and concentrations; the semivolatile compounds on soot particles were also affected. These semivolatile compounds were mostly organics. The organics in the particle phase were reduced efficiently due to the use of the DOC and especially the DOC & SCR. One should note that the effect of the ATS on organics was qualitatively similar to the effect on the NM particle number. Thus, organics seem to have a role in NM particle size and detectable NM particle number. This is in line with the results from previous studies (e.g. Rönkkö et al. (2007)) where the NM particle growth has been strongly affected by hydrocarbon compounds,

although the studies in **Paper 1** cannot confirm or exclude the role of the hydrocarbons in the nucleation process.

Also, there was not any indication of promoted nucleation caused by excess ammonia due to the use of the SCR, which is also considered to be possible (Lemmetty et al., 2007). On the contrary, there is an indication that undiluted exhaust carried NM core particles smaller than 7 nm in size. According to the literature, high NM particle concentrations without exhaust aftertreatment can be explained by the existence of core particles in raw exhaust gas (Rönkkö et al., 2007; Filippo and Maricq, 2008; Lähde et al., 2009). It appears that engine out core particles from Diesel 1 were removed to some extent in the DOC & SCR system, especially in the SCR where small particle diffusion collection can be efficient due to the relatively large volume of the SCR catalyst.

For modern gasoline engines the role of accelerations was dominant in nonvolatile particle emissions (**Paper 4**). Notwithstanding that, under steady combustion combustions the latest technology vehicle GDI 3 produced no detectable soot particles, and for GDIs 1 & 2, the concentrations were significantly higher during accelerations compared to constant speeds. Unlike in diesel exhaust, the nature of soot particle size distributions was different – the nonvolatile SM was bi-modal in the case of GDI, which has also been reported by Barone et al. (2012), for example.

The real-world study of GDI 3 conducted on the road shows that the observations in laboratory are relevant also from the viewpoint of the real emissions of GDI vehicles. It should be noted that, overall, the GDI technologies are diverse, even more diverse than PFI or diesel, with multiple degrees of freedom in how to choose the parameters of operation. Differences in technologies and operation parameter choices and as well as in drivers' behaviors can lead to different emission profiles than reported here.

The upcoming legislation limits for PN of GDI vehicles will enforce modifications for technologies related to gasoline engines. Based on the results, a combination of PFI and GDI technologies, as in GDI 3, can be advantageous when the limited solid particle number is considered. The legislation will focus only on solid particles larger than 23 nm in diameter. There is an indication that a major share of solid particles in the modern gasoline vehicle exhaust can be below this particle size limit. If the future PN limit is achieved by adding particle filters, then there should not be any problems in removing the nonvolatile sub-23 nm particles at the same time.

4.3   Sulfur driven nucleation with an oxidative ATS

Sulfur processes can significantly affect the NM formation when the exhaust temperature in the oxidative aftertreatment system is high enough. Semivolatile NM particle emissions were studied in **Papers 2 & 4**.

4.3.1 Nucleation mode formation and particle properties

The SO_2–SO_3 conversion in the aerosol laboratory study of **Paper 2** was a function of temperature; at 220 °C the conversion was below 5% but when the temperature was increased up to 400 °C the conversion increased up to 50% (Figure 4.10a). The measured NM concentration (N) in Figure 4.10a and size distributions in Figure 4.10b followed the increasing trend of the SO_2–SO_3 conversion. The SO_2 concentration (Figure 4.10c) had a similar effect to the temperature (Figure 4.10b) on particle size distributions. The higher the concentration or temperature were, the more and the larger the NM particles detected.
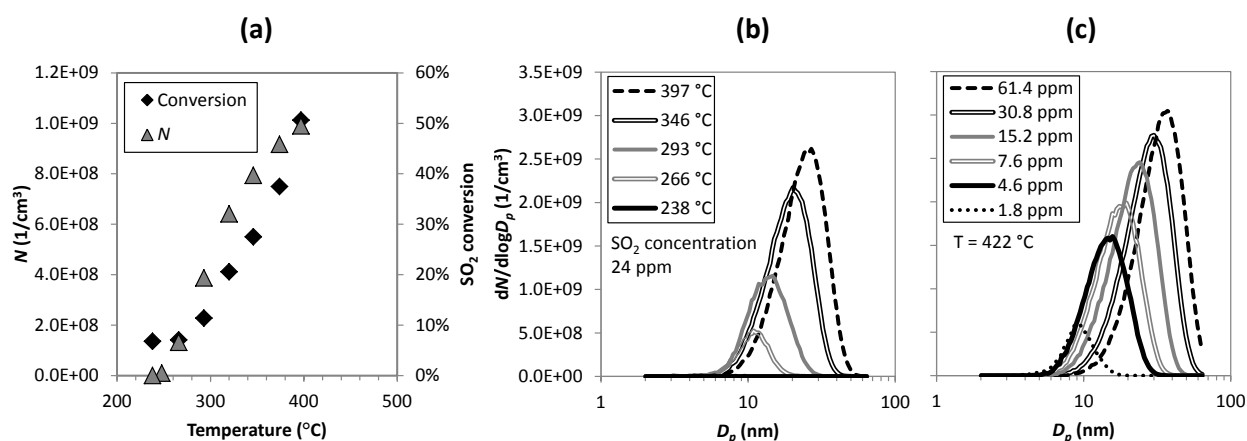

Figure 4.10: Sulfur driven nucleation mode formation in the aerosol laboratory tests (**Paper 2**). The effect of pre-pDPF gas temperature on particle concentration (N) and SO_2 conversion rate in (a), the effects of SO_2 concentrations and temperatures in NM size distributions (Nano-SMPS) in (b) and (c), respectively.

The NM was observed to completely vanish in the TD treatment, which is in line with results from previous studies (Filippo and Maricq, 2008; Lähde et al., 2009; Burtscher, 2005). The state of charge of the particles was measured in the aerosol laboratory study, and the particles were observed to be electrically neutral which, again, is in line with the results from earlier engine exhaust studies (Maricq, 2006; Lähde et al., 2009). This indicates that NM particles were formed during the dilution with cool air, not in the hot test gas before that. In this case, there was no detectable NM when the catalyst temperature was below 250 °C.

4.3.2 Storage and release of sulfur

In the aerosol laboratory study of sulfur storage and release (**Paper 2**), the NM was not observed immediately after the increase in temperature (Figure 4.11a). However, when the air temperature increased enough, NM particles were formed so that the particle number and size reached a maximum after eight minutes from the time the heater was set to increased
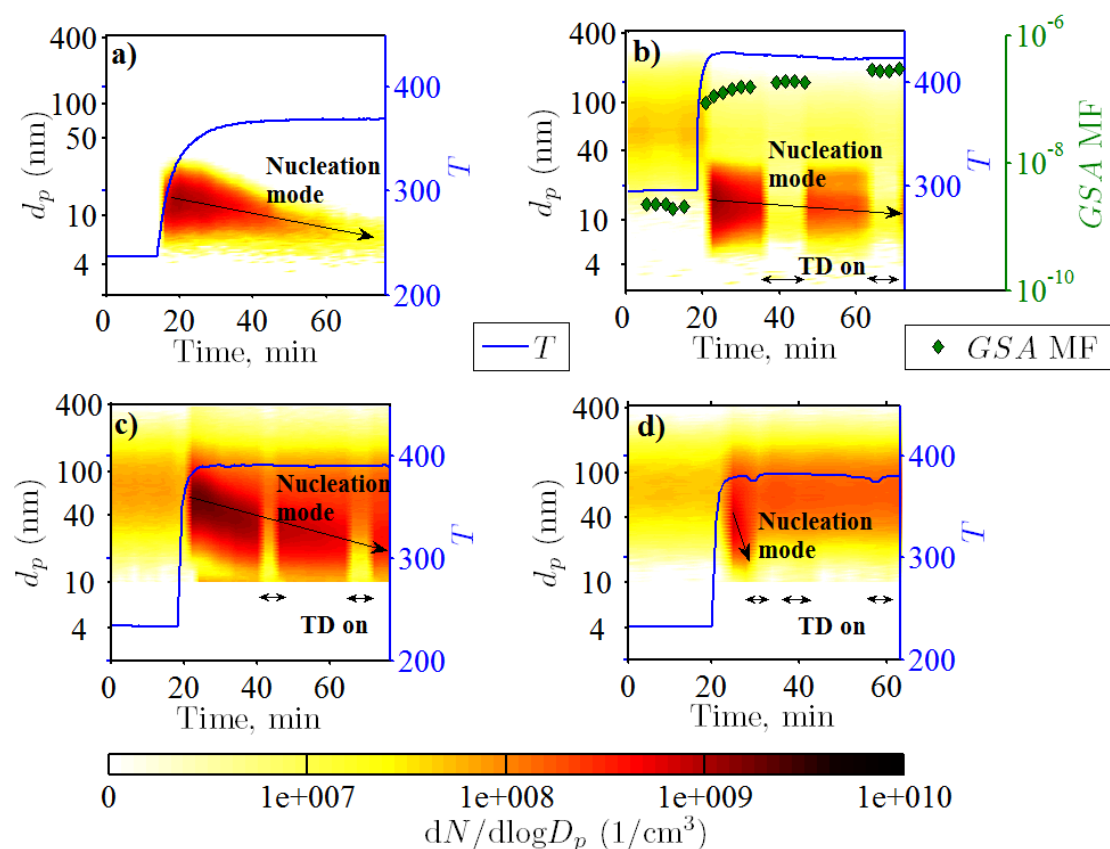
Figure 4.11: Sulfur driven NM formation when higher temperature phase followed low temperature phase (**Paper 2**). The aerosol laboratory experiment in (a) (Nano-SMPS), heavy-duty engine laboratory with FSC = 6 mg/kg in (b) (Nano-SMPS + SMPS) the GSA concentration is also shown, and light-duty engine laboratory tests in (c) for FSC = 340 mg/kg (SMPS) and (d) for FSC = 65 mg/kg (SMPS). Double-ended arrows (TD on) indicate the periods when the diluted exhaust was fed through the thermodenuder system (heated to 265 °C).

power. After that, both the particle concentration and the particle size decreased and reached the zero level after 45 minutes from the beginning of the high temperature phase. Both in the HD (Figure 4.11b) and LD (Figure 4.11c, 4.11d) engine experiments, the NM particle concentration increased from zero to very high values instantly after the increase in the engine load and reached the maximum value within a few minutes. After that, the particle concentrations decreased gradually and stabilized. The FSC had an effect on NM particle concentrations and the NM stabilization time in the LD engine experiments. The NM was present for about 8 minutes with a FSC of 65 ppmw (Figure 4.11c), whereas with a FSC of 340 ppmw (Figure 4.11d) the already stabilized NM was detected after one hour during the high temperature phase. This experiment was also repeated with a FSC of 6

ppmw, but without the observation of NM particles. A longer loading time or a higher temperature regeneration would have been needed for the NM formation with a fuel meeting the European standards (EN590). In all the engine experiments, the TD treatment removed the NM particles, so that solely the SM was left.

Thus, merging together the aerosol laboratory and engine exhaust studies, the results show that sulfur compounds can be stored on the catalyst substrate, and when the catalyst temperature is increased, the sulfur compounds can be released in a form capable to initiate the NM particle formation. This is possible even with ultra-low sulfur diesel fuel (< 10 ppmw of S) in the case of a HD engine. However, in the measurements with a HD diesel engine (Figure 4.11b), the concentration of gaseous sulfuric acid (GSA), measured downstream of the heated ejector diluter by a CIMS, did not follow the temporal behavior of NM number or size. Instead, the GSA concentration increased relatively rapidly to a mole fraction level above 10^{-7} and after that increased slowly through the remaining test period. Thus, although the change in engine load affected the GSA as reported before, higher load causes higher GSA concentration to the exhaust (Arnold et al., 2012; Rönkkö et al., 2013). This result indicates that the NM particle bursts caused by sulfur storage and release are not caused by the GSA. Actually, the initial nucleation process may still have been caused by the GSA, but the NM particle size and number did not correlate with the GSA concentrations.

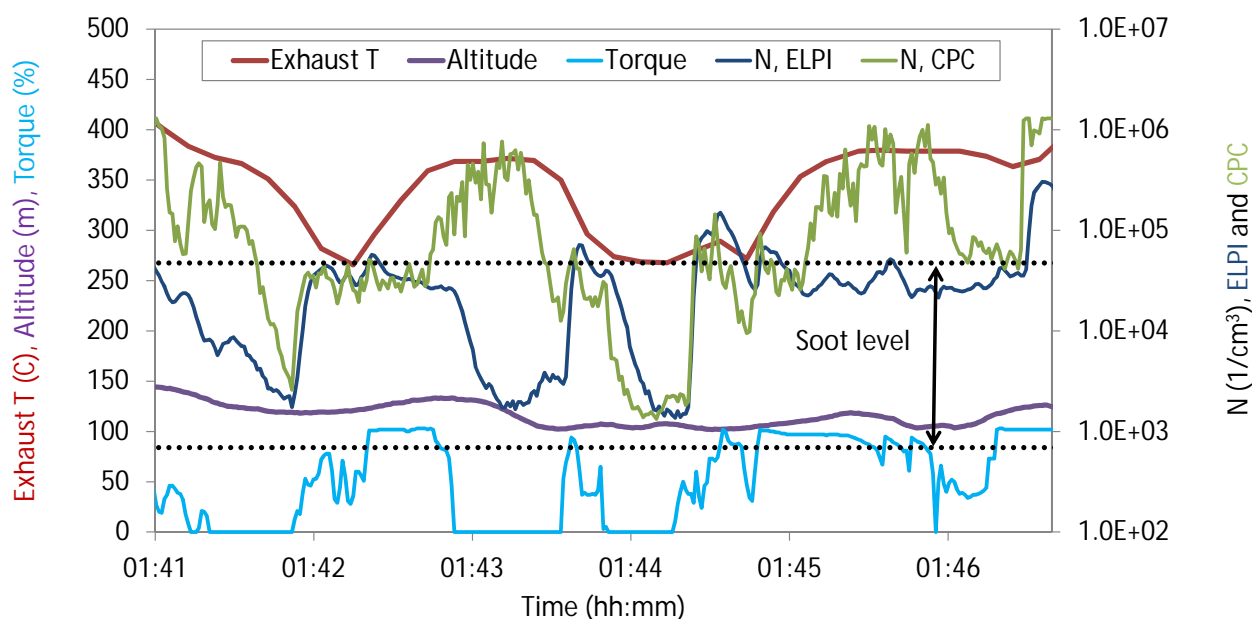Figure 4.12: Example of time-series of the on-road truck chasing study from **Paper 2**, about 250 km from the terminal in Oulu. Dotted lines represent the maximum and minimum soot concentrations, measured through the TD, during the whole test route.

In the on-road experiments of Diesel 4 equipped with a DOC & pDPF (Paper 2), the particle concentration of the exhaust plume (no DR correction) measured by the UCPC

varied over about 3 orders of magnitude (Figure 4.12). The highest concentration peaks were observed during uphill driving and at the hilltop when the exhaust temperature was above 350 °C. Measured through the TD, the particle concentration was 5×10^4 1/cm^3 at maximum during a 15-min-period over a hilly section of the route. In the particle size distribution, these particles formed a typical SM. Without the TD, the concentrations even reached a level over 1×10^6 1/cm^3.

Occasionally, the NM particles formed were smaller than 7 nm in aerodynamic diameter, so that the ELPI was unable to detect them, but the UCPC was able to see an NM peak. It can be seen from Figure 4.12 that when the truck was going downhill and the demanded torque was 0% (at ∼1:43 AM), the exhaust temperature remained at a high level (375 °C). This is mainly due to the heat stored in the engine and exhaust system. The particle concentrations measured by the ELPI decreased, but simultaneously, particle concentrations measured by the UCPC increased. The measuring range of the ELPI is limited to $D_a =$ 7 nm and the range of the UCPC to $D_p = 2.5$ nm. Similar behavior was never observed following the TD treatment of the exhaust sample. Thus, the measurements indicate that there was an increased amount of particles below the detection limit of the ELPI, particles were semivolatile NM particles, and that the precursors of particles did not originate directly from the combustion of fuel. It should be noted here that during downhill driving, fuel was not injected into the combustion chambers, and that the downhill driving was conducted systematically with engine braking without the use of wheel brakes.

During an 80 km long relatively hilly test section, the fraction of nucleation particles was calculated to be 60% of total particle number emissions. The calculation is based on particle concentrations measured by the ELPI so that the TD was used over half of the test section, and the nonvolatile particle losses in the TD were taken into account. For the UCPC, the TD loss correction is not possible. However, the results shown in Figure 4.12 indicate that a significant fraction of particles was in the particle size range below 7 nm. Thus, if the smallest (< 7 nm) particles are also taken into account, the fraction of semivolatile particles may be significantly larger than 60%.

4.3.3 Semivolatile particle emissions from gasoline vehicles

Looking back at time-resolved particle emissions of the test vehicle (GDI 2) in Figure 4.5 over the whole NEDC in terms of semivolatile particles, the particle emissions measured by the ELPI and the UCPC were strongly decreased, about an order of magnitude, by the TD treatment when the vehicle speed was over 100 km/h. At the highest speeds, the particle emissions measured by the UCPC without the TD treatment were higher than the ones measured by the ELPI and the EEPS, which indicates that a significant fraction of the emitted particles was 2.5–6 nm in diameter. Size distributions measured by the EEPS (Figure 4.6) indicate a very large concentration of sub-20 nm particles with a GMD of ∼10 nm. Similarly, during the 20 kW steady driving mode (at 80 km/h), there was a significant number of semivolatile NM particles. This was seen as a decrease in the concentration

measured by the UCPC when the sample was passed through the TD (not plotted). In that case, the NM particles were below 6 nm, since they were not detected by the ELPI when measured simultaneously.

In general, the total particle number emission factors were smaller during the UDC compared to the EUDC when the semivolatile particles were included in the numbers, i.e. the measurement was conducted without the TD (Table 4.1). Thus, when the results are studied from the viewpoint of distance traveled, the measurement shows that the semivolatile particles were emitted mainly during the EUDC phase of the NEDC (higher speeds).

The emission of these small and semivolatile particles also depended on the driving history. This was seen, for example, when the particle emissions over the EUDC were studied from one NEDC to another. During the first EUDC the particle emission measured by the UCPC without the TD was 3.0×10^{13} 1/km, in the following EUDCs it was 2.3×10^{13} 1/km, 5.0×10^{12} 1/km and 4.5×10^{12} 1/km. The emission of these small semivolatile particles was related to the occurrence of high exhaust gas temperature (above 700 °C in the catalyst). Because the driving history also affected the emissions, the formation of these particles seems to be caused by the release of semivolatile compounds from the aftertreatment system, engine or exhaust line surfaces.

The semivolatile particle mode was not observed during the on-road tests of GDI 3, where the maximum vehicle speed was limited by the mobile laboratory (90 km/h) and the engine loading was relatively low. If higher engine loading and thus higher exhaust temperatures are achieved in the on-road testing e.g. driving on a freeway or uphill, semivolatile NM formation is also expected.

4.3.4   Discussion

Sulfur, originating from the fuel or from the lubricant, seems to be the driving force in semivolatile NM formation. However, the semivolatile NM formation requires an ATS with oxidation potential and high enough exhaust temperature. In the studies of **Papers 2 & 4** semivolatile NM particles were detected, but in the studies of **Paper 1** there was no observation of sulfur driven NM formation, most likely due to relatively low exhaust temperature during the test cycle (232–246 °C). For instance, at temperatures above 380 °C, the SCR has previously been observed to increase NM particle emissions (Thiruvengadam et al., 2011; Herner et al., 2011). Note however that direct comparison of NM particle results between different dilution techniques is difficult since the particle formation is highly sensitive to how the sampling and dilution have been executed.

The results from the aerosol laboratory study **(Paper 2)** supported the earlier observations in engine exhaust studies that the formation of semivolatile and uncharged NM is a sulfur driven process, and therefore no evidence of ion-induced nucleation during the cooling and dilution was observed. The aerosol study was performed using only filtered air–SO_2 mixtures, and the results indicated that the NM formation did not require compounds such as hydrocarbons, sulfated hydrocarbons, or salts. However, in a larger perspective, in real

applications the NM size, number and particle properties are sensitive to nonvolatile particle and condensable hydrocarbon concentrations, and also to changes in gas humidity.

With a DOC or a DPF, the formation of semivolatile NM particles has been associated with moderate or high FSC and high load conditions (Vaaraslahti et al., 2005; Arnold et al., 2012; Maricq et al., 2002; Giechaskiel et al., 2007; Rönkkö et al., 2013; Vogt et al., 2003; Lähde et al., 2009; Schneider et al., 2005). In addition, it seems that at high load and during DPF regeneration nucleation can occur even with ultra low FSC fuels (Arnold et al., 2012; Uhrner et al., 2007; Wehner et al., 2009). With the combination of a DOC and a pDPF, the semivolatile NM particle formation was qualitatively similar, as previously reported for the DOC or the DPF. The NM was not observed at low load; but at medium load, the NM was observed with ultra low sulfur diesel fuel for a HD engine (Diesel 2), but not for the LD engine (Diesel 3). In addition, this result is dependent on the driving history, engine oil sulfur level, oil consumption, and the temperature during regeneration. For instance, during regeneration the temperature was higher for the HD engine compared to the LD engine. Oil consumption may also vary significantly between different engine types, technologies and ages.

Similarly, for a modern LD gasoline vehicle (GDI 2, **Paper 4**) semivolatile and history dependent NM was present when the exhaust temperature was over 700 °C. This NM formation is also considered to be sulfur driven. Comparing gasoline and diesel technologies, it appears that much higher exhaust temperatures are needed for gasoline vehicles to generate transient NM emissions. This can be affected – for instance – by different catalyst types and materials, as well as the totally different range of semivolatile components in the exhaust. In general, the hydrocarbons that form gasoline fuel are smaller and more volatile than the hydrocarbons found in diesel fuel.

The aerosol laboratory study **(Paper 2)** produced strong evidence that the sulfur compounds were stored within the pDPF and that the storage-release and its effect on NM are not measurement artifacts caused by, for example, sulfur storage in some part of the exhaust sampling system. The engine laboratory studies showed significant emissions of NM particles when the driving condition changed from a low load to a high load. This effect was more intensive when the FSC was higher. Although this behavior seems to be sulfur driven, the NM formed cannot be explained only by the GSA. For instance, hydrocarbon compound storage, release and chemical transformation (like partial oxidation or formation of organosulfates (Arnold et al., 2012)) in exhaust aftertreatment systems cannot be excluded in NM formation during transients. It has to be noted that in general, in engine exhaust studies, the sulfur or hydrocarbon compound storage and release in the exhaust sampling lines may also affect the measured NM.

From total particle number emission point of view (including semivolatile particles), the storage and release of sulfur compounds is important; it seems that because of this process, the NM particles can dominate (over 60% of particles) particle number emissions, even with low FSC. It is arguable that the behavior is similar with other oxidative exhaust

aftertreatment systems like older technology containing solely a DOC, and state-of-the-art technologies: the DOC & DPF, the DOC & SCR and the DOC & DPF & SCR. When a DPF is applied, the emissions of NM particles can be even higher, because of lower soot particle emissions, and hence the lack of a condensation sink. In general, semivolatile NM particles are practically not considered in emission regulations, since the NM particle mass is moderately low due to small particle size, and also because they are not counted as PN in the Euro emissions standards. The particle number emissions of modern vehicles equipped with oxidative exhaust aftertreatment systems also seem to be very significant during downhill driving, due to the release of semivolatile compounds from the catalyst.

4.4   Particle emissions under engine braking conditions

An unexpected observation was made during the studies of **Papers 3 & 4**, namely that vehicle engines can emit nanoparticles while the vehicle is rolling with engine braking. For direct injection engines the instantaneous fuel consumption is zero. The following subsections discuss experimental findings of engine braking-related exhaust particles for a HD diesel truck and GDI passenger cars.

4.4.1   Heavy-duty diesel truck

Figure 4.13a shows a typical driving condition dependent exhaust particle number concentration recording over a half-hour driving sequence in a relatively hilly part of the test route near Jyväskylä. Interestingly, the highest particle concentration peaks were detected during downhill driving. The peaks were repetitive appearing throughout the downhill sections of the driving sequence. The CPC consistently measured higher number concentrations than the ELPI. During another drive when there was solely the SM present (no sub-7 nm particles), due to use of a pDPF (Heikkilä et al., 2009; Karjalainen et al., 2010), the concentration levels of both instruments were equal. Given the different size ranges of the two instruments (CPC and ELPI count particles larger than 2.5 nm and 7 nm, respectively) this indicates that the high particle concentrations during downhill driving (engine braking) are dominated by particles of size below 7 nm.

Figure 4.13b zooms in one example period of moderate downhill driving, where the speed control was achieved by engine braking without the use of the wheel brakes. As a result, the engine maintained speed but the torque produced by the engine was practically zeroed. The particle concentration in the 2.5–7 nm size range, estimated as the difference between the CPC and ELPI recordings, reached high levels directly after the engine torque dropped. Size distribution measurements also indicated the small size of particles formed during engine braking (Figure 4.13c). Practically, no SM ($D_p > 50$ nm) was observed during engine braking while the concentration of particles below 10 nm exceeded typical concentrations in normal operation. It should be noted that in normal operation the particle size distribution consisted
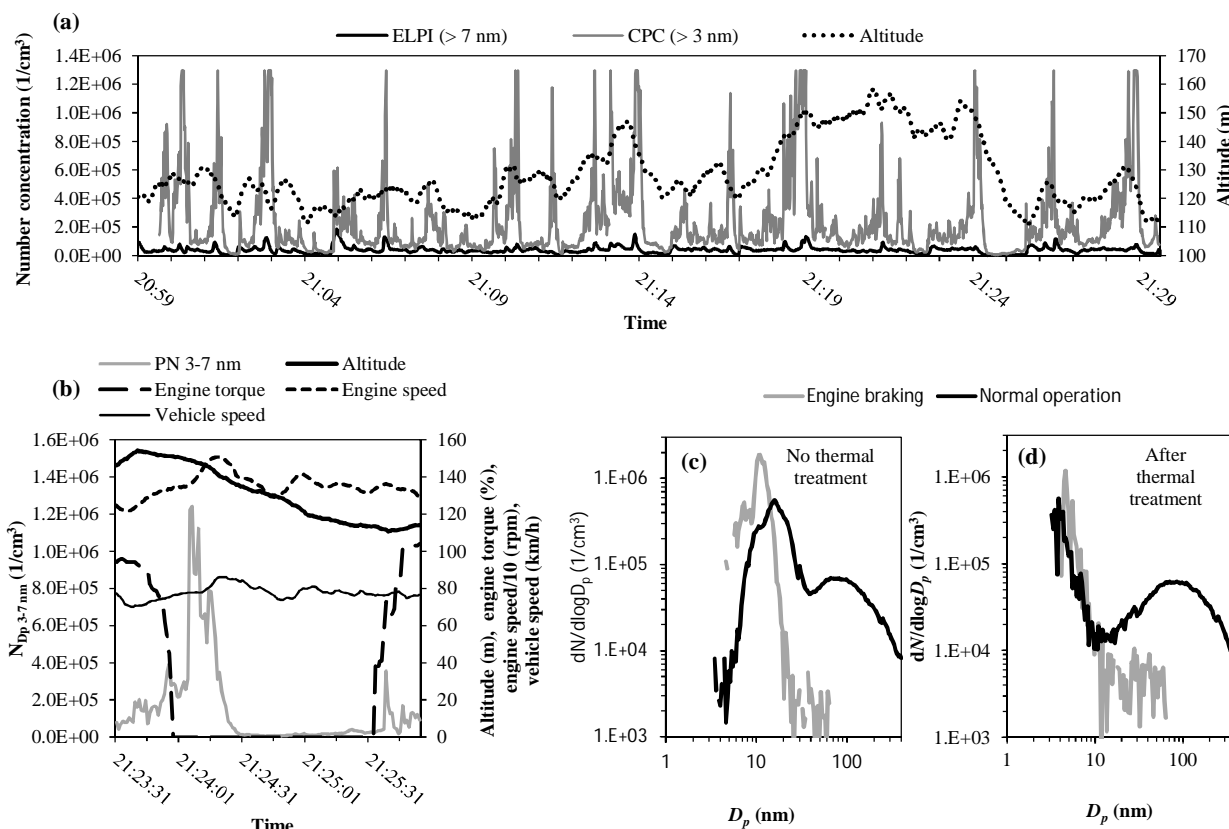
Figure 4.13: Particle concentrations and size distributions in the exhaust plume of a HD diesel truck. (a) Particle concentrations measured by an ELPI ($D_p > 7$ nm) and a UCPC ($D_p > 2.5$ nm) at variable road gradients. (b) Engine operation, altitude profile, and concentration of particles in the 2.5–7 nm size range (PN 2.5–7 nm) during downhill driving. (c) Particle size distributions measured by SMPSs under engine braking conditions and at normal operation. (d) Similar to (c), but conducted after the thermal treatment of the aerosol in the TD. Note that size distributions in parts (c) and (d) are indicative because of the low time resolution of SMPS instruments. (**Paper 3**)

of the SM and NM, as expected based on the results of other studies conducted with HD diesel engines and vehicles without exhaust aftertreatment (Rönkkö et al., 2007). Here, "normal operation" means driving flat part of the test route under modest torque conditions — mean values and standard deviations for vehicle speed, engine speed and engine torque were 78 ± 10 km/h, 1430 ± 85 rpm and $50 \pm 31\%$, respectively.

Thermal treatment (TD) had only a limited impact on the SM particles formed under normal operation conditions and significantly decreased the size of the NM particles (geometric mean diameter decreased from 10 nm to 4 nm) (Figure 4.13d). In contrast, the same thermal treatment had only a limited impact on particles formed during engine braking. Thus, the
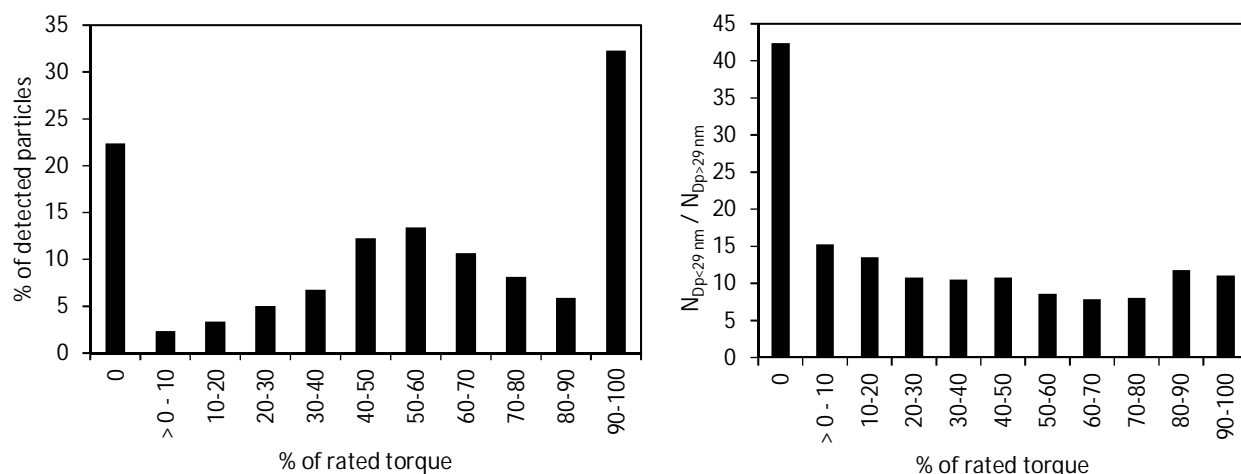
Figure 4.14: Fractions of particles detected by a UCPC ($D_p > 2.5$ nm) (left) and the ratio of particle number of small ($D_p < 29$ nm) and large particles ($D_p > 29$ nm) (right) under different torque conditions of a HD diesel truck. The data covers the entire test route. The concentration of large particles ($N_{D_p>29\text{nm}}$) was determined from the particle size distributions measured by an ELPI with enhanced nanoparticle resolution. The concentration of small particles ($N_{D_p<29\text{nm}}$) was determined by subtracting $N_{D_p>29\text{nm}}$ from the total particle concentration measured by CPC. (**Paper 3**)

results indicate that the particles emitted during engine braking were nonvolatile at 265 °C, the operating temperature of the TD. It should be noted that due to the presence of other (disturbing) traffic, the results have a higher uncertainty, compared to on-road experiments on a closed track or road. However, the experiments were made late in the evening and at night when disturbing traffic was at a minimum. Also, the background concentrations, measured occasionally by laboratory vehicle in front of the test truck, were low; e.g. the particle concentrations measured by the ELPI and NO_x concentrations in the background aerosol were typically below 2000 1/cm^3 and 0.01 ppm.

The contribution of these particles formed unconventionally under engine braking conditions to total emissions was significant. The total number of detected particles was distributed rather in proportion to the time spent by the engine in each torque class (Figure 4.14); 22% of detected particles by number were observed at engine braking (0% of rated torque) which covered 16% of measurement time and 32% were detected under full load conditions (> 90% of rated torque) where the engine spent 22% of the time. However, the contribution of engine braking to nanometer-sized particles differed from the other driving conditions when the particle size was considered; at engine braking the small particle (here $D_p < 29$ nm) concentration was 42 times higher than large particle ($D_p > 29$ nm) one, while under other driving conditions the ratio of small to large particle concentrations was around 10. It should be noted that the numbers presented in Figure 4.14 are for the whole measure-

ment period. Based on the results in Figure 4.13, it is quite clear that when the analysis is focused on the hilly sections only, the role of engine braking is much more emphasized.

4.4.2 Light-duty gasoline vehicles

Observations in the laboratory
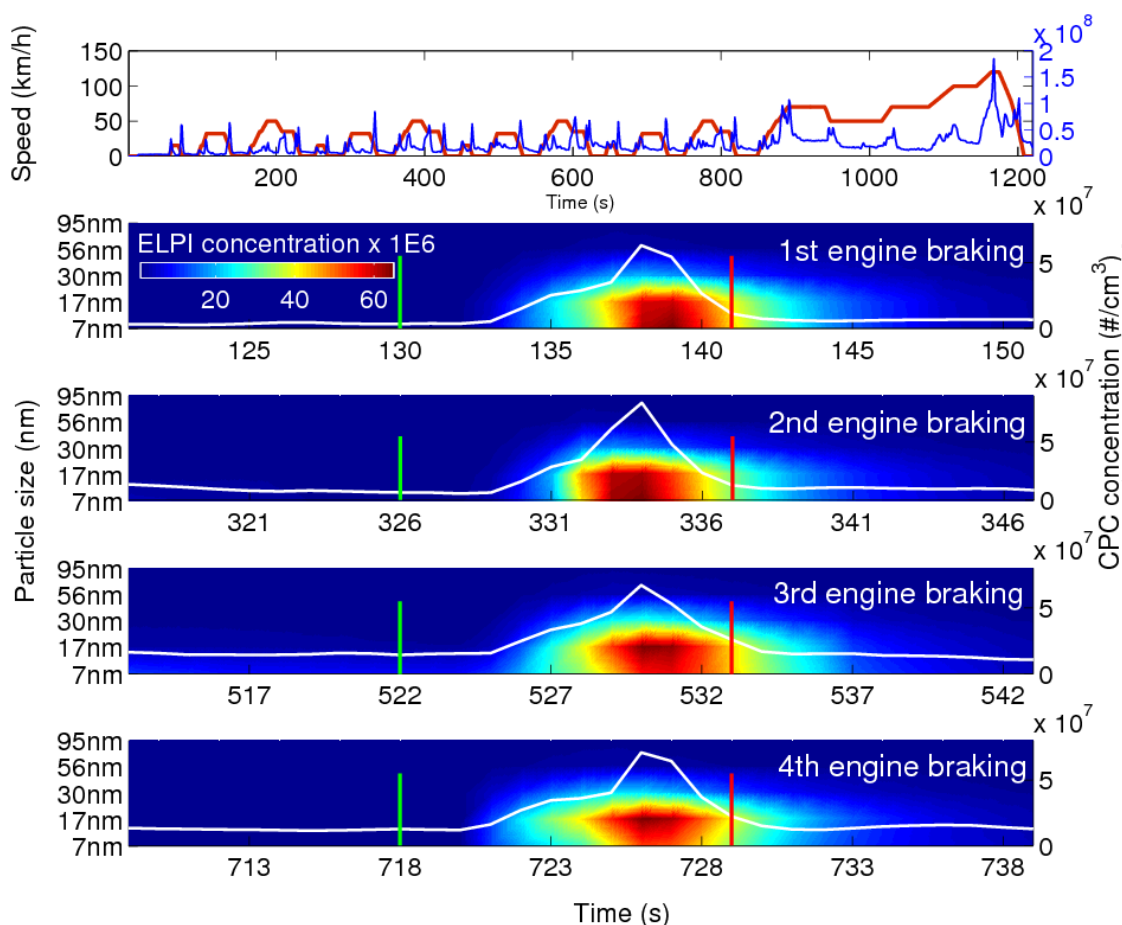
Figure 4.15: Top graph: GDI vehicle speed and exhaust particle concentration over the NEDC. Lower graphs: Exhaust particle size distributions measured by an ELPI (color map) and particle concentration measured by a CPC (white line) during individual engine braking conditions (speed change from 32 km/h to 0 km/h). The starting point of engine braking is marked by a vertical green line, and the end point is marked by a vertical red line. The exhaust sample was taken from the exhaust manifold. (**Paper 3**)

Engine braking particles were also observed in the experiments conducted with modern GDI vehicles during the NEDC. Continuous exhaust samples were studied in real-time using

two alternative sampling points, one in the engine bay directly downstream of the exhaust manifold and one at the end of the tailpipe. Repeatedly high concentrations of particles were observed during engine braking in decelerations, when the sampling was conducted directly downstream of the exhaust manifold (Figure 4.15). The mean diameter of these particles varied from less than 10 nm to slightly larger than 20 nm, depending on the deceleration pattern (Figure 4.16). When sampled downstream of the complete exhaust line including the TWC (not plotted), the particle concentration was lower and mean particle size larger, probably due to the strongly size dependent diffusional particle losses. Alternative measurements at the exhaust manifold and tailpipe outlet positions also led to an additional interesting observation; due to the decreased exhaust flow rate, particles formed during engine braking appeared in the tailpipe outlet when the engine had already reached idle operation. In this experiment, with a modern GDI passenger car (GDI 1) and measured at the tailpipe outlet position over the whole NEDC, as much as 23–29% of all emitted particles in number were observed during engine braking operation.
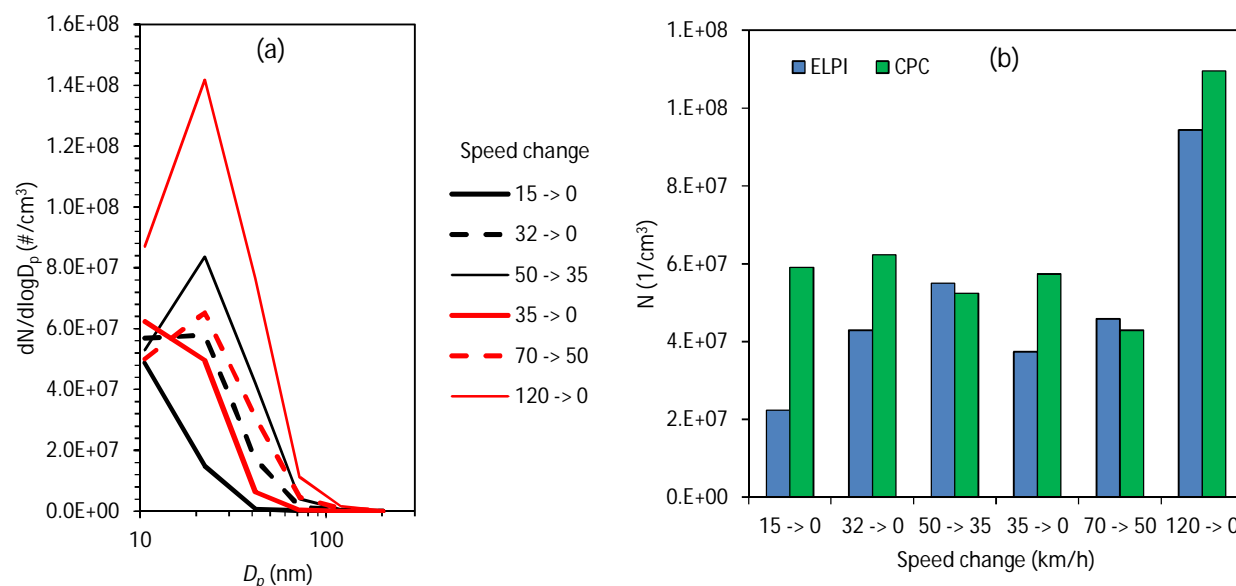
Figure 4.16: (a) Exhaust particle size distributions of the GDI passenger car during engine braking, measured using an ELPI after the exhaust sampling from the exhaust manifold, and (b) particle number emissions measured by an ELPI and a CPC. The legend shows the change of wheel speed in km/h. (**Paper 3**)

GDI vehicle (GDI 2) exhaust particle samples were collected and analyzed by the TEM for shape, and by EDS for elemental composition (Figure 4.17). Two distinct particle types were observed for samples collected over the whole NEDC. First, 10–20% of collected particles, counted from the TEM images obtained, were nearly spherical, often including small enclosures. These particles contained oxygen, zinc, phosphorous and calcium. Zinc, phos-

phorous and calcium can be found in engine oil, but not in gasoline fuel. Second, the soot particles had a typical agglomerated structure and consisted of elemental carbon but also of oxygen, zinc, phosphorous and calcium. When the particle sample was collected during steady state driving, the agglomerated particles contained carbon but not any metals. Thus, this result indicates that engine braking particles emitted during transient driving cycles are associated in some way with engine oil consumption. For GDI 2, the engine braking related particles added up to $\sim$10% of the total emitted particles over the NEDC test cycle (Karjalainen et al., 2014).
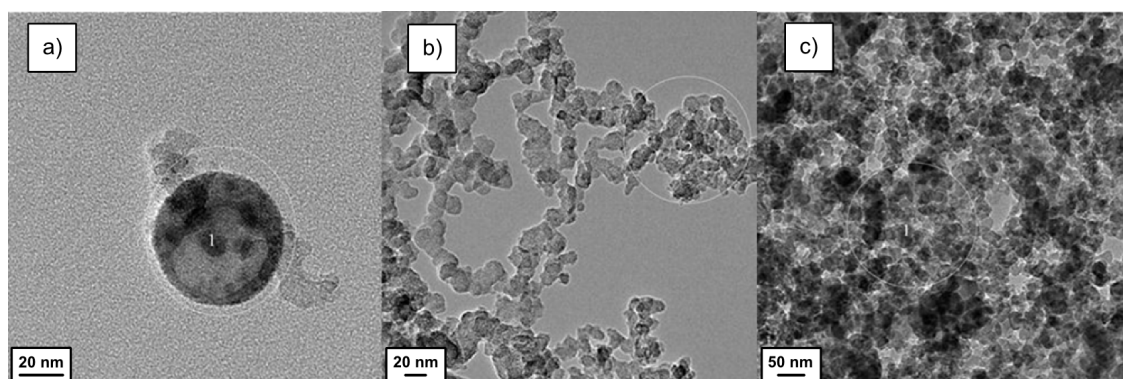

Figure 4.17: Transmission electron microscope (TEM) images of particles collected from an exhaust aerosol sample of a GDI passenger car (1.8 l engine). (a) A spherical O-Zn-P-Ca containing particle with enclosures, sampled during the NEDC cycle. (b) Soot-like C-O-Zn-P-Ca containing agglomerated particles sampled during the NEDC cycle. (c) Heavily loaded particle sample taken during steady-state driving where no elements such as Zn, P, and Ca were found. The circles show the focus of the EDS for elemental analyses. (**Paper 3**)

Observations on the road

Small but distinguishable exhaust plume concentration peaks (particle concentration between $\sim$3000–5000 1/cm^3) were associated with the start of deceleration by engine braking (Figure 4.8a). At this time the concentration of CO_2 was at a minimum. Because CO_2 can be used as a tracer gas for combustion generated particles, the result shows that those particles emitted during engine braking do not originate from combustion. To give a rough estimation for exhaust emission factors by estimating the dilution ratio from CO_2 concentrations of diluted sample and raw exhaust at 70 km/h constant speed and taking into account the exhaust flow rates, the number emission factor was during the deceleration was 3.1×10^{10} 1/s.

Comparison of exhaust plume particle concentrations during acceleration-deceleration routines are shown in Figure 4.8b. All the repetitions of experiments (**Paper 4**) were analyzed. The concentrations presented here are the average maximum concentrations reached

during accelerations and decelerations, measured by the UCPC. The error bars indicate the standard deviation of maximum concentrations. In general, particle emissions during engine braking were higher when the deceleration started at higher engine speed, compared to lower speed situations. The particle concentration levels were still too low or the particle size was too small for size distributions measurement with the ELPI or EEPS. It has to be mentioned that although engine braking increases the total particle number emission of the studied vehicle, the total emission was dominated by particles emitted during accelerations. Overall, the engine braking particle emissions added up to 3–18% of the total particle emissions during different acceleration and deceleration routines (Karjalainen et al., 2014).

4.4.3   Discussion

The clear advantage of engine braking is the effect on fuel economy; for engines with direct fuel injection technology, the fuel consumption during the engine braking is zero. In principle, during engine braking, the inertia of a moving vehicle maintains the rotation of a crankshaft, and thus, the movement of pistons, without simultaneous fuel combustion. The magnitude of engines intake air flow depends on the engine technology and design. In gasoline engines, the intake air flow is typically restricted by the throttles and/or valves. In diesel engines, in general, the resistance for the intake air flow is lower, and the braking effect can be weaker. During engine braking, the engines intake air goes to the cylinder, where it is compressed to elevated pressures, its temperature raises, and, finally, it is exhausted to the atmosphere.

Both the HD diesel truck (**Paper 3**) and the LD gasoline vehicles (**Papers 3-4**) were seen to emit markedly high emissions of exhaust particles also under engine braking conditions. One must note that these vehicles are typical representatives of the total fleet but the results so far cover only a few vehicles. Both the characteristics of these particles and the mechanism by which they form seem to differ significantly from those of SM and NM particles. For the first time, these new exhaust particles were observed by following a HD diesel truck (Diesel 4) under real-world conditions. The truck operated on its daily route, when the driving pattern, road conditions, and vehicle loading were typical of a normal scheduled day. Thus, the emissions of these engine braking particles were part of the real particle emissions of the truck. Because similar particles were observed in the exhaust of modern GDI passenger cars (GDIs 1–3), it is obvious that the emissions are not characteristics of one vehicle or technology type only. Also, because of increased use of fuel direct injection technologies in gasoline fueled vehicles not equipped with particle filters, the exhaust particle emission during engine braking will remain a problem in the future.

In principle, the lubricant oil or some compounds within it can end up in the cylinder by spouting through the piston ring gap, due to their evaporation from the cylinder liner or via the crankcase ventilation system, which conducts the crankcase vapors into the engine's intake air. The lubricant oil consumption has been reported to depend on driving conditions, especially transients. Thus, it seems evident that the direct origin of these particles is not the combustion of fuel, but rather, the engine oil. Because the observed particles are not

formed by direct combustion, they may contain chemical compounds similar to those of the engine oil. Although only metal compounds were observed, it is possible that these particles also contain hydrocarbon compounds from the engine oil. Because of their origin, in principle, no correlation between the emissions of these engine braking particles and CO_2 is expected. It is therefore possible that the approach typically used to determine emission factors (measuring particles and carbon dioxide concentrations simultaneously in an urban environment and using these quantities to calculate particles per unit of fuel combusted), has – at least partially – failed.

Particle number populations in the urban atmosphere have been frequently observed to be dominated by nanoparticles. Although in several countries, high quality fuels are in use, and new vehicles are typically equipped with modern emissions reduction technologies, vehicles still represent one of the most significant particulate pollution sources in the urban environment. Particles with similar physical characteristics as those in this study have been found in urban environments with high human populations. Observations indicate that these particles are emitted in short time bursts, causing high and instantaneous increases of particle concentrations. In addition to downhill driving, these particles may be emitted while approaching locales where people are frequently present, such as when decelerating at crossroads, traffic lights with pedestrian crossings, or bus stops. Particularly in urban environments, this can lead to significant human exposure to these particle emissions.

The contribution of nanoparticles emitted during engine braking to total particle number emissions can be highly significant, as shown in the tests on the HD truck (Diesel 4) 20–30% and on the gasoline vehicles (GDIs 1–3) 3–30% (Karjalainen et al., 2014). These numbers are however very sensitive to the testing procedure and the driving style. These particles have not been taken into account in emission regulations and in the assessment of associated health risks. The fraction of these particles is not dominating but the role of these particles can be very important when adverse health effects are consired, due to the fact that particles contain lubricant-derived metals. For instance, zinc has been lately associated with increased cell deaths (Leskinen et al., 2014).

For example, in the case of gasoline vehicles and nonroad engines, standards controlling particle number emissions have not yet been established, and the proper emission reduction technologies have not yet been applied. However, the results indicate that the particles were nonvolatile, formed before the catalyst, and originate from the engine oil. Hence, it seems that the emissions of engine braking particles can be reduced using exhaust particle filtration systems. Additionally, another potential but less direct way to reduce the emissions of these particles may be the modification of engine oil characteristics, such as metal content or viscosity. From an emissions control perspective, the problem remains for those older vehicle types that are not equipped with particle filters and possibly for new vehicle technologies for which particle filters have not been mandated, such as GDI vehicles. Another aspect is that these particles can also affect the performance and eventually lifetime of DPF systems since the particles contain ash originating from the oil. Ash containing particles can increase

the pressure drop over the DPF and furthermore, in the worst case eventually clog the DPF channels.

Chapter 5

Conclusions and final remarks

This thesis covers results of transient exhaust particle emission measurements including both diesel and gasoline engines/vehicles. The transient phenomena here include accelerations, decelerations by engine braking and sulfur storage/release effects. From the regulatory point of view, the increase in solid particle number ($D_p > 23$ nm) during acceleration is covered in the NEDC and ETC tests for LD and HD vehicles, respectively. Engine braking and sulfur related small particles are not much taken into account in the regulatory testing and validation of the vehicles. The emission of these particle is, however a real-world phenomenon that can affect local and global air quality, causing a potential risk for the human health and the environment.

During accelerations, the engine loading and fuel consumption are high. During transient cycles, there were observations for both the HD diesel nonroad engine and the gasoline passenger car that during accelerations the particle concentrations were 2–10 times higher than the the average concentrations during the test cycles, most likely due to turbocharger lag. In addition, in on-road chase measurements on a gasoline passenger car (GDI 3) the particle concentrations during steady vehicle speeds were at background level (2000–3000 1/cm^3), but during acceleration the exhaust plume particle concentrations reached up to 100000 1/cm^3. So, in fact, on the road practically all the soot particle emissions were associated with emissions during accelerations. In the case of GDI technologies, the characteristics of soot particles were different than typically observed with diesel; the soot particles appeared in two particle modes, where the smaller is considered to consist of primary spheres and the larger of agglomerates. Note that currently in new vehicles neither gasoline passenger car engines nor HD nonroad diesel engines need to employ particle filtration in the exhaust system mandatorily.

Sulfur originating from the fuel or lubricant oil can be stored inside catalytic aftertreatment systems. In catalysts, SO_2 is oxidized to SO_3 which later forms GSA in the presence of water. The sources for engine out SO_2 are the fuel and the lubricant oil, where the role of the latter is emphasized when ultra low sulfur diesel fuels or totally sulfur free biofuels are used. The stored sulfur compounds will be released, forming a high concentration of semivolatile NM particles when the exhaust temperature rises (Vaaraslahti et al., 2005; Giechaskiel et al., 2007; Herner et al., 2011). This observation was detected for LD and HD vehicles in the engine laboratory, for a HD vehicle on the road and in a simplified measurement setup in an

aerosol laboratory. The NM emission emission burst from the ATS is not explained by GSA based on the results of the HD road engine experiment. The sulfur storage and release phenomenon depends greatly on the driving history, and it was seen to make the emission of NM particles plausible, even with the ultra low sulfur diesel fuel. Overall, about 60% of the total particle number emissions from the HD truck equipped with a DOC & pDPF (retrofit) were caused by semivolatile NM particles. When catalytic particle filtration (a DPF or pDPF) is used the amount of soot is reduced and the nonvolatile NM cores are practically removed which will increase the likelihood of semi-volatile NM existence, and hence high real-world NM particle emissions.

Somewhat unexpectedly, an observation was made that some engines produce nanoparticles even while not fueled at the time. Exhaust particles were observed during decelerations by engine braking for a HD diesel truck and three GDI gasoline passenger cars. Here, engine braking refers to a situation when the gear is engaged and accelerator pedal is depressed. Thus, on flat ground, vehicles were decelerating and during downhill driving the vehicle speed remained more or less constant. For the truck engine, the engine braking related particle emissions added up to 20–30% of the total particles during the test sections. For the three GDI vehicles tested, these particles accounted for 3–30% of the total emitted particles, depending on the vehicle and the test routine. In the case of a GDI engine, these particles were considered to contain lubricant oil derived metals: zinc, phosphorus and calcium. Therefore the particles of this type are suggestive of health risks at least similar to, or even higher than, those of exhaust particles observed before. These particles' characteristics indicate that they are expected to be removed by exhaust filtration, but the emissions of the particles can be a reality for older diesel vehicle types without particle filters, as well as all gasoline vehicles, including the ones with the latest technology. In particle filters, engine braking related particles can have an impact on the ash accumulation and transport mechanisms, which may lead to worse performance and eventually reduced lifetime of the devices.

The most important recent development in regulatory particle emission testing in Europe has for sure been the introduction of the PN emission limit for LD and now HD diesel vehicles. Hence more understanding of exhaust particles and technologies affecting them is required, but the regulation has shortcomings. The semivolatile particle material is not counted, and the cut size for nonvolatile particles is set to an artificial value ($D_p > 23$ nm). A big share of nonvolatile particles can even be below this cut size, especially in the case of GDI technology. The development of particle emission testing and research is going to a direction that the real-world situations (e.g. on-board diagnostics (OBD) research and testing, transient conditions) are emphasized more than in the past. The number of regulated emission components (e.g. NH_3, NO_2 and specific organics) can increase in the future. Further away in the future, NM particle emissions and secondary organic aerosol (SOA) emissions are potential targets for regulations. We know now at least that the secondary particles, minutes or hours after their emission, can be quite different from freshly emitted particles. At least on a global scale, the amount of SOA due to emissions is emphasized, since it can have effects on climate change.

Whatever the development in the particle emissions will be in the future, the emissions related to transient phenomena of engines and aftertreatment systems are in an important role, potentially in the most important role.

Bibliography

Aakko, P. and Nylund, N.-O. Particle emissions at moderate and cold temperatures using different fuels. *SAE Technical Papers*, 2003-01-3285, 2003.

Agarwal, J. and Sem, G. Continuous flow, single-particle-counting condensation nucleus counter. *Journal of Aerosol Science*, 11(4):343–357, 1980.

Alkidas, A. Combustion advancements in gasoline engines. *Energy Conversion and Management*, 48(11):2751–2761, 2007.

Arnold, F., Pirjola, L., Rönkkö, T., Reichl, U., Schlager, H., Lähde, T., Heikkilä, J., and Keskinen, J. First online measurements of sulfuric acid gas in modern heavy-duty diesel engine exhaust: Implications for nanoparticle formation. *Environmental Science & Technology*, 46(20):11227–11234, 2012.

Barone, T., Storey, J., Youngquist, A., and Szybist, J. An analysis of direct-injection spark-ignition (DISI) soot morphology. *Atmospheric Environment*, 49:268–274, 2012.

Bergmann, M., Kirchner, U., Vogt, R., and Benter, T. On-road and laboratory investigation of low-level pm emissions of a modern diesel particulate filter equipped diesel passenger car. *Atmospheric Environment*, 43(11):1908–1916, 2009.

Bielaczyc, P., Keskinen, J., Dzida, J., Sala, R., Rönkkö, T., Kinnunen, T., Matilainen, P., Karjalainen, P., and Happonen, M. Performance of particle oxidation catalyst and particle formation studies with sulphur containing fuels. *SAE International Journal of Fuels and Lubricants*, 5(2):611–619, 2012.

Braisher, M., Stone, R., and Price, P. Particle number emissions from a range of European vehicles. *SAE Technical Papers*, 2010-01-0786, 2010.

Burtscher, H. Physical characterization of particulate emissions from diesel engines: A review. *Journal of Aerosol Science*, 36(7):896–932, 2005.

Canagaratna, M., Jayne, J., Jimenez, J., Allan, J., Alfarra, M., Zhang, Q., Onasch, T., Drewnick, F., Coe, H., Middlebrook, A., Delia, A., Williams, L., Trimborn, A., Northway, M., DeCarlo, P., Kolb, C., Davidovits, P., and Worsnop, D. Chemical and microphysical characterization of ambient aerosols with the aerodyne aerosol mass spectrometer. *Mass Spectrometry Reviews*, 26(2):185–222, 2007.

CARB. Proposed amendments to Californias low-emission vehicle regulations – particulate matter mass, ultrafine solid particle number, and black carbon emissions. Workshop report, California Air Resources Board, 2010.

Chase, R., Duszkiewicz, G., Richert, J., Lewis, D., Maricq, M., and Xu, N. PM measurement artifact: Organic vapor deposition on different filter media. *SAE Technical Papers*, 2004-01-0967, 2004.

Chen, D., Pui, D., Hummes, D., Fissan, H., Quant, F., and Sem, G. Design and evaluation of a nanometer aerosol differential mobility analyzer (Nano-DMA). *Journal of Aerosol Science*, 29(5–6):497–509, 1998.

Dieselnet, 2014. URL http://www.dieselnet.com/. 25.8.2014.

Dockery, D., Pope III, C., Xu, X., Spengler, J., Ware, J., Fay, M., Ferris Jr., B., and Speizer, F. An association between air pollution and mortality in six U.S. cities. *New England Journal of Medicine*, 329:1753–1759, 1993.

Eastwood, P. *Particulate Emissions from Vehicles*. John Wiley & Sons, Ltd., Chichester, West Sussex, England, 2008.

Filippo, A. and Maricq, M. Diesel nucleation mode particles: Semi-volatile or solid? *Environmental Science & Technology*, 42:7957–7962, 2008.

Gasmet Technologies, 2014. URL http://www.gasmet.com/technology/ftir. 3.10.2014.

Giakoumis, E., Rakopoulos, C., Dimaratos, A., and Rakopoulos, D. Exhaust emissions of diesel engines operating under transient conditions with biodiesel fuel blends. *Progress in Energy and Combustion Science*, 38(5):691–715, 2012.

Giechaskiel, B., Ntziachristos, L., Samaras, Z., Casati, R., Scheer, V., and Vogt, R. Effect of speed and speed-transition on the formation of nucleation mode particles from a light duty diesel vehicle. *SAE Technical Papers*, 2007-01-1110, 2007.

Heikkilä, J., Rönkkö, T., Lähde, T., Lemmetty, M., Arffman, A., Virtanen, A., Keskinen, J., Pirjola, L., and Rothe, D. Effect of open channel filter on particle emissions of modern diesel engine. *Journal of the Air & Waste Management Association*, 59:1148–1154, 2009.

Herner, J., Hu, S., Robertson, W., Huai, T., Collins, J., Dwyer, H., and Ayala, A. Effect of advanced aftertreatment for PM and NOx control on heavy-duty diesel truck emissions. *Environmental Science & Technology*, 43:5928–5933, 2009.

Herner, J., Hu, S., Robertson, W., Huai, T., Chang, M.-C., Rieger, P., and Ayala, A. Effect of advanced aftertreatment for PM and NOx reduction on heavy-duty diesel engine ultrafine particle emissions. *Environmental Science & Technology*, 45:2413–2419, 2011.

Högström, R., Karjalainen, P., Yli-Ojanperä, J., Rostedt, A., Heinonen, M., Mäkelä, J., and Keskinen, J. Study of the PM gas-phase filter artifact using a setup for mixing diesel-like soot and hydrocarbons. *Aerosol Science and Technology*, 46(9):1045–1052, 2012.

Hu, S., Herner, J., Shafer, M., Robertson, W., Schauer, J., Dwyer, H., Collins, J., Huai, T., and Ayala, A. Metals emitted from heavy-duty diesel vehicles equipped with advanced PM and NOx emission controls. *Atmospheric Environment*, 43:2950–2959, 2009.

Janssen, N., Hoek, G., Simic-Lawson, M., Fischer, P., van Bree, L., Brink, H., Keuken, M., Atkinson, R., Ross Anderson, H., Brunekreef, B., and Cassee, F. Black carbon as an additional indicator of the adverse health effects of airborne particles compared with pm 10 and pm 2.5. *Environmental Health Perspectives*, 119(12):1691–1699, 2011.

Johnson, J. E. and Kittelson, D. B. Deposition, diffusion and adsorption in the diesel oxidation catalyst. *Applied Catalysis B: Environmental*, 10:117–137, 1996.

Johnson, T. Review of diesel emissions and control. *International Journal of Engine Research*, 10(5):275–285, 2009.

Johnson, T., Caldow, R., Pöcher, A., Mirme, A., and Kittelson, D. A new electrical mobility particle sizer spectrometer for engine exhaust particle measurements. *SAE Technical Papers*, 2004-01-1341, 2004.

Karjalainen, P., Heikkilä, J., Rönkkö, T., Keskinen, J., Lehtoranta, K., Matilainen, P., and Kinnunen, T. Effect of exhaust flow conditions and external cooling on the performance of the particle oxidation catalyst (POC). *SAE Technical Papers*, 2010-01-2158, 2010.

Karjalainen, P., Pirjola, L., Heikkilä, J., Lähde, T., Hillamo, R., Keskinen, J., and Rönkkö, T. Exhaust particles formed during engine braking: contribution on total particle emissions of GDI vehicles. *18th ETH Conference on Combustion Generated Nanoparticles*, 2014.

Keskinen, J. and Rönkkö, T. Can real-world diesel exhaust particle size distribution be reproduced in the laboratory? A critical review. *Journal of the Air & Waste Management Association*, 60(10):1245–1255, 2010.

Keskinen, J., Pietarinen, K., and Lehtimäki, M. Electrical low pressure impactor. *Journal of Aerosol Science*, 23:353–360, 1992.

Ketzel, M., Wåhlin, P., Berkowicz, R., and Palmgren, F. Particle and trace gas emission factors under urban driving conditions in copenhagen based on street and roof-level observations. *Atmospheric Environment*, 37(20):2735–2749, 2003.

Kittelson, D., Johnson, J., Watts, W., Wei, Q., Drayton, M., Paulsen, D., and Bukowiecki, N. Diesel aerosol sampling in the atmosphere. *SAE Technical Papers*, 2000-01-2212, 2000.

Kittelson, D. B. Engines and nanoparticles: A review. *Journal of Aerosol Science*, 29: 575–588, 1998.

Krahl, J., Munack, A., Grope, N., Ruschel, Y., Schröder, O., and Bünger, J. Biodiesel, rapeseed oil, gas-to-liquid, and a premium diesel fuel in heavy duty diesel engines: Endurance, emissions and health effects. *Clean*, 35(5):417–426, 2007.

Lähde, T., Rönkkö, T., Virtanen, A., Schuck, T. J., L., Hämeri, K., Kulmala, M., Arnold, F., Rothe, D., and Keskinen, J. Heavy duty diesel engine exhaust aerosol particle and ion measurements. *Environmental Science & Technology*, 43:163–168, 2009.

Lähde, T., Rönkkö, T., Happonen, M., Söderström, C., Virtanen, A., Solla, A., Kytö, M., Rothe, D., and Keskinen, J. Effect of fuel injection pressure on a heavy-duty diesel engine nonvolatile particle emission. *Environmental Science & Technology*, 45(6):2504–2509, 2011.

Lapuerta, M., Oliva, F., Agudelo, J., and Boehman, A. Effect of fuel on the soot nanostructure and consequences on loading and regeneration of diesel particulate filters. *Combustion and Flame*, 159(2):844–853, 2012.

Lehtoranta, K., Matilainen, P., Åsenbrygg, J., Lievonen, A., Kinnunen, T., Keskinen, J., and Solla, A. Particle oxidation catalyst in light duty and heavy duty diesel applications. *SAE Technical Papers*, 2004-24-0093, 2007.

Lemmetty, M., Vehkamäki, H., Virtanen, A., Kulmala, M., and Keskinen, J. Homogeneous ternary H_2SO_4–NH_3–H_2O nucleation and diesel exhaust: a classical approach. *Aerosol and Air Quality Research*, 7(4):489–499, 2007.

Leskinen, J., Tissari, J., Uski, O., Virn, A., Torvela, T., Kaivosoja, T., Lamberg, H., Nuutinen, I., Kettunen, T., Joutsensaari, J., Jalava, P., Sippula, O., Hirvonen, M.-R., and Jokiniemi, J. Fine particle emissions in three different combustion conditions of a wood chip-fired appliance - particulate physico-chemical properties and induced cell death. *Atmospheric Environment*, 86:129–139, 2014.

Lipsky, E. and Robinson, A. Effects of dilution on fine particle mass and partitioning of semivolatile organics in diesel exhaust and wood smoke. *Environmental Science & Technology*, 40(1):155–162, 2006.

Liu, Z., Vasys, V., and Kittelson, D. Nuclei-mode particulate emissions and their response to fuel sulfur content and primary dilution during transient operations of old and modern diesel engines. *Environmental Science & Technology*, 41(18):6479–6483, 2007.

Logan, W. Mortality in the london fog incident, 1952. *The Lancet*, 261(0):336–338, 1953.

Longley, I., Gallagher, M., Dorsey, J., Flynn, M., Allan, J., Alfarra, M., and Inglis, D. A case study of aerosol (4.6 nm $< D_p <$ 10 m) number and mass size distribution measurements in a busy street canyon in Manchester, UK. *Atmospheric Environment*, 37(12):1563–1571, 2003.

Mamakos, A., Dardiotis, C., Marotta, A., Martini, G., Manfredi, U., Colombo, R., Sculati, M., Lijour, P. L., and Lanappe, G. Particle emissions from a Euro 5a certified diesel passenger car. *JRC Scientific and Technical Reports*, JRC-IE, 2011.

Maricq, M. Chemical characterization of particulate emissions from diesel engines: A review. *Journal of Aerosol Science*, 38(11):1079–1118, 2007.

Maricq, M., Chase, R., Xu, N., and Laing, P. The effects of the catalytic converter and fuel sulfur level on motor vehicle particulate matter emissions: Light duty diesel vehicles. *Environmental Science & Technology*, 36(2):283–289, 2002.

Maricq, M. On the electrical charge of motor vehicle exhaust particles. *Journal of Aerosol Science*, 37(7):858–874, 2006.

Maricq, M., Podsiadlik, D., Brehob, D., and Haghgooie, M. Particulate emissions from a direct-injection spark-ignition (DISI) engine. *SAE Technical Papers*, 1999-01-1530, 1999a.

Maricq, M., Podsiadlik, D., and Chase, R. Examination of the size-resolved and transient nature of motor vehicle particle emissions. *Environmental Science & Technology*, 33(10): 1618–1626, 1999b.

Maricq, M., Podsiadlik, D., and Chase, R. Gasoline vehicle particle size distributions: Comparison of steady state, FTP, and US06 measurements. *Environmental Science & Technology*, 33(12):2007–2015, 1999c.

Marjamäki, M., Ntziachristos, L., Virtanen, A., Ristimäki, J., Keskinen, J., Moisio, M., Palonen, M., and Lappi, M. Electrical filter stage for the ELPI. *SAE Technical Papers*, 2002-01-0055, 2002.

Mathis, U., Mohr, M., and Forss, A.-M. Comprehensive particle characterization of modern gasoline and diesel passenger cars at low ambient temperatures. *Atmospheric Environment*, 39(1):107–117, 2005.

Mathis, U., Ristimäki, J., Mohr, M., Keskinen, J., Ntziachristos, L., Samaras, Z., and Mikkanen, P. Sampling Conditions for the Measurement of Nucleation Mode Particles in the Exhaust of a Diesel Vehicle. *Aerosol Science and Technology*, 38(12):1149–1160, 2004.

Mohr, M., Forss, A.-M., and Lehmann, U. Particle emissions from diesel passenger cars equipped with a particle trap in comparison to other technologies. *Environmental Science & Technology*, 40(7):2375–2383, 2006.

Mollenhauer, K. and Tschoeke, H. *Handbook of Diesel Engines.* Springer, Germany, 2010.

Ng, N., Canagaratna, M., Zhang, Q., Jimenez, J., Tian, J., Ulbrich, I., Kroll, J., Docherty, K., Chhabra, P., Bahreini, R., Murphy, S., Seinfeld, J., Hildebrandt, L., Donahue, N., Decarlo, P., Lanz, V., Prvt, A., Dinar, E., Rudich, Y., and Worsnop, D. Organic aerosol components observed in northern hemispheric datasets from aerosol mass spectrometry. *Atmospheric Chemistry and Physics*, 10(10):4625–4641, 2010.

Ng, N., Herndon, S., Trimborn, A., Canagaratna, M., Croteau, P., Onasch, T., Sueper, D., Worsnop, D., Zhang, Q., Sun, Y., and Jayne, J. An aerosol chemical speciation monitor (ACSM) for routine monitoring of the composition and mass concentrations of ambient aerosol. *Aerosol Science and Technology*, 45(7):770–784, 2011.

Ntziachristos, L., Giechaskiel, B., Pistikopoulos, P., Samaras, Z., Mathis, U., Mohr, M., Ristimäki, J., Keskinen, J., Mikkanen, P., Casati, R., Scheer, V., and Vogt, R. Performance evaluation of a novel sampling and measurement system for exhaust particle characterization. *SAE Technical Papers*, 2004-01-1439, 2004.

Oberdörster, G., Oberdörster, E., and Oberdörster, J. Nanotoxicology: An emerging discipline evolving from studies of ultrafine particles. *Environmental Health Perspectives*, 113 (7):823–839, 2005.

Olfert, J., Symonds, J., and Collings, N. The effective density and fractal dimension of particles emitted from a light-duty diesel vehicle with a diesel oxidation catalyst. *Journal of Aerosol Science*, 38(1):69–82, 2007.

Petzold, A. and Schönlinner, M. Multi-angle absorption photometry - a new method for the measurement of aerosol light absorption and atmospheric black carbon. *Journal of Aerosol Science*, 35(4):421–441, 2004.

Pirjola, L., Parviainen, H., Hussein, T., Valli, A., Hämeri, K., Aalto, P., Virtanen, A., Keskinen, J., Pakkanen, T., Mäkelä, T., and Hillamo, R. "Sniffer" – a novel tool for chasing vehicles and measuring traffic pollutants. *Atmospheric Environment*, 38:3625–3635, 2004.

Pirjola, L., Paasonen, P., Pfeiffer, D., Hussein, T., Hämeri, K., Koskentalo, T., Virtanen, A., Rönkkö, T., Keskinen, J., Pakkanen, T., and Hillamo, R. Dispersion of particles and trace gases nearby a city highway: Mobile laboratory measurements in finland. *Atmospheric Environment*, 40(5):867–879, 2006.

Putaud, J.-P., Van Dingenen, R., Alastuey, A., Bauer, H., Birmili, W., Cyrys, J., Flentje, H., Fuzzi, S., Gehrig, R., Hansson, H., Harrison, R., Herrmann, H., Hitzenberger, R., Hglin, C., Jones, A., Kasper-Giebl, A., Kiss, G., Kousa, A., Kuhlbusch, T., Löschau, G., Maenhaut, W., Molnar, A., Moreno, T., Pekkanen, J., Perrino, C., Pitz, M., Puxbaum,

H., Querol, X., Rodriguez, S., Salma, I., Schwarz, J., Smolik, J., Schneider, J., Spindler, G., ten Brink, H., Tursic, J., Viana, M., Wiedensohler, A., and Raes, F. A European aerosol phenomenology - 3: Physical and chemical characteristics of particulate matter from 60 rural, urban, and kerbside sites across Europe. *Atmospheric Environment*, 44 (10):1308–1320, 2010.

Rakopoulos, C. D. and Giakoumis, E. *Diesel Engine Transient Operation.* Springer, 2009.

Rakopoulos, C., Dimaratos, A., Giakoumis, E., and Rakopoulos, D. Investigating the emissions during acceleration of a turbocharged diesel engine operating with bio-diesel or n-butanol diesel fuel blends. *Energy*, 35(12):5173–5184, 2010.

Ristimäki, J., Vaaraslahti, K., Lappi, M., and Keskinen, J. Hydrocarbon condensation in heavy-duty diesel exhaust. *Environmental Science & Technology*, 41(18):6397–6402, 2007.

Robinson, A., Donahue, N., Shrivastava, M., Weitkamp, E., Sage, A., Grieshop, A., Lane, T., Pierce, J., and Pandis, S. Rethinking organic aerosols: Semivolatile emissions and photochemical aging. *Science*, 315(5816):1259–1262, 2007.

Rogge, W., Hildemann, L., Mazurek, M., Cass, G., and Simoneit, B. Sources of fine organic aerosol. 2. noncatalyst and catalyst-equipped automobiles and heavy-duty diesel trucks. *Environmental Science & Technology*, 27(4):636–651, 1993.

Rönkkö, T., Virtanen, A., Vaaraslahti, K., Keskinen, J., Pirjola, L., and Lappi, M. Effect of dilution conditions and driving parameters on nucleation mode particles in diesel exhaust: Laboratory and on-road study. *Atmospheric Environment*, 40(16):2893–2901, 2006.

Rönkkö, T., Virtanen, A., Kannosto, J., Keskinen, J., Lappi, M., and Pirjola, L. Nucleation mode particles with a nonvolatile core in the exhaust of a heavy duty diesel vehicle. *Environmental Science & Technology*, 41:6384–6389, 2007.

Rönkkö, T., Arffman, A., Lähde, T., Karjalainen, P., Heikkilä, J., Pirjola, L., Rothe, D., and Keskinen, J. Diesel exhaust nanoparticle volatility studies by a new thermodenuder with low solid nanoparticle losses. *15th ETH Conference on Combustion Generated Nanoparticles*, 2011.

Rönkkö, T., Lähde, T., Heikkilä, J., Pirjola, L., Bauschke, U., Arnold, F., Schlager, H., Rothe, D., Yli-Ojanperä, J., and Keskinen, J. Effects of gaseous sulphuric acid on diesel exhaust nanoparticle formation and characteristics. *Environmental Science & Technology*, 47(20):11882–11889, 2013.

Sappok, A., Santiago, M., Vianna, T., and Wong, V. Characteristics and effects of ash accumulation on diesel particulate filter performance: Rapidly aged and field aged results. *SAE Technical Papers*, 2009.

Schneider, J., Hock, N., Weimer, S., Borrmann, S., Kirchner, U., Vogt, R., and Scheer, V. Nucleation particles in diesel exhaust: Composition inferred from in situ mass spectrometric analysis. *Environmental Science & Technology*, 39:6153–6161, 2005.

Sementa, P., Maria Vaglieco, B., and Catapano, F. Thermodynamic and optical characterizations of a high performance gdi engine operating in homogeneous and stratified charge mixture conditions fueled with gasoline and bio-ethanol. *Fuel*, 96:204–219, 2012.

Sgro, L., Sementa, P., Vaglieco, B., Rusciano, G., D'Anna, A., and Minutolo, P. Investigating the origin of nuclei particles in GDI engine exhausts. *Combustion and Flame*, 159(4):1687–1692, 2012.

Speidel, M., Nau, R., Arnold, F., Schlager, H., and Stohl, A. Sulfur dioxide measurements in the lower, middle and upper troposphere: Deployment of an aircraft-based chemical ionization mass spectrometer with permanent in-flight calibration. *Atmospheric Environment*, 41(11):2427–2437, 2007.

Stolzenburg, M. and McMurry, P. An ultrafine aerosol condensation nucleus counter. *Aerosol Science and Technology*, 14(1):48–65, 1991.

Thiruvengadam, A., Besch, M., Carder, D., Oshinuga, A., and Gautam, M. Influence of real-world engine load conditions on nanoparticle emissions from a DPF and SCR equipped heavy-duty diesel engine. *Environmental Science & Technology*, 46:1907–1913, 2011.

Uhrner, U., von Löwis, S., Vehkamäki, H., Wehner, B., Bräsel, S., Hermann, M., Stratmann, F., Kulmala, M., and Wiedensohler, A. Dilution and aerosol dynamics within a diesel car exhaust plume-CFD simulations of on-road measurement conditions. *Atmospheric Environment*, 41(35):7440–7461, 2007.

Vaaraslahti, K., Virtanen, A., Ristimäki, J., and Keskinen, J. Nucleation mode formation in heavy-duty diesel exhaust with and without a particulate filter. *Environmental Science & Technology*, 38(18):4884–4890, 2004.

Vaaraslahti, K., Keskinen, J., Giechaskiel, B., Solla, A., Murtonen, T., and Vesala, H. Effect of lubricant on the formation of heavy-duty diesel exhaust nanoparticles. *Environmental Science & Technology*, 39(21):8497–8504, 2005.

Vaaraslahti, K., Ristimäki, J., Virtanen, A., Keskinen, J., Giechaskiel, B., and Solla, A. Effect of oxidation catalysts on diesel soot particles. *Environmental Science & Technology*, 40:4776–4781, 2006.

Vogt, R., Scheer, V., Casati, R., and Benter, T. On-road measurement of particle emission in the exhaust plume of a diesel passenger car. *Environmental Science & Technology*, 37 (18):4070–4076, 2003.

Wang, J., Storey, J., Domingo, N., Huff, S., Thomas, J., and West, B. Studies of diesel engine particle emissions during transient operations using an engine exhaust particle sizer. *Aerosol Science and Technology*, 40(11):1002–1015, 2006.

Wang, J.-F., Hu, M.-G., Xu, C.-D., Christakos, G., and Zhao, Y. Estimation of citywide air pollution in Beijing. *PLoS ONE*, 8(1), 2013.

Wang, S. and Flagan, R. C. Scanning electrical mobility spectrometer. *Aerosol Science and Technology*, 13:230–240, 1990.

Wehner, B., Birmili, W., Gnauk, T., and Wiedensohler, A. Particle number size distributions in a street canyon and their transformation into the urban-air background: Measurements and a simple model study. *Atmospheric Environment*, 36(13):2215–2223, 2002.

Wehner, B., Uhrner, U., von Löwis, S., Zallinger, M., and Wiedensohler, A. Aerosol number size distributions within the exhaust plume of a diesel and a gasoline passenger car under on-road conditions and determination of emission factors. *Atmospheric Environment*, 43 (6):1235–1245, 2009.

Whittaker, A., BeruBe, K., Jones, T., Maynard, R., and Richards, R. Killer smog of london, 50 years on: particle properties and oxidative capacity. *Science of the Total Environment*, 334–335(0):435–445, 2004.

Yli-Ojanperä, J., Kannosto, J., Marjamäki, M., and Keskinen, J. Improving the nanoparticle resolution of the ELPI. *Aerosol and Air Quality Research*, 10(4):360–366, 2010.

Paper 1

Panu Karjalainen, Topi Rönkkö, Tero Lähde, Antti Rostedt, Jorma Keskinen, Sanna Saarikoski, Minna Aurela, Risto Hillamo, Aleksi Malinen, Liisa Pirjola and Arno Amberla.
Reduction of Heavy-Duty Diesel Exhaust Particle Number and Mass at Low Exhaust Temperature Driving by the DOC and the SCR. *SAE International Journal of Fuels and Lubricants*, 2012, 5(3), doi: 10.4271/2012-01-1664.

SAE International®

Reduction of Heavy-Duty Diesel Exhaust Particle Number and Mass at Low Exhaust Temperature Driving by the DOC and the SCR

Panu Karjalainen, Topi Ronkko, Tero Lahde, Antti Rostedt and Jorma Keskinen
Tampere Univ of Technology

Sanna Saarikoski, Minna Aurela and Risto Hillamo
Finnish Meteorological Institute

Aleksi Malinen and Liisa Pirjola
Metropolia Univ of Applied Sciences

Arno Amberla
Proventia Emission Control Oy

ABSTRACT

The effect of SCR on nanoparticle emissions has been a subject for some recent diesel particle emission related studies. In this study, the effect of after-treatment (DOC and SCR) on particle emissions was studied with a heavy-duty off-road diesel engine (emission level stage 3b with an SCR). A special "transient cold test cycle" (TCTC) was designed to describe the SCR system operation at low exhaust gas temperatures. The particle instrumentation made it possible to measure on-line the particle number concentration, particle size distribution and chemical composition of particles. The largest particle number concentrations were measured after the exhaust manifold. The exhaust after-treatment was observed to reduce the total particle number concentration by 82.5% with the DOC and 95.7% with the DOC+SCR. Also the mean particle composition was affected by the after-treatment; while the organics formed the main fraction of the particulate mass without exhaust after-treatment, after the DOC and especially after the DOC+SCR the organic particulate matter was reduced so that most significant particle fraction was soot. The effect of after-treatment was similar both on exhaust particle number and mass concentration of organics. The SCR system itself was not observed to cause an increase in particle number concentrations by promoting new particle formation. In general, the results indicate that the semi-volatile organic fraction, formed in exhaust cooling and dilution process, can play a significant role in the PM emissions of a modern off-road diesel engine in low exhaust temperature situations. On the other hand, the semi-volatile components, which participate in gas-to-particle conversion during cooling and dilution, were effectively removed by exhaust after-treatment.

CITATION: Karjalainen, P., Ronkko, T., Lahde, T., Rostedt, A. et al., "Reduction of Heavy-Duty Diesel Exhaust Particle Number and Mass at Low Exhaust Temperature Driving by the DOC and the SCR," *SAE Int. J. Fuels Lubr.* 5(3):2012, doi: 10.4271/2012-01-1664.

INTRODUCTION

Exhaust particles are emitted in the close vicinity of people, e.g. in city centers, road canyons [1,2,3] and highways [4-5]; thus their contribution on the total particle exposure of people is emphasized. The emission related aerosol particles worsen the air quality and pose a threat to human health. High particulate matter concentrations together with high concentrations of sulphur compounds in urban air are associated with increased human morbidity and mortality (e.g. [6]). A major source of urban aerosol particles is diesel engines. The diesel engine related aerosol particle emissions are affected by the fuel quality, lubricant oil, engine design and operation, and particularly exhaust gas after-treatment. These after-treatment devices are a method to control regulated exhaust emissions: carbon monoxide (CO),

hydrocarbons (HC), nitrous oxides (NO_x) and particulate matter (PM) - the components that are controlled by legislation all over the world.

The submicron diesel exhaust particles can be divided into two separate groups depending on particle size, properties and formation mechanisms. In a number size distribution, the two groups form typically two modes, most frequently named as *nucleation mode* and *accumulation mode* [7]. The mean particle diameters of the nucleation mode and the accumulation mode are typically between 3-40 nm and 30-100 nm, respectively. The accumulation mode consists of solid agglomerated soot particles and semi-volatile compounds adsorbed or condensed on these particles. The nucleation mode particles have been reported to consist mainly of water, sulphur compounds, and hydrocarbons and they have frequently been reported to be semi-volatile. However, in several studies during the last five years, the nucleation mode has been reported to consist of non-volatile core particles and semi-volatile compounds condensed on these core particles [8,9,10]. Some studies have indicated that the core particle formation occurs during the combustion process or just after that; the core particle mode is partly electrically charged and the existence of the mode is strongly dependent on the exhaust after-treatment [9,10,11]. The existence of the core particles makes nucleation mode formation possible also in situations where the exhaust sulphuric acid concentration is not high enough for the nucleation mode particle formation during the exhaust dilution and cooling process. Regardless of several studies on the non-volatile core particles, the elemental and chemical composition of these particles is yet unknown.

The selective catalytic reduction (SCR) method is used to reduce NO_x emissions that are formed during high temperature combustion within the engine cylinder. The increase in fuel injection pressure drops down the soot particle size and decreases the PM emission while more NO_x and core particles are formed during the combustion of diesel fuel [12]. The NO_x emission is addressed by an SCR-system that is installed in the tailpipe. NO_x is reduced in a selective catalyst using ammonia as a reductant. Ammonia is generated by hydrolysis of urea solution which is injected into the hot exhaust gas. However, the efficiency of the SCR depends on various parameters such as urea injection placement and operational parameters, the SCR catalyst and exhaust gas temperatures [13]. Overall, the SCR allows a diesel engine to be run at maximum efficiency generating high amounts of NO_x. At the same time with high fuel injection pressure, soot particle mass is reduced. However, the SCR system can be a potential source of new exhaust particles if ammonia is able to penetrate the system or by other means. In some cases, an oxidative "slip catalyst" is installed at the back end of the SCR to oxidize excess ammonia.

The SCR effect on emission related particles is not yet a well-known subject, but there exist a few studies concerning the topic [14,15,16,17,18]. Both Thiruvendagam et al. (2012) [14] and Herner et al. (2011) [15] measured particles with a DPF+SCR after-treatment in heavy-duty diesel application. Thiruvendagam et al. (2012) [14] found out that after the SCR small nanoparticle concentrations were over an order of magnitude larger than with an after-treatment that consisted solely of a DPF. The higher the exhaust temperature was, the higher the nucleation mode particle concentrations were. Under threshold temperature 380 °C, there was no significant amount of nucleation mode particles. Results of Herner et al. (2011) [15] confirm that after the DPF+SCR, large quantity of small particles ($D_p < 20$ nm) can be observed. Concluding, both studies indicate an increase of nucleation mode particle number emissions when the SCR system is used and the exhaust temperature is high enough. The formation is explained by the oxidative potential of the SCR system, by increasing the oxidation of SO_2 to SO_3, therefore, promoting the formation of sulphur-driven nucleation mode. This is in correlation with the study of Hu et al. 2009 [18], however, they observed also that a vanadium-based SCR system emitted considerable amounts of vanadium in the nanoparticle size range. This can also cause an increase in the nucleation mode particle emissions. Based on the exhaust particle modeling studies, it is also possible that ammonia can promote the exhaust particle formation by changing the nucleation process; e.g. Lemmetty et al. (2007) [19] proposed that the SCR equipped diesel engine can emit more nucleation particles than the engine without an SCR system. Typically the effects of SCR on soot particles have been reported to be nearly negligible.

The functioning of an SCR system is challenged during low load conditions and cold ambient temperatures. At these conditions the urea injection changes strongly depending on temporary exhaust gas temperature which can lead to excess particle emissions. In this study, the effect of after-treatment (DOC and SCR) on the particle emissions was studied with a modern off-road diesel engine during low exhaust temperature operation conditions. Special attention was paid to composition and volatility of particles during transient driving operation, and especially the effect of SCR after-treatment on particle emissions.

EXPERIMENTAL

The experiments were performed in the engine laboratory of Proventia Emission Control Oy. Test engine was a Stage 3b off-road 6 cylinder heavy-duty diesel rated to 200 kW. The engine was operated with ultra-low-sulphur diesel fuel (less than 10 mg/kg sulphur) and equipped with a diesel oxidation catalyst (DOC) and a modern SCR system in serial configuration.

The driving operation consisted of dozens of "transient cold test cycles" (TCTC) in a day. The TCTC was designed to describe the SCR system operation at challenging low exhaust gas temperatures. The TCTC was constructed of parts of the NRTC where exhaust gas temperature upstream of the SCR catalyst was less than 250 °C. During the TCTC

cycle, rate of the SCR urea dosing depended on the pre-SCR exhaust temperature. A single TCTC lasts 275 seconds, and at least six cycles were run consecutively in each sampling point. Engine speed, torque, and exhaust gas temperature after the turbocharger during a TCTC are shown in Figure 1. The average engine parameters and exhaust gas temperature profile in the tail pipe are shown in Table 1.
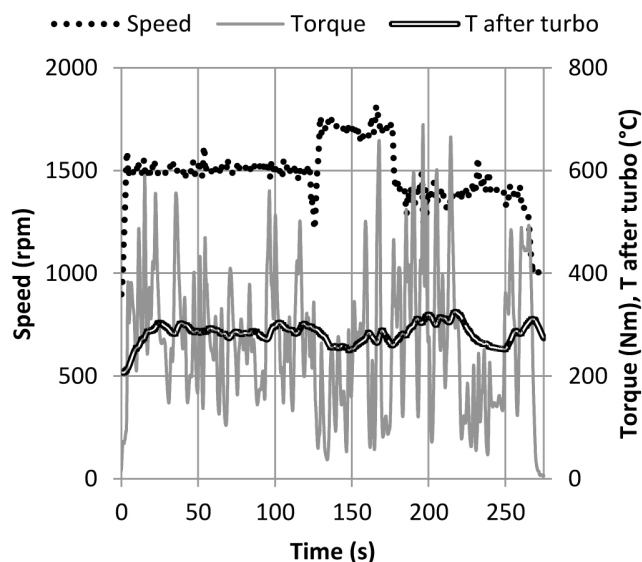

Figure 1. Transient cold test cycle speed, torque and temperature (after turbo) profiles for the test engine.

Table 1. Transient cold test cycle average properties with standard deviation.

Speed	1480 ± 149 rpm
Torque	266 ± 136 Nm
Power (kW)	41.2 ± 20.1 kW
Air mass flow	467 ± 59 kg/h
Lambda ratio	3.64 ± 1.63
T, after turbo (SP 1)	282 ± 20.6 °C
T, before SCR (SP 2)	239 ± 3.3 °C
T, after SCR (SP 3)	237 ± 5.2 °C

The experimental setup is shown in Figure 2. Three sampling points (SP) were used: (1) after the exhaust manifold (NONE), (2) after the DOC and (3) after the SCR. In order to dilute the exhaust gas for sampling, two primary diluters were used; a porous tube diluter (PTD) [20,21] and a hot ejector diluter [12,22]. The dilution air temperature in the PTD was set to 30 °C. After the PTD, diluted exhaust is led to an ageing chamber and a secondary diluter, an ejector. When the results measured using the dilution system consisting of PTD, ageing chamber and secondary dilution have been compared to real-world studies, the dilution system has been observed to mimic the real-world nanoparticle formation reasonably well [23,24]. This was the reason to use this dilution system in this study also; we aimed to get

information about the effects of the exhaust after-treatment on the real particle emissions. In the other primary diluter, the hot ejector, the dilution air temperature was set to 250 °C. A secondary ejector (in room temperature) was installed right after the first ejector in order to cool and dilute the sample appropriate for the aerosol instruments. This dilution pathway is now on called as *double ejector dilution* (DED). In contrary to the system consisting of PTD, ageing chamber and secondary dilution, the DED system enables the study of non-volatile particles, since the high temperature of primary dilution air reduces the nucleation and condensation of semi-volatile compounds by decreasing significantly the vapour pressures of semi-volatile compounds before the decrease of sample temperature. After the dilution setups a thermodenuder (TD), with low nanoparticle losses [25] operated at 265 °C, was used occasionally. The TD allows the study of particle volatility when the PTD dilution is used. The dilution ratio corrections were calculated according to measured CO_2 concentrations from the tailpipe and diluted sample.
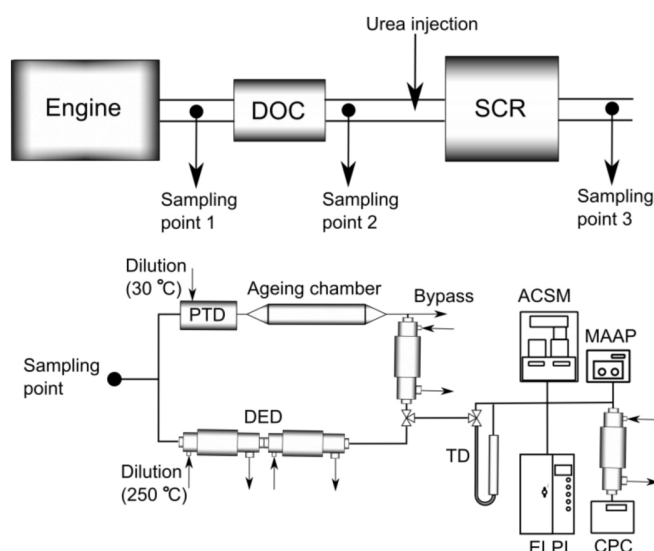

Figure 2. Experimental setup describing three sampling points, dilution setups and aerosol instruments. See text for more details.

After sampling, the aerosol particles were measured with following instruments: an ELPI (Electrical low pressure impactor, Dekati Ltd.) with a filter stage and improved nanoparticle size resolution [26,27,28], a CPC (Condensation particle counter, ultrafine CPC model 3025, TSI Inc.), an ACSM (Aerosol chemical speciation monitor, Aerodyne Research Inc.) and a MAAP (Multi-angle absorption photometer, Thermo Electron Corporation). Both the ELPI and CPC measured the particle number concentration ($\#/cm^3$) in real-time (1 s time resolution) with different minimum particle size detection limits; around 7 nm and 2.5 nm, respectively. The ELPI also measures the particle number size distribution (7 nm - 10 μm). There was an ejector

(dilution ratio 8) placed in front of the CPC to avoid the exceeding of the maximum concentration limit (100 000 #/ cm^3) of the instrument.

The ACSM is an instrument that characterizes and monitors the mass and chemical composition of non-refractory submicron particulate matter in real time [29]. It measures particulate inorganic components, nitrate, sulfate, ammonium and chloride, and the total amount of organic compounds in particles. An aerodynamic lens is used to sample and focus submicron particles into the ACSM. The 50% transmission range of the lens is 75-650 nm [30]. Aerosol mass concentrations measured by the ACSM need to be corrected for particle collection efficiency (CE). CE values can be less than 1 due to collection losses at the vaporizer from inefficient focusing of non-spherical particles, particle losses at the vaporizer because of bouncing of solid particles, and particle losses in the aerodynamic inlet as a function of particle diameter [31]. As the ACSM use the identical aerodynamic lens and vaporizer design used in Aerodyne aerosol mass spectrometer (AMS) [32] similar CE values to those observed in the AMS measurements can be expected. The large database of AMS field results indicates that a CE value of 0.5 gives AMS mass concentrations for ambient particles to within 25% of those measured by collocated instruments [33]. Because of that, a CE of 0.5 was used also in this study for the ACSM data. The ACSM was used only when the PTD system was used in particle sampling and dilution. Each ACSM measurement consisted of three TCTCs averaged together, resulting in the time-resolution of ~15 minutes.

The MAAP was used to measure the soot content of the exhaust particles. Empirically determined mass-specific aerosol absorption coefficient (σ_{abs}) of 6.6 m^{2}g^{-1} is used in the MAAP in order to get soot concentrations in μg m^{-3}. The data averaging time for the MAAP was 1 min and the flow rate varied from 6.7 to 7.5 l/min. A cyclone with a cut-off size of 1 μm was used prior to the MAAP in order to remove large particles. A more detailed description of the MAAP is given in the literature [34,35].

In summary, the instrumentation for the study was chosen so that it produced versatile information about the exhaust particle population and about the effects of exhaust after-treatment on it. Using the CPC and ELPI we got information on the particle number, using the ELPI also on particle size distribution. Combining the ACSM and MAAP we measured the particle composition, and when all particle number, size distribution and composition measurements were combined together with knowledge related to exhaust dilution systems, we got information on the formation of particulate matter. It should be noted that all the instruments produced their data on-line. Therefore this kind of measurement system is suitable on the rapid screening and development work related to vehicle technologies.
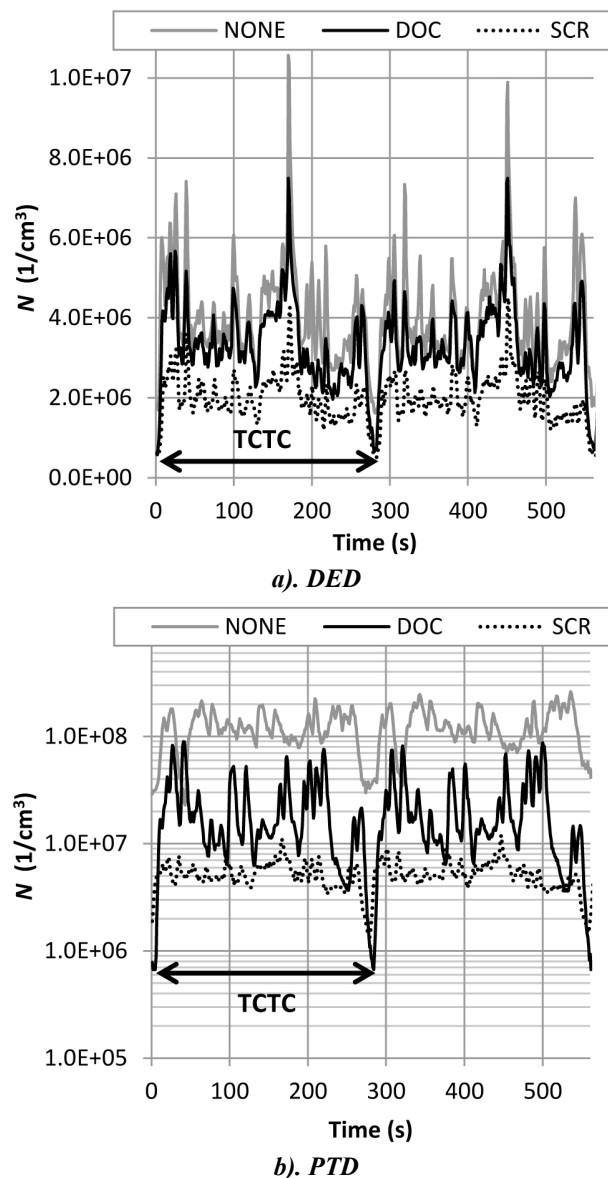
RESULTS

a). DED

b). PTD

Figure 3. Total particle number concentration with the a) DED dilution and b) PTD dilution measured with the CPC during two consecutive example TCTCs and with three exhaust after-treatments: NONE, DOC and DOC +SCR.

Figure 3 shows the total particle number concentrations during two example TCTCs. The upper part (Figure 3a) shows the concentrations measured after the DED system, Figure 3b the concentrations after the PTD system without the thermodenuder. Concentrations were measured using the CPC and thus they cover the exhaust particles larger than 2.5 nm in diameter. Three results can be observed. At first, in all the measurements, the exhaust particle number concentration varied strongly. This variation was caused mainly by rapid changes in engine torque during the TCTC. The variation was

highly repeatable resulting in practically identical concentration from a cycle to another and even from a day to another. Secondly, it can be seen that the choice of the sampling system affected the particle concentrations greatly. In the PTD system, the semi-volatile nucleation mode formation and condensation of semi-volatile compounds on existing non-volatile particles is possible, but in the DED system these processes have been suppressed. Thus based on the results in Figure 3, the exhaust particle number depends on the gas-to-particle conversion processes of semi-volatile compounds in exhaust dilution and cooling. Thirdly, it can be seen that the exhaust after-treatment had extremely high effect on exhaust particle number concentration, almost two orders of magnitude when measured after the PTD system. The effects were reductive so that both the DOC and the SCR decreased the concentrations. In addition, it can be seen that the DOC and the SCR reduced both the non-volatile particle concentrations (DED dilution, Figure 3a) and total particle concentrations and the effects were qualitatively similar throughout the cycle. It can be seen also that the exhaust after-treatment affected the variation of particle concentrations, both absolute values (seen in Figure 3) and relative values (showed as standard deviations in Figure 4). Combining these three results, it seems that both the DOC and the SCR affect the semi-volatile exhaust compounds so that the formation of new particles during the exhaust cooling is reduced. However, it should be noted that semi-volatile compounds can also condensate on existing particles affecting particle sizes and thus also on particle losses in sampling line. Because of that, the particle concentration measured with different sampling and dilution setups are not fully comparable.

Dilution ratio corrected number concentration ($\#/cm^3$) averages (arithmetic mean) over the TCTC are shown in Figure 4. With the DED sampling and CPC (Figure 4a), the DOC reduced total particle number concentration/emission ($D_p > 2.5$ nm) 17.7% and the DOC+SCR 50.8%. The particle number reduction rates were larger with the PTD (Figure 4b), 82.5% for the DOC and 95.7% for the DOC+SCR. The standard deviation of concentrations was significantly the largest with the PTD & DOC, ~80% of the average number concentration; otherwise the deviation was 25-40% of the average concentrations.

The particle size distributions measured using the ELPI (Figure 5) show typical diesel exhaust particle size distributions; most of the particles were smaller than 100 nm in aerodynamic diameter and the size distributions consisted of one or two modes. The nucleation mode particles, observed only with the PTD sampling, were smaller than soot mode particles. In addition, the existence and particle size of the nucleation mode was affected by the after-treatment; the highest concentrations were at the extra stage of ELPI (17-29 nm) without after-treatment and at the filter stage (7-17 nm) with the DOC. Additionally, after the SCR there was no nucleation mode in the measurement range of the ELPI. The

highest soot mode particle concentrations, with the DED, were seen on the extra stage (17-29 nm). The relatively small soot mode mean diameter is in agreement with the study by Lähde et al. 2011, where the soot mode GMD was under 40 nm when high fuel injection pressure was used with similar diesel engine. It is important to note that the soot mode number concentration was not much affected by the exhaust after-treatment. Instead, the size of the soot particles was affected by semi-volatile compounds.
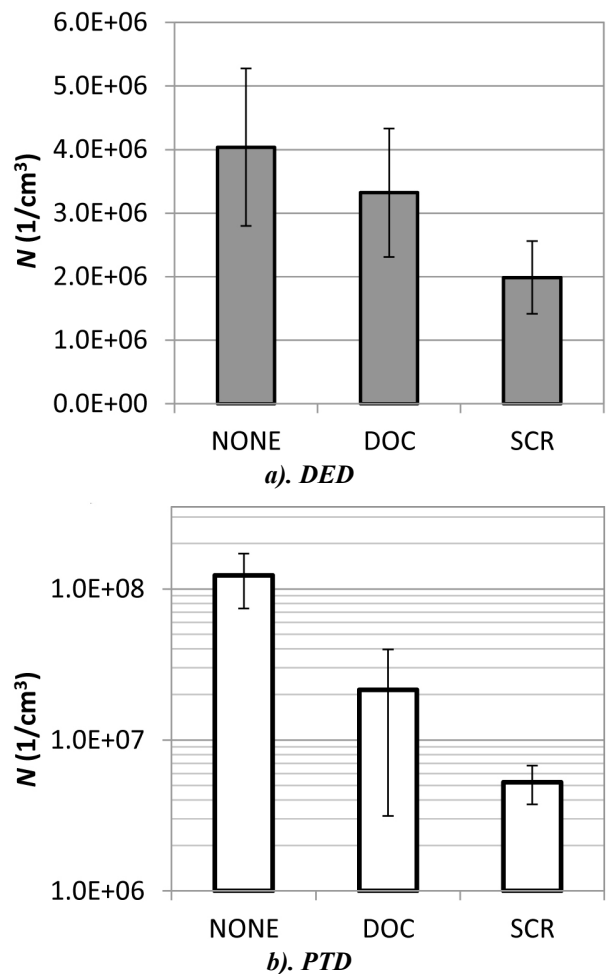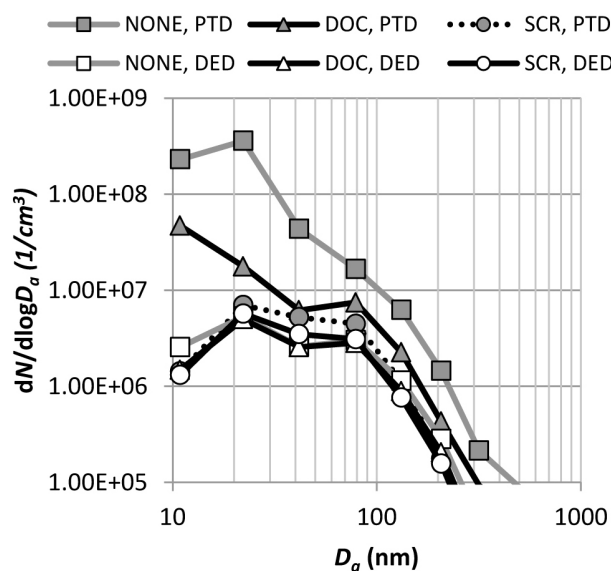

Figure 4. Particle number concentration ($D_p > 2.5$ nm) averages with standard deviations over the TCTC cycle and with the a) DED and b) PTD dilution measured with the CPC.

Results in Figure 3a and Figure 4a indicate a reductive effect of the exhaust after-treatment on non-volatile particle number concentrations. Concentrations were measured using the CPC. However, seen in the exhaust particle size distributions in Figure 5 with the DED sampling and measured with the ELPI, the soot particle concentrations were practically not influenced by the after-treatment at all. The total particle number reduction caused by the DOC+SCR after-treatment of detectable particles for the ELPI was only ~10%. The main difference between these two particle instruments, the CPC and the ELPI, is the detection limit for the smallest particles. The CPC is able to detect particles larger than 3 nm and the ELPI particles larger than 7 nm. The detection limit for the ELPI comes from the small diffusion charging probability of smaller particles. The result indicates that during the cycle there are substantial amounts of particles in the exhaust gas that the ELPI is unable to detect but the CPC is, and the exhaust after-treatment seems to affect those particles. This phenomenon was consistent throughout all the experiments and was also observed when the PTD sampling was used with the TD. It is possible that the difference exists due to very small non-volatile core particles [8,9,10] existing in undiluted exhaust. If so, results indicate that these small particles with high diffusion coefficient are collected or removed by other means in the screens of the DOC and SCR. If the core particle mode exists during the TCTC, similarly as in several other studies, it could explain the origin of nucleation mode without exhaust after-treatment and with the DOC.

Without exhaust after-treatment, the exhaust particles were mostly composed of organics and soot, measured by the ACSM and MAAP, respectively. The mass concentration as well as the chemistry of particles changed due to the after-treatment. Without after-treatment, the fraction of organics dominated the submicron particle mass (81%; Fig. 6a). Organic compounds were oxidized in the DOC and SCR so that their contribution on mass emission reduced to 53% after the DOC and 37% after the SCR. The amount of soot remained the same after the DOC and SCR. After the SCR, the concentration of total organics was 15% of that without the after-treatment, and soot constituted a larger portion of the particle mass (63%) than organics. The concentrations of particulate inorganic components (nitrates, sulfates, ammonium and chlorides) were below the detection limit of the instrument.

The volatility of organics was investigated by using a thermodenuder. In the TD (temperature 265 °C), semi-volatile organics (and other semi-volatile compounds) are evaporated from the particles whereas soot and low-volatility compounds remain in the particle phase. The volatility of organics was found to decrease because of the after-treatment devices. Without after-treatment, most of the organics were semi-volatile (84%; Figure 6b). After the DOC, organics consisted of nearly equal fractions of semi-volatile and non-volatile components (53% and 47%, respectively). The decrease in the total concentration of organics was caused

dominantly by semi-volatile components. After the DOC and SCR only a small portion (3%) of organics was made of semi-volatile compounds. After the DOC and SCR the concentrations of non-volatile and semi-volatile organics were 92% and 0.5% of those without the after-treatment, respectively.
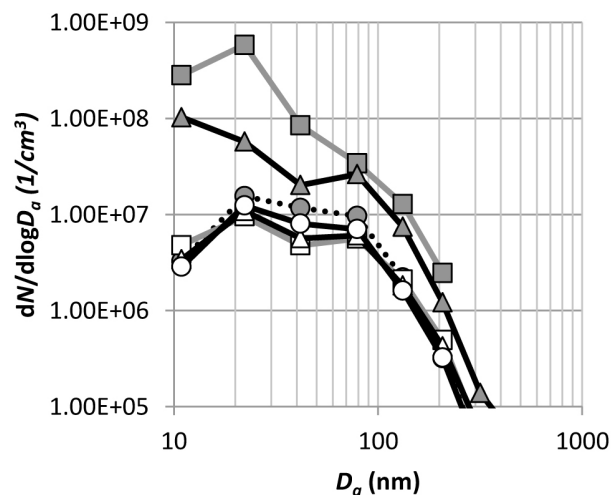
Figure 5. Particle size distributions measured with the ELPI a) on average over the TCTC and b) at the time of the maximum particle number concentration (165 s).
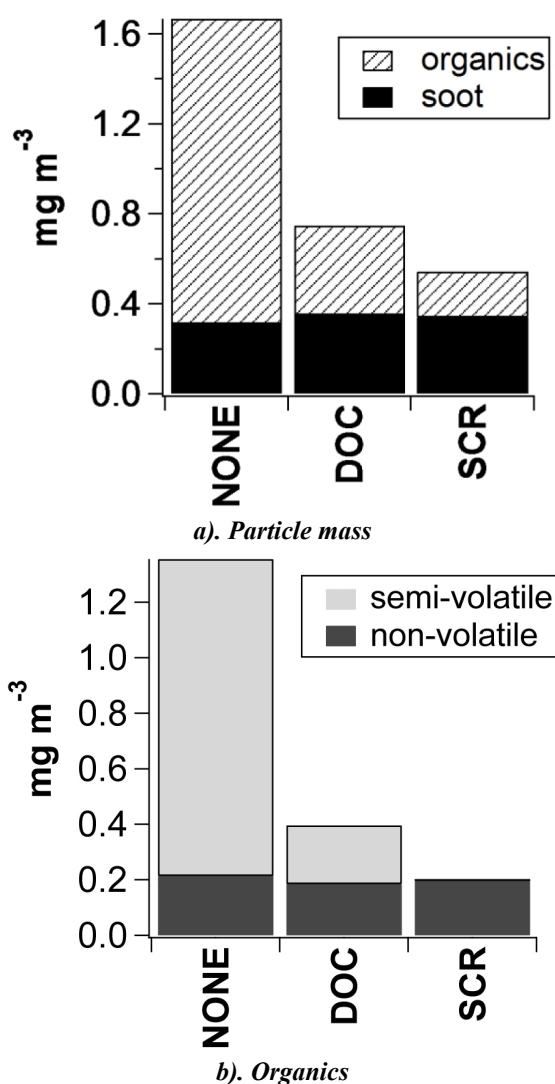
a). Particle mass

b). Organics

Figure 6. The effect of after-treatment on the mass concentration and chemical composition (a) and the volatility of organics (b) in submicrometer particles. In (a) "organics" means total organics observed by the ACSM. In (b) "semi-volatile" organics indicates the fraction that is reduced by the TD and "non-volatile" organics the fraction that remains in the particle phase after the TD treatment.

DISCUSSION AND SUMMARY

Results indicate that the soot particle concentrations and the soot emissions were not affected by the exhaust after-treatment. Instead, the exhaust after-treatment affected significantly the semi-volatile particle compounds; nucleation mode particle emission and concentrations and semi-volatile compounds on soot particles. These semi-volatile compounds were mostly organics. Organics in particle phase were reduced efficiently due to the use of the DOC and DOC +SCR. It should be noted that the effect of after-treatment on

organics was qualitatively similar as on nucleation mode particle number. Thus, organics seem to have a role in nucleation mode appearance. This is in line with previous studies (e.g. [8]) where the nucleation mode particle growth has been strongly affected by hydrocarbon compounds, although the current study cannot confirm or exclude the role of the hydrocarbons in the nucleation. Also, we do not have any indication about promoted nucleation caused by excess ammonia due to the use of the SCR. Instead there is an indication that undiluted exhaust carried small nucleation mode core particles smaller than 7 nm in size. According to literature and authors' knowledge, the high nucleation mode particle concentrations without exhaust after-treatment can be explained by the existence of core particles in undiluted exhaust. Thus also in this study the high nucleation mode particle concentration without exhaust after-treatment could be due to the existence of core particles and their growth in cooling dilution. This study was focused on particles during transient test cycle. Therefore phenomena in particle formation can differ from those observed at steady state driving modes. Also it should be kept in mind that these measurements covered very narrow operation temperature window from the viewpoint of the SCR; the exhaust temperature in the SCR varied between 232-246 °C. Thus e.g. at high load conditions the results can be very different. In temperatures above 380 °C, the SCR has previously observed to increase particle number emissions [14,15].

To summarize, the after-treatment devices reduced particle concentrations overall. The non-volatile particle concentrations were decreased 17.7% and 50.8% due to the use of DOC and DOC+SCR, respectively. The particle number reduction rates were larger when the formation of semi-volatile particle fraction was enabled; decreases were 82.5% for the DOC and 95.7% for the DOC+SCR. Without after-treatment, the fraction of organics dominated the particle mass (81%). Organic compounds were oxidized in the DOC and SCR so that their contribution on mass emission reduced to 53% after the DOC and 37% after the SCR. The exhaust after-treatment affected also organic fraction volatility; without after-treatment most organics were semi-volatile (84%), after the DOC organics consisted of nearly equal fractions of semi-volatile and non-volatile components (53% and 47%, respectively), and after the DOC and SCR only a very small portion (3%) of organics was composed of semi-volatile compounds. The concentrations of non-volatile and semi-volatile organics were 92% and 0.5% of those without the after-treatment, respectively.

Online aerosol mass spectrometers have not been used widely in engine exhaust studies. However, clearly the mass spectrometer methods can produce efficiently information on how the engine and vehicle technologies affect particle emission. In addition, clearly the best results can be achieved when the mass spectrometer measurements are combined with other real-time and online exhaust particle measurements, and with well-defined and well-known exhaust particle sampling and dilution methods.

REFERENCES

1. Wehner, B.; Birmili, W.; Gnauk, T.; Wiedensohler, A. Particle number size distributions in a street canyon and their transformation into the urban-air background: Measurements and a simple model study. *Atmospheric Environment* 2002, 36, 2215-2223.
2. Ketzel, M.; Wåhlin, P.; Berkowicz, R.; Palmgren, F. Particle and trace gas emission factors under urban driving conditions in Copenhagen based on street and roof-level observations. *Atmospheric Environment* 2003, 37, 2735-2749.
3. Longley, I.; Gallagher, M.; Dorsey, J.; Flynn, M.; Allan, J.; Alfarra, M.; Inglis, D. A case study of aerosol (4.6 nm < Dp < 10 μm) number and mass size distribution measurements in a busy street canyon in Manchester, UK. *Atmospheric Environment* 2003, 37, 1563-1571.
4. Pirjola, L.; Paasonen, P.; Pfeiffer, D.; Hussein, T.; Hämeri, K.; Koskentalo, T.; Virtanen, A.; Rönkkö, T.; Keskinen, J.; Pakkanen, T. Dispersion of particles and trace gases nearby a city highway: mobile laboratory measurements in Finland, *Atmospheric Environment* 2006, 40, 867-879.
5. Kittelson, D., Johnson, J., Watts, W., Wei, Q. et al., "Diesel Aerosol Sampling in the Atmosphere," SAE Technical Paper 2000-01-2212, 2000, doi:10.4271/2000-01-2212.
6. Dockery, D.; Pope, A.; Xu, X.; Spengler, J.; Ware, J.; Fay, M.; Ferris, B.; Speizer, F. An Association between Air Pollution and Mortality in Six U.S. Cities. *The New England Journal of Medicine* 1993, 329, 1753-1759.
7. Kittelson, D.B. Engines and nanoparticles: a review, *Journal of Aerosol Science* 1998, 29, 5-6, 575-588.
8. Rönkkö, T.; Virtanen, A.; Kannosto, J.; Keskinen, J.; Lappi, M.; Pirjola, L. Nucleation mode particles with a nonvolatile core in the exhaust of a heavy duty diesel vehicle. *Environ. Sci. Technol.* 2007, 41, 6384-6389.
9. Lähde, T.; Rönkkö, T.; Virtanen, A.; Schuck, T. J.; Pirjola, L.; Hämeri, K.; Kulmala, M.; Arnold, F.; Rothe, D.; Keskinen, J. Heavy Duty Diesel Engine Exhaust Aerosol Particle and Ion Measurements. *Environ. Sci. Technol.* 2009, 43, 163-168.
10. Filippo, A. D.; Maricq, M. M. Diesel Nucleation Mode Particles: Semi-volatile or Solid? *Environ. Sci. Technol.* 2008, 42, 7957-7962.
11. Heikkilä, J.; Rönkkö, T.; Lähde, T.; Lemmetty, M.; Arffman, A.; Virtanen, A.; Keskinen, J.; Pirjola, L.; Rothe, D. Effect of open channel filter on particle emissions of modern diesel engine. *Journal of the Air & Waste Management Association* 2009, 59 (10), 1148.
12. Lähde, T.; Rönkkö, T.; Happonen, M.; Söderström, C., Virtanen, A.; Solla, A.; Kytö, M.; Rothe, D; Keskinen, J. Effect of Fuel Injection Pressure on a Heavy-Duty Diesel Engine Non-volatile Particle Emission. *Environ. Sci. Technol.* 2011.
13. Johnson, T. V. Review of diesel emissions and control, *International Journal of Engine Research* 2009, 10(5), 275-285.
14. Thiruvengadam, A.; Besch, M.; Carder, D.; Oshinuga, A.; Gautam, M. Influence of Real-World Engine Load Conditions on Nanoparticle Emissions from a DPF and SCR Equipped Heavy-Duty Diesel Engine. *Environ. Sci. Technol.* 2012.
15. Herner, J.; Hu, S.; Robertson, W.; Huai, T.; Chang, M.-C.; Rieger, P.; Ayala, A. Effect of Advanced Aftertreatment for PM and NOx Reduction on Heavy-Duty Diesel Engine Ultrafine Particle Emissions. *Environ. Sci. Technol.* 2011, 45, 2413-2419.
16. Herner, J.; Hu, S.; Robertson, W.; Huai, T.; Collins, J.; Dwyer, H.; Ayala, A. Effect of Advanced Aftertreatment for PM and NOx Control on Heavy-Duty Diesel Truck Emissions. *Environ. Sci. Technol.* 2009, 43, 5928-5933.
17. Krahl, J.; Munack, A.; Grope, N.; Ruschel, Y.; Schröder, O.; Bünger, J. Biodiesel, Rapeseed Oil, Gas-To-Liquid, and a Premium Diesel Fuel in Heavy Duty Diesel Enginens: Endurance, Emissions and Health Effects. *Clean* 2007, 35(5), 417-426.
18. Hu, S.; Herner, J.; Shafer, M.; Robertson, W.; Schauer, J.; Dwyer, H.; Collins, J.; Huai, T.; Ayala, A. Metals emitted from heavy-duty diesel vehicles equipped with advanced PM and NOx emission controls. *Atmospheric Environment* 2009. 43, 2950-2959.
19. Lemmetty, M.; Vehkamäki, H.; Virtanen, A.; Kulmala, M.; Keskinen, J. Homogeneous ternary H_2SO_4-NH_3-H_2O nucleation and diesel exhaust: a classical approach. *Aerosol and Air Quality Research* 2007, 7, 489-499.
20. Mikkanen, P., Moisio, M., Keskinen, J., Ristimäki, J. et al., "Sampling Method for Particle Measurements of Vehicle Exhaust," SAE Technical Paper 2001-01-0219, 2001, doi:10.4271/2001-01-0219.
21. Mathis, U.; Ristimäki, J.; Mohr, M.; Keskinen, J.; Ntziachristos, L.; Samaras, Z.; Mikkanen, P. Sampling Conditions for the Measurement of Nucleation Mode Particles in the Exhaust of a Diesel Vehicle, *Aerosol Science and Technology* 2004, 38, 1149-1160.
22. Karjalainen, P., Heikkila, J., Ronkko, T., Keskinen, J. et al., "Effect of Exhaust Flow Conditions and External Cooling on the Performance of the Particle Oxidation Catalyst (POC)," SAE Technical Paper 2010-01-2158, 2010, doi:10.4271/2010-01-2158.
23. Rönkkö, T.; Virtanen, A.; Vaaraslahti, K.; Keskinen, J.; Pirjola, L.; Lappi, M. Effect of dilution conditions and driving parameters on nucleation mode particles in diesel exhaust: laboratory and on-road study. *Atmospheric Environment* 2006, 40, 2893-2901.
24. Keskinen, J.; Rönkkö, T. Can Real-World Diesel Exhaust Particle Size Distribution be Reproduced in the Laboratory? A Critical Review. *Journal of the Air & Waste Management Association* 2010, 60, 1245-1255.
25. Rönkkö, T.; Arffman, A.; Lähde, T.; Karjalainen, P.; Heikkilä, J.; Pirjola, L.; Rothe, D. and Keskinen, J. (2011) Diesel exhaust nanoparticle volatility studies by a new thermodenuder with low solid nanoparticle losses, *15th ETH Conference on Combustion Generated Nanoparticles*.
26. Keskinen, J.; Pietarinen, K.; Lehtimäki, M. Electrical low pressure impactor. *Journal of Aerosol Science* 1992, 23, 4, 353-360.
27. Marjamäki, M., Ntziachristos, L., Virtanen, A., Ristimäki, J. et al., "Electrical Filter Stage for the ELPI," SAE Technical Paper 2002-01-0055, 2002, doi:10.4271/2002-01-0055.
28. Yli-Ojanperä, J., Kannosto, J.; Marjamäki, M.; Keskinen, J. Improving the Nanoparticle Resolution of the ELPI. *Aerosol and Air Quality Research.* 10, 360-366, 2010.
29. Ng, N.L.; Herndon, S.C.; Trimborn, A.; Canagaratna, M.R.; Croteau, P.L.; Onasch, T.B.; Sueper, D.; Worsnop, D.R.; Zhang, Q.; Sun, Y.L. and Jayne, J.T. An Aerosol Chemical Speciation Monitor (ACSM) for Routine Monitoring of the Composition and Mass Concentrations of Ambient Aerosol, *Aerosol Sci. Technol.* 2011, 45, 770-784.
30. Liu, P.S.K.; Deng, R.; Smith, K.A.; Williams, L.R.; Jayne, J.T.; Canagaratna, M.R.; Moore, K.; Onasch, T.B.; Worsnop, D.R. and Deshler, T. Transmission Efficiency of an Aerodynamic Focusing Lens System: Comparison of Model Calculations and Laboratory Measurements for the Aerodyne Aerosol Mass Spectrometer. *Aerosol Sci. Technol.* 2007, 41, 721-733.
31. Matthew, B. M.; Middlebrook, A. M., and Onasch, T. B. Collection Efficiencies in an Aerodyne Aerosol Mass Spectrometer as a Function of Particle Phase for Laboratory Generated Aerosols, *Aerosol Sci. Technol.* 2008, 42, 884-898.
32. Jayne, J. T.; Leard, D. C.; Zhang, X.; Davidovits, P.; Smith, K. A.; Kolb, C. E., and Worsnop, D. R. Development of an Aerosol Mass Spectrometer for Size and Composition, Analysis of Submicron Particles, *Aerosol Sci. Technol.* 2000, 33, 49-70.
33. Canagaratna, M. R.; Jayne, J. T.; Jimenez, J. L.; Allan, J. D.; Alfarra, M. R.; Zhang, Q.; Onasch, T. B.; Drewnick, F.; Coe, H.; Middlebrook, A.; Delia, A.; Williams, L. R.; Trimborn, A. M.; Northway, M. J.; DeCarlo, P. F.; Kolb, C. E.: Davidovits, P., and Worsnop, D. R. Chemical and Microphysical Characterization of Ambient Aerosols with the Aerodyne Aerosol Mass Spectrometer, *Mass Spectrometry Reviews* 2007, 26, 185-222.
34. Petzold, A. and Schönlinner, M. Multi-angle absorption photometry - a new method for the measurement of aerosol light absorption and atmospheric black carbon. *J. Aerosol Sci.* 2004, 35, 421-441.
35. Petzold, A.; Kramer, H. and Schönlinner, M. Continuous Measurement of Atmospheric Black Carbon Using a Multi-angle Absorption Photometer. *Environ Sci & Pollut Res.* 2002, 4, 78-82.

CONTACT INFORMATION

Panu Karjalainen
panu.karjalainen@tut.fi

Sanna Saarikoski
sanna.saarikoski@fmi.fi

Liisa Pirjola
liisa.pirjola@metropolia.fi

ACKNOWLEDGMENTS

DEFINITIONS/ABBREVIATIONS

ACSM - Aerosol chemical speciation monitor

CPC - Condensation particle counter

D_a - Particle aerodynamic diameter

DOC - Diesel oxidation catalyst

D_p - Particle diameter

DPF - Diesel particulate filter

ELPI - Electrical low pressure impactor

DED - Double ejector dilution

MAAP - Multi-angle absorption photometer

NONE - Without after-treatment

PTD - Porous tube diluter

SCR - Selective catalytic reduction

SP - Sampling point

TD - Thermodenuder

Paper 2

Panu Karjalainen, Topi Rönkkö, Liisa Pirjola, Juha Heikkilä, Matti Happonen, Frank Arnold, Dieter Rothe, Piotr Bielaczyc and Jorma Keskinen. Sulfur Driven Nucleation Mode Formation in Diesel Exhaust under Transient Driving Conditions. *Environmental Science & Technology*, 2014, 48, 2336–2343, doi: 10.1021/es405009g.

Sulfur Driven Nucleation Mode Formation in Diesel Exhaust under Transient Driving Conditions

Panu Karjalainen,[†] Topi Rönkkö,[*,†] Liisa Pirjola,[‡] Juha Heikkilä,[†] Matti Happonen,[†] Frank Arnold,[§] Dieter Rothe,[∥] Piotr Bielaczyc,[⊥] and Jorma Keskinen[†]

[†]Aerosol Physics Laboratory, Department of Physics, Tampere University of Technology, Tampere 33720, Finland

[‡]Department of Technology, Metropolia University of Applied Sciences, P.O. Box 4000, FIN-00180 Helsinki, Finland

[§]Atmospheric Physics Division, Max Planck Institute for Nuclear Physics (MPIK), P.O. Box 103980, D-69029 Heidelberg, Germany

[∥]MAN Truck & Bus AG, EPRE - Engineering Powertrain Research Exhaust Aftertreatment, Vogelweiherstrasse 33, 90441 Nürnberg, Germany

[⊥]BOSMAL Automotive Research and Development Institute Ltd., Bielsko-Biala 43-300, Poland

S *Supporting Information*

ABSTRACT: Sulfur driven diesel exhaust nucleation particle formation processes were studied in an aerosol laboratory, on engine dynamometers, and on the road. All test engines were equipped with a combination of a diesel oxidation catalyst (DOC) and a partial diesel particulate filter (pDPF). At steady operating conditions, the formation of semivolatile nucleation particles directly depended on SO_2 conversion in the catalyst. The nucleation particle emission was most significant after a rapid increase in engine load and exhaust gas temperature. Results indicate that the nucleation particle formation at transient driving conditions does not require compounds such as hydrocarbons or sulfated hydrocarbons, however, it cannot be explained only by the nucleation of sulfuric acid. A real-world exhaust study with a heavy duty diesel truck showed that the nucleation particle formation occurs even with ultralow sulfur diesel fuel, even at downhill driving conditions, and that nucleation particles can contribute 60% of total particle number emissions. In general, due to sulfur storage and release within the exhaust aftertreatment systems and transients in driving, emissions of nucleation particles can even be the dominant part of modern diesel vehicle exhaust particulate number emissions.
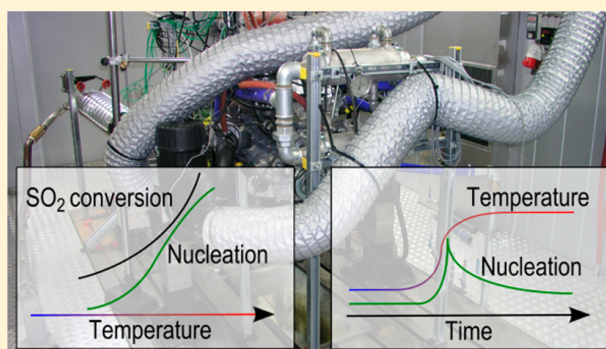
INTRODUCTION

Air quality and traffic-related emissions have been a major concern during recent decades, and in developing countries especially, air quality problems may even increase in the future. High particulate matter concentrations, together with high concentrations of sulfur compounds in urban air are associated with increased human morbidity and mortality.[1] The World Health Organization (WHO) has recently updated the classification for diesel exhaust to be *carcinogenic* to humans, whereas previously it was considered as *probably carcinogenic*.[2] From the human health point of view, traffic-related emissions are of particular importance, since the source is in our immediate environment. Fuel sulfur content (FSC) affects the number concentration of exhaust particles,[3−6] and the physical and chemical characteristics of particles emitted by vehicles and engines, and may also affect the particle formation processes in the atmosphere on longer time scales. Although the limits for FSC have become stricter globally and the advantages of sulfur free fuels are well-known, in several areas, FSC has remained high. For example, in the largest developing countries, such as

Brazil, Russia, India, and China, the amount of sulfur in diesel is generally 1 or 2 orders of magnitude higher than in Europe or the U.S.[7]

Modern diesel vehicles are typically equipped with diesel oxidation catalysts (DOC) to reduce the emissions of hydrocarbons and carbon monoxide; many new road vehicle types are also with equipped diesel particle filters (DPF) to reduce particle emissions. The DOC has not been reported to significantly affect the nonvolatile particle size distribution. Instead, both the DOC and DPF, which often contain catalytic material, can change the semivolatile fraction of exhaust particles via hydrocarbon oxidation and promotion of the conversion of SO_2 to SO_3.[8−10] In the exhaust gas, SO_3 reacts with water molecules forming gaseous sulfuric acid (GSA).[4,5,11] Later, based on both modeling and experimental studies, the

Table 1. Description of Measurements Conducted in the Engine Laboratory, Aerosol Laboratory and On-Road[a]

experiment	engine type	FSC or SO$_2$	ATS	Cpsi	Pgm (g/ft^3)	diameter (mm)	length (mm)
1. aerosol laboratory		SO$_2$ (1.8−61.4 ppm)	pDPF	400	10	29	150
2. engine laboratory, heavy-duty	10.5 l TD on-road engine, Euro 4 level with a pDPF	FSC 36 mg/kg	DOC	200	40	334	75
			pDPF	400	10	334	225
3. engine laboratory, light-duty	1.9 l TD passenger car engine, Euro 4 level	Three FSCs: 6 mg/kg, 65 mg/kg and 340 mg/kg	DOC	200	40	127	74.5
			pDPF	400	10	127	150
4. on-road (chasing), heavy-duty truck	11.7 l, Euro II, mileage 800 000 km	FSC < 10 mg/kg	DOC	120	40	334	74.5
			pDPF (retrofitted)	400	10	334	152

[a]Experiments with engines/vehicles FSC is shown; in the aerosol laboratory setup SO$_2$ concentration is shown. Channels per square inch (cpsi), precious metal content (pgm), diameter, and length of the catalysts are shown. Metal substrates of DOCs and pDPFs were coated with alumina based coatings where Pt was added as the active metal. In experiment 4, the real emission level of the truck is unknown since the DOC and pDPF system was retrofitted.

GSA in diesel exhaust gas can nucleate when the exhaust gas is cooled and diluted in the atmosphere or in a sampling device.[5,11−13] Experimental studies indicate that when the engine or vehicle is equipped with a DOC or another oxidative aftertreatment system, semivolatile *nucleation mode* (NM) particles can exist at high load and high FSC. Instead, without oxidative aftertreatment, the NM did not exist[8,14] or, the NM formation happened due to the formation of so-called nonvolatile core particles.[15] The initial formation of nonvolatile NM core particles seems to take place at high temperatures within the cylinder; the cooling dilution of the exhaust gas only affects the particle growth.[15−17] The sulfur driven nucleation process can be separated from the process based on core particles by measuring particle characteristics or by using a DPF or partial diesel particulate filters (pDPF) in the exhaust line.[11,17] Both of these devices have been observed to efficiently remove the core particles from exhaust.[17−19]

A significant part of particle emissions of traffic originates from diesel passenger cars and light and heavy duty diesel vehicles, especially in the case of those older than Euro 5/Euro VI technology. The particle size distribution of urban air is generally dominated by NM particles, especially near traffic. In urban areas, the highest particle concentrations have typically been observed on roads, highways,[20,21] and in street canyons.[22−24] In comparison, the submicrometer size diesel exhaust particles are typically NM particles of the same size as in the urban atmosphere, or so-called *accumulation mode* (AM) particles.[25] While NM particles have been commonly reported to consist of water, sulfur compounds, and hydrocarbons, AM particles are mainly solid agglomerated soot particles that can contain volatile or semivolatile components (e.g., sulfur compounds, water, hydrocarbons) on their surface. In general, the relative importance of the different exhaust particle modes depends on technologies like fuel injection and exhaust aftertreatment, and driving conditions, but also on the measurement systems used in the studies. For example, although traffic related NM particles frequently dominate particle number in the urban atmosphere, due to their small size and their sensitivity to sampling methods, NM particles have practically not been included in the emission standards of vehicles.

Due to the increased need for emissions reduction, the use of different exhaust aftertreatment devices is becoming more common also in applications where FSC is still high. While the regulated CO and HC emissions are reduced efficiently by oxidation catalysts, the oxidative exhaust aftertreatment may have potential to increase especially the nanoparticle emissions of vehicles by increasing the possibility of sulfur driven NM formation.[26]

In general, some studies[3,6,9,10] have indicated that the exhaust sulfur compounds can be partially stored in the exhaust aftertreatment systems and that these compounds can be released when the exhaust temperature rises. Sulfur has been reported to be stored in the alumina support material in the form of Al$_2$(SO$_4$)$_3$, or by mechanical adsorption of SO$_3$ or H$_2$SO$_4$.[27−29] The release phenomenon is often linked to the regeneration process of a DPF, followed by increased emission of NM particles. In real driving, these sulfur storage and release phenomena can be expected to be common because the engine loading and thus the temperatures of exhaust gas and catalytic converters are continuously changing. It is not yet well-known how often NM particles are emitted in real driving when engines are running with ultralow sulfur diesel.

In this work, we study the effect of these storage and release processes related to fuel sulfur and particle formation and properties of semivolatile nucleation particles. The study includes several experiments. In the aerosol research laboratory study, processes were studied by oxidizing SO$_2$ from pure SO$_2$−air mixture in an oxidative catalyst followed by cooling and dilution of test aerosol. In the diesel engine exhaust measurements, test engines were equipped with a DOC and a pDPF, both using platinum as the catalytic material. The possibility of nonvolatile core particles was excluded by the use of the pDPF. Finally, the exhaust NM particle studies were conducted on-road with a heavy-duty truck using a similar type of exhaust aftertreatment: a combination of a DOC and a pDPF. Similar exhaust aftertreatment is a solution for Euro IV trucks and Euro 3/4 diesel passenger cars, and for vehicles of corresponding emission levels[7] elsewhere, and a significant number of existing vehicles use this technology. In developing countries, high sulfur level fuels are used together with this technology. For nonroad engines, this may be a potential configuration in the future as well, potentially applied together with an SCR system. It should be noted that the most important findings of this work can be generalized for all exhaust aftertreatment systems, including oxidative functions, like the DOC, DPF, and pDPF.

■ EXPERIMENTAL SECTION

The study consisted of four different experiments: (1) laboratory experiments where the sulfur driven nucleation particle formation was simulated using different gas mixtures at highly controlled conditions; (2) engine laboratory experiments conducted with a heavy duty diesel engine on a test bench; (3)

engine laboratory experiments with a passenger car diesel engine on a test bench; and (4) on-road experiments with a heavy duty diesel truck (Table 1). Engine experiments were performed with different FSC levels and under different driving conditions. In all the engine/vehicle measurement experiments, the test engines and vehicles were equipped with a combination of a diesel oxidation catalyst (DOC) and a partial diesel particle filter (pDPF), both having platinum (Pt) as the catalytic active metal within an alumina based washcoat. Thus, the test engines and the test vehicle represented an example of typical modern systems in terms of oxidative conditions. Note that the oxidation conditions of modern Euro 6/VI aftertreatment systems containing a combination of a DOC, an SCR and a DPF can be even more effective than in the aftertreatment system tested here. However, the use of a pDPF ensured that the so-called core particles were removed from the exhaust before dilution, since the particle reduction efficiency of the pDPF is near 100% for particles smaller than 10 nm.[18,19] A short summary of the measurements and details of the catalysts are described in Table 1.

Experiments on engine dynamometers and in the laboratory were conducted using an exhaust sampling and dilution system[30] (porous tube diluter, PTD) observed to mimic the NM particle formation in the real exhaust dilution and cooling process in the atmosphere.[31,32] With the heavy-duty diesel truck (experiment 4), the exhaust particle measurement was conducted by chasing the test truck using the "Sniffer" mobile laboratory van.[33] Particle instrumentation consisted of an electrical low pressure impactor (ELPI, Dekati Oy), two scanning mobility particle sizers (Nano-SMPS and SMPS, TSI Inc.), and a condensation particle counter (CPC, TSI Inc.). The particle volatility was studied in all of the measurements using a thermodenuder (TD) with low nanoparticle losses[34]— 32% and 50% for mobility sizes 10 and 4.5 nm, respectively. In the TD, the diluted exhaust sample is first heated to 265 °C to evaporate the semivolatile compounds from the particles, and after that, the sample is gradually cooled in the denuder part. The denuder section is used to decrease the concentration of evaporated vapors by collecting them in charcoal. In addition, in the heavy-duty diesel engine study (experiment 2) a Chemical Ionization Mass Spectrometer (CIMS) was used to measure the GSA concentration of the hot exhaust gas. Details of the CIMS can be found in Speidel et al. (2007),[35] and the experimental setup here was similar to that employed by Arnold et al. (2012)[5] and Rönkkö et al. (2013).[11] Experimental setups are described in the Supporting Information, SI (Figures S1 and S2).

The aerosol laboratory studies (experiment 1) were performed using different mixtures of SO_2 and filtered air (~5% relative humidity at 25 °C), passing this mixture through heaters and a small scale pDPF, sampling from the test gas by the PTD system, and measuring the particle size distribution with a Nano-SMPS. The small scale pDPF was designed so that the gas flow velocity and residence time were comparable to the real-world application.[18] The SO_2–SO_3 conversion was calculated by measuring the decrease in SO_2 concentration over the pDPF with an FTIR analyzer (Gasmet model DX4000). The test was conducted at a temperature range of 238–412 °C and over the SO_2 concentration range of 1.8–61.4 ppm. If SO_2 is assumed to originate solely from the pure combustion of the fuel, then 1.8 ppm corresponds to FSC = 32 mg/kg and 61.4 ppm corresponds to FSC = 1100 mg/kg.

To study the role of storage and release of sulfur compounds in an oxidative catalyst, there was first a low temperature phase which enabled sulfur compound storage and then the test gas temperature was increased to decompose and desorb the accumulated sulfur species. In experiment 1, an SO_2–air mixture (50 ppm SO_2) was passed through a pDPF at 240 °C at first in order to simulate the adsorption conditions of sulfur compounds. The sulfur storage into the sampling and dilution system was prevented during this storage phase by flushing the PTD with filtered instrument air. After one hour, the SO_2 feed was shut off, the sample flow was taken through the PTD and the temperature of the air flowing through the pDPF was increased to 370 °C. In the engine experiments (2 and 3), the increase in temperatures was caused by increasing the engine load. In the light-duty case, the low-temperature period took 48 h, whereas with the heavy-duty engine the corresponding time was 40 min.

In order to investigate the nucleation independently of exhaust dilution and cooling systems, we studied the exhaust particles of a heavy-duty diesel truck on the road under its real driving and loading on its normal transportation route. This means that the driving conditions changed continuously, mostly depending on the altitude profile of the route (see SI Figure S4). The exhaust residence time in the atmosphere before aerosol sampling was ca. 1.5 s, calculated assuming a vehicle speed 80 km/h and a probe inlet distance from the end of the tailpipe of 34 m. This means that the dilution factor was high and, alternatively, the cooling and the fast gas-to-particle processes like nucleation were completed before sampling took place.[32]

RESULTS AND DISCUSSION

The SO_2–SO_3 conversion in the aerosol laboratory study (experiment 1) was a function of temperature; at 220 °C, the conversion was below 5%, but when the temperature increased to 400 °C, the conversion increased to 50% (Figure 1a). The measured NM concentration (a) and size distributions (b) followed the increasing trend of the SO_2–SO_3 conversion. The SO_2 concentration (Figure 1c) had a similar effect to the temperature (Figure 1b) on the particle size distributions. The higher the concentration or temperature became, the more numerous and the larger the NM particles were detected. The NM was observed to totally vanish in the thermodenuder treatment, which is in line with previous studies.[16,17,36] The charging state of the particles was measured in the aerosol laboratory study (test protocol in SI), and the particles were observed to be electrically neutral which, again, is in line with the earlier engine exhaust studies.[17,37] This indicates that NM particles were formed during dilution with cool air, not in the hot test gas beforehand. There was no NM when the catalyst temperature was below 250 °C.

In Western Europe and North America, FSC is lower than 10 or 15 mg/kg, respectively, and thus the nucleation particle formation presented above could be assumed to be relatively unusual. However, there are some indications that at low exhaust temperatures, sulfur can be stored in the catalyst, and in some circumstances, it can be released. In principle, these releases can cause periods of high sulfur compound emissions—and thus higher particle emissions.

In the aerosol laboratory study (experiment 1) on sulfur storage and release, the NM was not observed immediately after the increase in test gas temperature (Figure 2a). However, when the air temperature increased enough, NM particles were
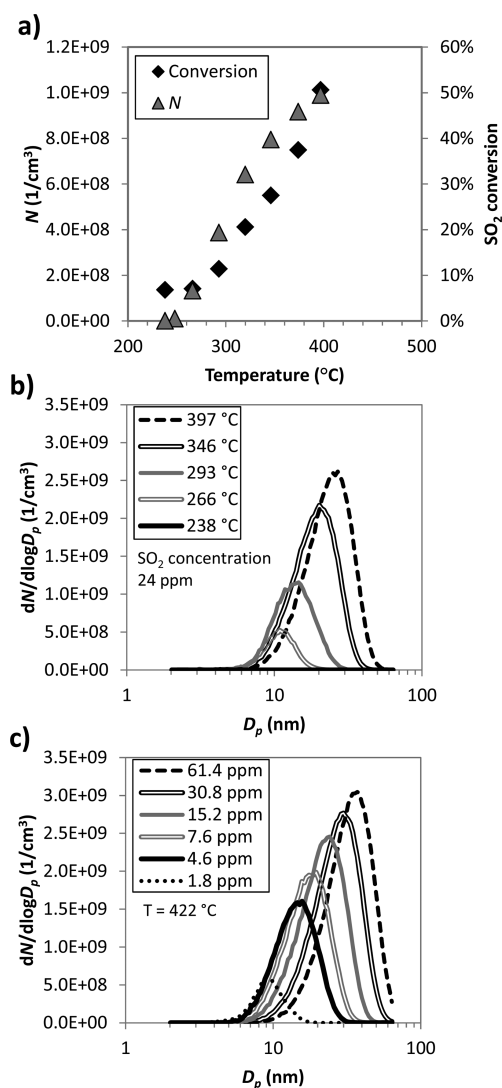
Figure 1. Results of the aerosol laboratory study (experiment 1): (a) The SO_2 conversion and nucleation particle number as a function of temperature, (b) particle number size distributions for various temperatures (SO_2 pre pDPF was 24 ppm), and (c) particle number size distributions for various SO_2 concentrations (temperature was 422 °C).

formed so that the particle number and size reached a maximum after 8 min from the time the heater power was increased. After that, both the particle concentration and the particle size decreased and reached the zero level 45 min after the beginning of the high temperature phase. Both in the heavy-duty (Figure 2b) and light-duty (Figure 2c,d) engine experiments, the NM particle concentration increased from zero to very high values instantly after the increase in engine load and reached its maximum value within a few minutes. After that, the particle concentrations decreased gradually and stabilized. The FSC had an effect on NM particle concentrations and NM stabilization time in the light-duty engine experiments. The NM was present for about 8 min with FSC = 65 mg/kg (Figure 2c), whereas with FSC = 340 mg/kg (Figure 2d) the already stabilized NM was detected after 1 h at the high temperature phase. This experiment was repeated also with FSC = 6 mg/kg, but without the observation of NM
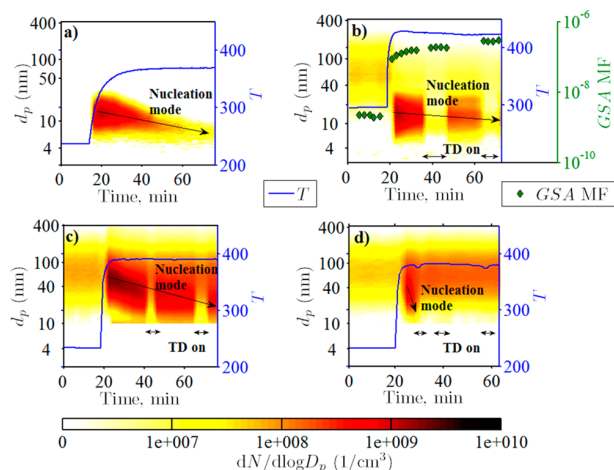

Figure 2. Sulfur-driven NM formation when higher temperature phase followed low temperature phase. The aerosol laboratory experiment in (a) (Nano-SMPS), heavy-duty engine laboratory with FSC = 6 mg/kg in (b) (Nano-SMPS + SMPS) also shown is the GSA concentration, and light-duty engine laboratory tests in (c) for FSC = 340 mg/kg (SMPS) and (d) for FSC = 65 mg/kg (SMPS). Double-ended arrows (TD on) indicate the periods when the diluted exhaust was led through the thermodenuder system (heated to 265 °C).

particles. Thus, the result indicates that a longer loading time or a higher temperature regeneration would have been required for the NM formation with a ultralow sulfur fuel that meets European fuel quality standards. In all the engine experiments, the thermodenuder treatment removed the NM particles so that solely the soot mode was left.

Thus, merging together the aerosol and engine exhaust studies, the results show that sulfur compounds can be stored on the catalyst, and when the catalyst temperature is increased, the sulfur compounds can be released in a form capable of initiating the NM particle formation. This is possible even with ultralow sulfur diesel fuel in the case of a heavy-duty engine. However, in the measurements with a heavy-duty diesel engine (Figure 2b), the concentration of gaseous sulfuric acid (GSA), measured downstream of a heated ejector diluter and a heated transfer tube by a CIMS, did not follow the time behavior of the NM. Instead, the GSA concentration increased relatively rapidly to a mole fraction level above 10^{-7} and after that increased slowly throughout the whole test period. Thus, although the change in engine load affected the GSA, as reported previously (higher load causes higher GSA concentration to the exhaust),[5,11] our results indicate that the NM particle bursts caused by sulfur storage and release may not be caused by solely the GSA.

On the basis of previous laboratory measurements reported by several research groups,[8,9,14,38,39] sulfur-driven nucleation is not a common phenomenon when the FSC is low. However, several studies have been performed at steady state driving conditions, and the results have been affected by the design of sampling system, for example. The results presented above indicated that in addition to the direct conversion of SO_2 to SO_3, the storage and release of sulfur compounds had an effect on the nucleation. In principle, this effect may also make nucleation particle emissions possible with low FSCs.[40]

In experiment 4, the particle concentration of exhaust plume (no dilution ratio correction) measured by the CPC varied over about 3 orders of magnitude (Figure 3). The highest
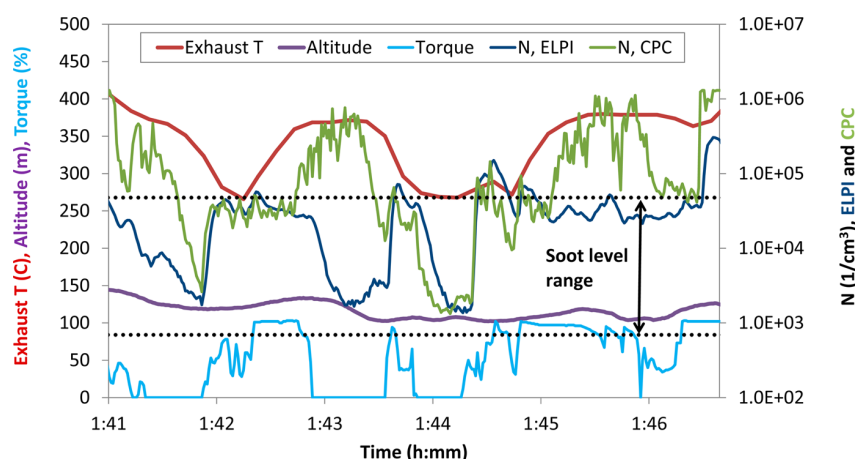
Figure 3. Time-series of the on-road truck chasing study (experiment 4), about 250 km from the terminal in Oulu (SI Figure S4). Dotted lines represent the maximum and minimum soot concentrations, measured through the TD, during the whole test route.

concentration peaks were observed during uphill driving and at the hilltop when the exhaust temperature was above 350 °C. Measured through the TD, the particle concentration was 5×10^4 1/cm^3 at maximum measured during a 15-min-period over a hilly section of the route. In the particle size distribution, these particles formed a typical soot mode. Without the TD, the concentrations even reached a level over 1×10^6 1/cm^3. It can be seen from Figure 3 that when the truck was going downhill and the demanded torque was 0% (at 1:43 AM), the exhaust temperature remained at a high level (375 °C). This is due to the thermal capacity of the engine and exhaust system. The particle concentrations measured by the ELPI decreased, but at the same time, particle concentrations measured by the CPC increased. The measuring range of the ELPI is limited to 7 nm (aerodynamic diameter of particles) and the range of the CPC to 2.5 nm (mobility diameter of particles). Similar behavior was never observed following thermodenuder treatment of the exhaust sample. Thus, the measurements indicate that there was an increased amount of particles below the detection limit of the ELPI, particles were semivolatile NM particles and that the precursors of particles did not originate directly from combustion. It should be noted here that during downhill driving, the fuel consumption was zero (fuel was not injected into the cylinders), and that the downhill driving was conducted systematically with engine braking without the use of the wheel brakes.

Figure 4 shows examples of instantaneous particle size distributions measured during experiment 4. Particle size distributions are shown separately for background aerosol and for exhaust plume aerosol at hilltop driving, at stable driving conditions (flat ground) and during downhill driving. At a hilltop, when the exhaust temperature was at its maximum value, the particulate number was dominated by small semivolatile NM particles. Compared to that, the particle concentration was significantly lower on flat ground; the particle size distribution measured by the ELPI consisted of soot mode only. During downhill driving, right after the hilltop, the particle size distribution consisted only of NM particles. In this case, there were no soot particle emissions since the particle concentration ($D_a > 60$ nm) was at the background level. Occasionally, the nucleation particles formed were smaller than 7 nm in aerodynamic diameter, so that the ELPI was unable to detect them, but the ultrafine condensation particle
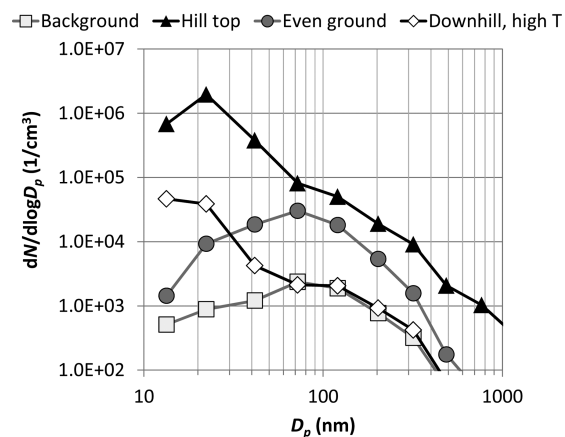

Figure 4. On-road measurement of a heavy-duty diesel truck: background aerosol particle size distribution and examples of instantaneous exhaust plume particle size distributions at different driving conditions.

counter (UCPC) was able to see a NM peak. During an 80 km long hilly test section, the fraction of nucleation particles was calculated to be 60%. The calculation is based on particle concentrations measured by the ELPI so that the TD was used over half of the test section, and the nonvolatile particle losses in the TD were taken into account. For the CPC, we are not able to make the TD loss correction. However, the results shown in Figure 3 indicate that a significant fraction of particles was in the particle sizes below 7 nm. Thus, if the smallest particles are also taken into account, the fraction of semivolatile particles may be significantly larger than 60%.

◼ DISCUSSION

The aerosol laboratory study reported above provided a means to simplify the exhaust system and to study the phenomenological effects of different factors independently. Here we focused on the effects of both SO_2 concentration and SO_2 conversion on the NM formation, and the transient nucleation particle bursts after an increase in the gas temperature. Both the increase of the SO_2 concentration and the increase of the SO_2 conversion enhanced NM particle formation. The NM formed consisted of electrically neutral particles, which were totally

volatile at a TD temperature of 265 °C. Thus, the results supported the earlier observations in engine exhaust studies that the formation of semivolatile and uncharged NM is a sulfur-driven process, and therefore no evidence of ion-induced nucleation during the cooling and dilution was observed. The aerosol study was performed using only filtered air−SO_2 mixtures, and the results indicated that the NM formation did not require compounds such as hydrocarbons, sulfated hydrocarbons, or salts. However, in a larger perspective the NM size, number and particle properties are sensitive to nonvolatile particle and condensable hydrocarbon concentrations,[15,31] and also to changes in gas humidity.[41]

With the DOC or the DPF, the formation of semivolatile NM particles has been reported to take place with moderate or high FSC and at high load.[3,5,8,9,11,14,17,38] In addition, it seems that at high load and during DPF regeneration nucleation can occur even with ultralow FSC fuels.[5,42,43] With the combination of a DOC and a pDPF, the semivolatile NM particle formation was qualitatively similar, as previously reported for the DOC or the DPF. The NM was not observed at low load; but at medium load, the NM was observed with ultralow sulfur diesel fuel for a heavy-duty engine, but not for the light-duty engine. In addition, this result is dependent on the driving history, engine oil sulfur level, oil consumption, and the temperature during regeneration. For instance, here the regeneration temperature was higher for the heavy-duty engine compared to the light-duty engine. Oil consumption may also vary significantly between different engine types, technologies and ages.

Previous studies have indicated that the substrate and support temperature has a crucial role in the means by which sulfur is stored in catalytic converters.[27−29] Sulfur has been reported to be stored in the alumina support in the form of $Al_2(SO_4)_3$ which is thermodynamically stable at low temperatures under lean conditions. The sulfate decomposition from alumina support under lean conditions may start when the temperature is above 400 °C, becoming higher at 600 °C. In the low temperature region, below 350 °C, sulfur storage in catalysts has been previously reported to also happen through the physical adsorption of SO_3 or H_2SO_4 on the substrate surfaces. This sulfur is in loose contact with the walls and easily gets released when the temperature is increased, or possibly when the flow velocity is changed. In this work, the storage phases were carried out at temperatures below 300 °C, most often below 250 °C, which suggests that SO_3 or H_2SO_4 may also adsorb onto the substrate surfaces, in addition to more stable aluminum sulfate species. Adsorbed sulfur may also react with the support to form alumina sulfates during the release phases (temperature near 400 °C). In addition to alumina, the DOC also contained also high surface area support materials (zeolites), which do not form stable sulfates, but may adsorb and desorb SO_x.

The aerosol laboratory study produced strong evidence that the sulfur compounds were stored into the pDPF and that the storage-release and its effect on NM are not measurement artifacts caused by, for example, sulfur storage in the exhaust sampling setup. The engine laboratory studies showed significant emissions of NM particles when the driving condition changed from a low load to a high load. This effect was more intensive when the FSC was higher. Although this behavior seems to be sulfur-driven, the NM formed cannot be explained only by the GSA. For instance, hydrocarbon compound storage, release and chemical transformation (like partial oxidation or formation of organosulfates[5]) in exhaust aftertreatment systems cannot be excluded in NM formation during transients. It has to be noted that, in general, in engine exhaust studies, the sulfur or hydrocarbon compound storage and release in the exhaust sampling lines may also affect the measured NM.

From total particle number emission point of view (including semivolatile particles), the storage and release of sulfur compounds is important; it seems that because of this process, the NM particle formation dominates particle number emissions, even with low FSC. It is arguable that the behavior is similar with other oxidative exhaust aftertreatment systems like older technology containing solely a DOC, and state-of-the-art technologies containing a combination of a DOC and DPF or a DOC, DPF, and SCR. When the DPF is applied, the emissions of NM particles can be even higher because of lower soot particle emissions. In general, semivolatile NM particles are practically not considered in the emission regulations since the NM particle mass is moderately low due to small particle size and they are not counted as particulate number in the European PMP protocol. Finally, the particle number emissions of modern vehicles equipped with oxidative exhaust aftertreatment systems seem to be very significant also during downhill driving, due to the release of semivolatile compounds from the catalyst.

■ ASSOCIATED CONTENT

ⓢ Supporting Information

The experimental setups of laboratory studies (experiments 1−3) (Figure S1). Nucleation mode particle size distributions with and without electrostatic precipitator (Figure S2). The experimental setup of chasing study (experiment 4) (Figure S3). Speed and altitude profiles of the route during on-road truck chasing measurements (Figure S4). This material is available free of charge via the Internet at http://pubs.acs.org.

■ AUTHOR INFORMATION

Corresponding Author
*Tel.: +358 40 198 1019; fax: +358 33 115 3015; e-mail: topi.ronkko@tut.fi.

Author Contributions

The manuscript was written through contributions of all authors. All authors have given approval to the final version of the manuscript.

Notes

The authors declare no competing financial interest.

■ ACKNOWLEDGMENTS

■ REFERENCES

(1) Dockery, D.; Pope, A.; Xu, X.; Spengler, J.; Ware, J.; Fay, M.; Ferris, B.; Speizer, F. An association between air pollution and mortality in six U.S. cities. *New Engl. J. Med.* **1993**, *329*, 1753−1759.

(2) IARC. Press release 213. Diesel Engine Exhaust Carsinogenic, 12/6/2012.

(3) Vaaraslahti, K.; Keskinen, J.; Giechaskiel, B.; Solla, A.; Murtonen, T.; Vesala, H. Effect of lubricant on the formation of heavy duty diesel exhaust nanoparticles. *Environ. Sci. Technol.* **2005**, *39*, 8497−8504.

(4) Arnold, F.; Pirjola, L.; Aufmhoff, H.; Schuck, T.; Lähde, T.; Hämeri, K. First gaseous sulfuric acid measurements in automobile exhaust: Implications for volatile nanoparticle formation. *Atmos. Environ.* **2006**, *40* (37), 7097−7105.

(5) Arnold, F.; Pirjola, L.; Rönkkö, T.; Reischl, U.; Schlager, H.; Lähde, T.; Heikkilä, J.; Keskinen, J. First online measurements of sulfuric acid gas in modern heavy-duty diesel engine exhaust: Implications for nanoparticle formation. *Environ. Sci. Technol.* **2012**, *46*, 11227−11234.

(6) Kittelson, D.; Watts, W.; Johnson, J.; Thorne, C.; Higham, C.; Payne, M.; Goodier, S.; Warrens, C.; Preston, H.; Zink, U.; Pickles, D.; Goersmann, C.; Twigg, M.; Walker, A.; Boddy, R. Effect of fuel and lube oil sulfur on the performance of a diesel exhaust gas continuously regenerating trap. *Environ. Sci. Technol.* **2008**, *42*, 9276−9282.

(7) Dieselnet website, http://www.dieselnet.com/standards/fuels.php, checked 7.1.2014.

(8) Maricq, M.; Chase, R.; Xu, N.; Laing, P. The effects of the catalytic converter and fuel sulphur level on motor vehicle particulate matter emissions: Light duty diesel vehicles. *Environ. Sci. Technol.* **2002**, *36*, 283−289.

(9) Giechaskiel, B.; Ntziachristos, L.; Samaras, Z.; Casati, R.; Scheer, V.; Vogt, R. Effect of speed and speed-transition on the formation of nucleation mode particles from a light duty diesel vehicle. *SAE Tech. Paper Ser.* **2007**, 2007−01−1110.

(10) Herner, J.; Hu, S.; Robertson, W.; Huai, T.; Chang, M.-C.; Rieger, P.; Ayala, A. Effect of advanced aftertreatment for PM and NO$_x$ reduction on heavy-duty diesel engine ultrafine particle emissions. *Environ. Sci. Technol.* **2011**, *45*, 2413−2419.

(11) Rönkkö, T.; Lähde, T.; Heikkilä, J.; Pirjola, L.; Bauschke, U.; Arnold, F.; Schlager, H.; Rothe, D.; Yli-Ojanperä, J.; Keskinen, J. Effects of gaseous sulphuric acid on diesel exhaust nanoparticle formation and characteristics. *Environ. Sci. Technol.* **2013**, *47*, 11882−11889.

(12) Lemmetty, M.; Rönkkö, T.; Virtanen, A.; Keskinen, J.; Pirjola, L. The effect of sulphur in diesel exhaust aerosol: models compared with measurements. *Aerosol Sci. Technol.* **2008**, *42*, 916−929.

(13) Du, H.; Yu, F. Role of the binary H$_2$SO$_4$−H$_2$O homogeneous nucleation in the formation of volatile nanoparticles in the vehicular exhaust. *Atmos. Environ.* **2006**, *40*, 7579−7588.

(14) Vogt, R.; Scheer, V.; Casati, R.; Benter, T. On-road measurement of particle emission in the exhaust plume of a diesel passenger car. *Environ. Sci. Technol.* **2003**, *37*, 4070−4076.

(15) Rönkkö, T.; Virtanen, A.; Kannosto, J.; Keskinen, J.; Lappi, M.; Pirjola, L. Nucleation mode particles with a nonvolatile core in the exhaust of a heavy duty diesel vehicle. *Environ. Sci. Technol.* **2007**, *41*, 6384−6389.

(16) Filippo, A. D.; Maricq, M. M. Diesel nucleation mode particles: Semi-volatile or solid? *Environ. Sci. Technol.* **2008**, *42*, 7957−7962.

(17) Lähde, T.; Rönkkö, T.; Virtanen, A.; Schuck, T. J.; Pirjola, L.; Hämeri, K.; Kulmala, M.; Arnold, F.; Rothe, D.; Keskinen, J. Heavy duty diesel engine exhaust aerosol particle and ion measurements. *Environ. Sci. Technol.* **2009**, *43*, 163−168.

(18) Karjalainen, P.; Heikkilä, J.; Rönkkö, T.; Keskinen, J.; Lehtoranta, K.; Matilainen, P.; Kinnunen, T. Effect of exhaust flow conditions and external cooling on the performance of the particle oxidation catalyst (POC). *SAE Tech. Paper Ser.* **2010**, 2010−01−2158.

(19) Heikkilä, J.; Rönkkö, T.; Lähde, T.; Lemmetty, M.; Arffman, A.; Virtanen, A.; Keskinen, J.; Pirjola, L.; Rothe, D. Effect of open channel filter on particle emissions of modern diesel engine. *J. Air Waste Manage. Assoc.* **2009**, *59* (10), 1148.

(20) Pirjola, L.; Paasonen, P.; Pfeiffer, D.; Hussein, T.; Hämeri, K.; Koskentalo, T.; Virtanen, A.; Rönkkö, T.; Keskinen, J.; Pakkanen, T. Dispersion of particles and trace gases nearby a city highway: Mobile laboratory measurements in Finland. *Atmos. Environ.* **2006**, *40*, 867−879.

(21) Kittelson, D. B.; Johnson, J.; Watts, W.; Wei, Q.; Drayton, M.; Paulsen, D.; Bukowiecki, N. Diesel aerosol sampling in the atmosphere. *SAE Tech. Paper Ser.* **2000**, 2000−01−2212.

(22) Wehner, B.; Birmili, W.; Gnauk, T.; Wiedensohler, A. Particle number size distributions in a street canyon and their transformation into the urban-air background: Measurements and a simple model study. *Atmos. Environ.* **2002**, *36*, 2215−2223.

(23) Ketzel, M.; Wåhlin, P.; Berkowicz, R.; Palmgren, F. Particle and trace gas emission factors under urban driving conditions in Copenhagen based on street and roof-level observations. *Atmos. Environ.* **2003**, *37*, 2735−2749.

(24) Longley, I.; Gallagher, M.; Dorsey, J.; Flynn, M.; Allan, J.; Alfarra, M.; Inglis, D. A case study of aerosol (4.6 nm < D_p < 10 μm) number and mass size distribution measurements in a busy street canyon in Manchester, UK. *Atmos. Environ.* **2003**, *37*, 1563−1571.

(25) Kittelson, D. B. Engines and nanoparticles: A review. *J. Aerosol Sci.* **1998**, *29* (5−6), 575−588.

(26) Liu, H.; Rönkkö, T.; Keskinen, J. Impact of vehicle development and fuel quality on exhaust nanoparticle emissions of traffic. *Environ. Sci. Technol.* **2013**, *47*, 8091−8092.

(27) Horiuchi, M.; Saito, K.; Ichihare, S. Sulfur storage and discharge behavior on flow-through type oxidation catalysts. *SAE Tech. Paper Ser.* **1991**, 910605.

(28) Henk, M.; Williamson, W.; Silver, R. Diesel catalysts for low particulate on low sulfate emissions. *SAE Tech. Paper Ser.* **1992**, 920368.

(29) Kröcher, O.; Widmer, M.; Elsener, M.; Rothe, D. Adsorption and desorption of S$_{ox}$ on diesel oxidation catalysts. *Ind. Eng. Chem. Res.* **2009**, *48*, 9847−9857.

(30) Ntziachristos, L.; Giechaskiel, B.; Pistikopoulos, P.; Samaras, Z.; Mathis, U.; Mohr, M.; Ristimäki, J.; Keskinen, J.; Mikkanen, P.; Casati, R.; Scheer, V.; Vogt, R. Performance evaluation of a novel sampling and measurement system for exhaust particle characterization. *SAE Tech. Paper Ser.* **2004**, 2004−01−1439.

(31) Rönkkö, T.; Virtanen, A.; Vaaraslahti, K.; Keskinen, J.; Pirjola, L.; Lappi, M. Effect of dilution conditions and driving parameters on nucleation mode particles in diesel exhaust: laboratory and on-road study. *Atmos. Environ.* **2006**, *40*, 2893−2901.

(32) Keskinen, J.; Rönkkö, T. Can real-world diesel exhaust particle size distribution be reproduced in the laboratory? A critical review. *J. Air Waste Manage. Assoc.* **2010**, *60*, 1245−1255.

(33) Pirjola, L.; Parviainen, H.; Hussein, T.; Valli, A.; Hämeri, K.; Aalto, P.; Virtanen, A.; Keskinen, J.; Pakkanen, T. A.; Mäkelä, T.; Hillamo, R. E. "Sniffer"—A novel tool for chasing vehicles and measuring traffic pollutants. *Atmos. Environ.* **2004**, *38*, 3625−3635.

(34) Rönkkö, T.; Arffman, A.; Lähde, T.; Karjalainen, P.; Heikkilä, J.; Pirjola, L.; Rothe, D.; Keskinen, J. Diesel exhaust nanoparticle volatility studies by a new thermodenuder with low solid nanoparticle losses, *15th ETH Conference on Combustion Generated Nanoparticles*, 2011.

(35) Speidel, M.; Nau, R.; Arnold, F.; Schlager, H.; Stohl, A. Sulfur dioxide measurements in the lower, middle and upper troposphere: Deployment of an aircraft-based chemical ionization mass spectrometer with permanent in-flight calibration. *Atmos. Environ.* **2007**, *41*, 2427−2437.

(36) Burtscher, H. Physical characterization of particulate emissions from diesel engines: A review. *J. Aerosol Sci.* **2005**, *36*, 896−932.

(37) Maricq, M. M. On the electrical charge of motor vehicle exhaust particles. *J. Aerosol Sci.* **2006**, *37*, 858−874.

(38) Schneider, J.; Hock, N.; Weimer, S.; Borrmann, S.; Kirchner, U.; Vogt, R.; Scheer, V. Nucleation particles in diesel exhaust: Composition inferred from in situ mass spectrometric analysis. *Environ. Sci. Technol.* **2005**, *39*, 6153−6161.

(39) Bielaczyc, P.; Keskinen, J.; Dzida, J.; Sala, R.; Rönkkö, T.; Kinnunen, T.; Matilainen, P.; Karjalainen, P.; Happonen, M.

2342

dx.doi.org/10.1021/es405009g | *Environ. Sci. Technol.* 2014, 48, 2336−2343

Performance of particle oxidation catalyst and particle formation studies with sulphur containing fuels. *SAE Int. J. Fuels Lubr.* **2012**, *5* (2), 2012−01−0366.

(40) Khalek, I. A.; Bougher, T. L.; Merritt, P. M.; Zielinska, B. Regulated and unregulated emissions from highway heavy-duty diesel engines complying with U.S. environmental protection agency 2007 emissions standards. *J. Air Waste Manage. Assoc.* **2011**, *61* (4), 427−442.

(41) Khalek, I.;Mamakos, A.; Premnath, V.; Mechler, R.; Preece, D. Particle generator for engine exhaust simulation. *17th ETH Conference on Combustion Generated Nanoparticles*, 2013.

(42) Uhrner, U.; von Löwis, S.; Vehkamäki, H.; Wehner, B.; Bräsel, S.; Hermann, M.; Stratmann, F.; Kulmala, M.; Wiedensohler, A. Dilution and aerosol dynamics within a diesel car exhaust plume— CFD simulations of on-road measurement conditions. *Atmos. Environ.* **2007**, *41*, 7440−7461.

(43) Wehner, B.; Uhrner, U.; von Löwis, S.; Zallinger, M.; Wiedensohler, A. Aerosol number size distributions within the exhaust plume of a diesel and a gasoline passenger car under on-road conditions and determination of emission factors. *Atmos. Environ.* **2009**, *43*, 1235−1245.

Sulfur driven nucleation mode formation in diesel exhaust under transient driving conditions

Panu Karjalainen[1], Topi Rönkkö*[1], Liisa Pirjola[2], Juha Heikkilä[1], Matti Happonen[1], Frank Arnold[3], Dieter Rothe[4], Piotr Bielaczyc[5] and Jorma Keskinen[1]

[1]Aerosol Physics Laboratory, Department of Physics, Tampere University of Technology, Tampere, Finland

[2]Metropolia University of Applied Sciences, Helsinki, Finland

[3]Max-Planck-Institute for Nuclear Physics, Atmospheric Physics Division, Heidelberg, Germany

[4]MAN Truck & Bus AG, EPRE - Engine Research Exhaust Aftertreatment, Nuremberg, Germany

[5]BOSMAL Automotive Research and Development Institute Ltd, Bielsko-Biala, Poland

6 Pages

4 Figures

Supporting information

Detailed experimental setups for all the four experiments performed are shown in Figures S1&S2. In the engine laboratories (Fig. S1a) and in the aerosol laboratory (Fig. S1b) the primary exhaust gas dilution was executed with a porous tube diluter (PTD). In the PTD the dry and filtered dilution air flow was 50 l/min, the temperature was 30 °C and the dilution ratio was maintained close to a constant value (12). With these parameters, nucleation mode formation was aimed to maintain repeatable. In the engine laboratories, the primary dilution ratio was determined by measuring the CO_2 concentrations both in hot exhaust and diluted exhaust. In the aerosol laboratory, the SO_2 concentrations were used in the dilution ratio determination. The secondary dilution was performed by an ejector type diluter (Dekati diluter) in order to reach suitable concentration levels for the instruments. The instrumentation consisted of Scanning mobility particle sizers (SMPS, TSI Inc.), both the Nano-SMPS and the SMPS in Fig. 1a and only the Nano-SMPS in Fig. 1b, and an Electrical low pressure impactor (ELPI, Dekati Oy) with extra impactor and filter stages. The instruments enabled particle number size distribution analysis over a broad particle size range (3 nm – 10 µm). Occasionally, a thermodenuder with low nanoparticle losses[1] was applied to test the aerosol upstream of the instruments.

Solely in the engine laboratory study of the heavy-duty diesel engine (experiment 2), the gaseous sulphuric acid (GSA) concentration was measured using a Chemical Ionization Mass Spectrometer (CIMS) setup which consisted of a flow tube reactor and an ion trap mass spectrometer. In the flow tube reactor, gaseous H_2SO_4 molecules undergo an ion-molecule reaction with the reagent ions (NO_3-HNO_3), leading to product ions of the HSO_4-HNO_3 type. The GSA concentration is determined from the abundance ratio of product and reagent ions measured with an ion trap mass spectrometer. Details of the instrument can be found in Speidel et al. (2007)[2].
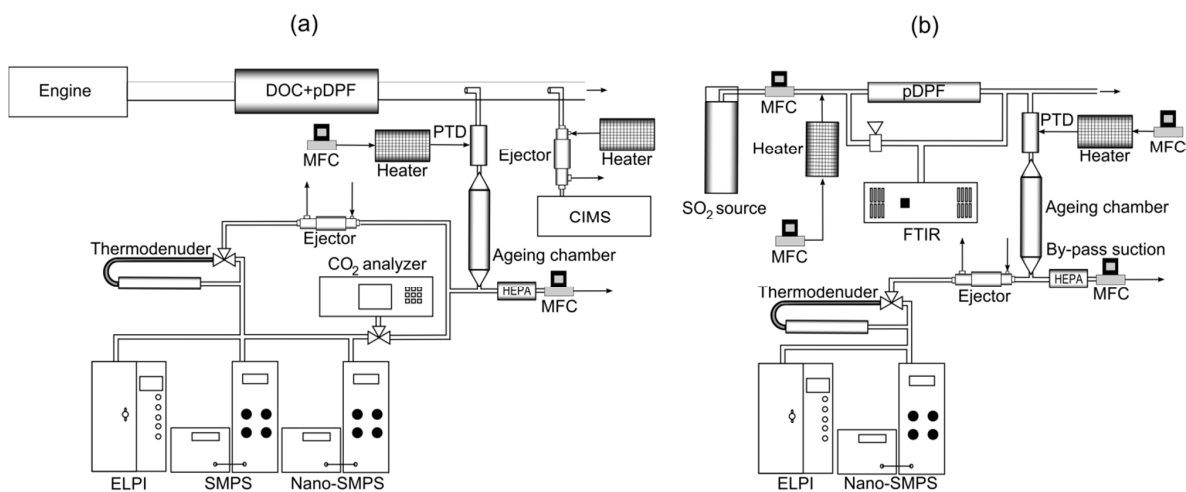
Figure S1. Experimental setups in the engine laboratory tests (a) and in the aerosol laboratory (b). The CIMS and the adjacent ejector diluter were only used in the heavy-duty engine laboratory experiment (experiment 2).

The nucleation mode particle characteristics were studied in the aerosol laboratory (experiment 1). The volatility of nucleation mode particles was tested by measuring the Nano-SMPS size distribution with and without thermodenuder treatment (at 265 °C). The particle mode was completely eliminated by the thermodenuder treatment, as presented in Rönkkö et al. 2011[1]. The particle charging state was studied by applying an efficient electrostatic precipitator with high voltage (3.75 kV) in the inlet of the Nano-SMPS (flow 1.5 l/min). The particle collection efficiency of the EPS was close to 100% for singly charged particles at nucleation mode size range. There was no change in the measured particle concentrations whether the high voltage was on or off (Fig. S2).
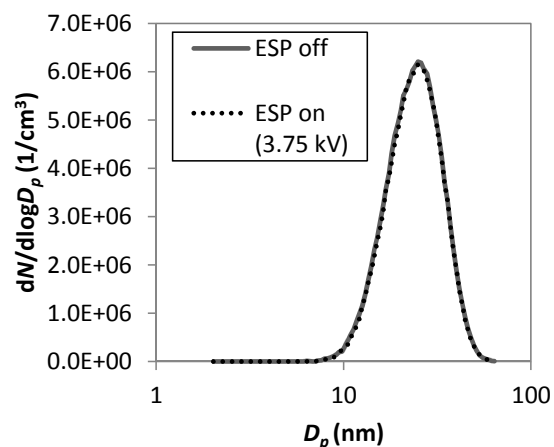
Figure S2. Nucleation mode particle size distributions in experiment 1 measured with and without

an electrostatic precipitator (ESP).

Particle concentrations of the exhaust plume were measured by chasing the truck with a trailer by the "Sniffer" mobile laboratory van. Using a laser based distance-meter, the distance between the truck and the laboratory vehicle was kept constant at 12 ± 2 m. The probe for sampling the exhaust plume aerosol was located above the front bumper of the laboratory vehicle. The sample was conveyed continuously to the particle instruments. The particle instrumentation inside the mobile laboratory consisted of an ELPI, an SMPS, a Nano-SMPS and an ultrafine CPC. Furthermore, thermodenuder treatment (at 265°C) was occasionally applied to the aerosol sample. The laboratory van was also equipped with gas analyzers for CO_2, CO and NO_x.
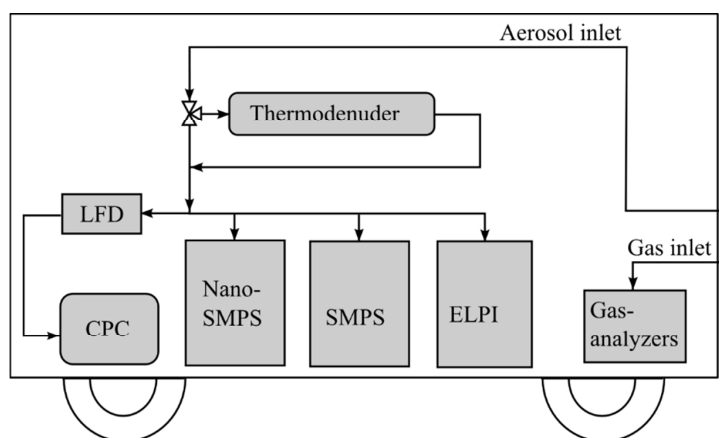

Figure S3. Experimental setup in the mobile laboratory.

Studies were conducted on Highway 4, Finland, between Oulu - Jyväskylä - Oulu. The distance between the two cities is 350 km. The long route was chosen in order to get statistical data and, in order to avoid the effects of other traffic, the measurements were performed during the late evening and at night. Fig. S4 shows the altitude profile for the test route. Near Jyväskylä, the test period consisted mainly of uphill and downhill driving conditions, while near Oulu the route was relatively flat. However, the vehicle speed was kept near 80 km/h throughout the test route. Although speed was relatively constant, engine load varied strongly, depending mainly on the altitude profile; during uphill driving engine torque was typically at maximum and during downhill it was zero, meaning driving at engine braking conditions. Here "torque" refers to the torque produced by the engine. The negative torque caused by the inertia of the truck was not measured.
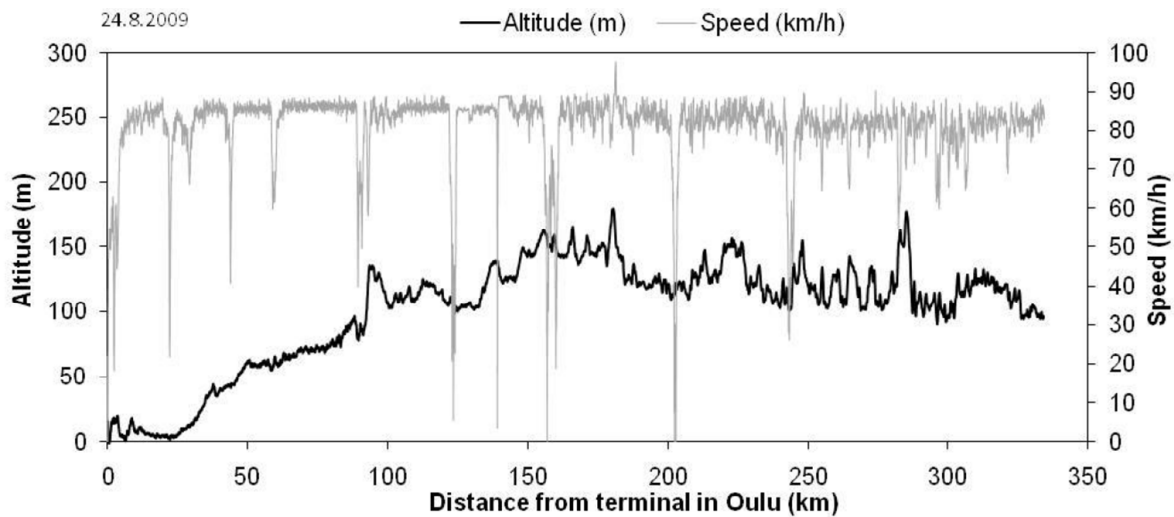

Figure S4. The speed and altitude profiles on the transportation route of the test truck

(Oulu – Jyväskylä, Finland).

References

1. Rönkkö, T.; Arffman, A.; Lähde, T.; Karjalainen, P.; Heikkilä, J.; Pirjola, L.; Rothe, D. and Keskinen, J. Diesel exhaust nanoparticle volatility studies by a new thermodenuder with low solid nanoparticle losses, *15th ETH Conference on Combustion Generated Nanoparticles* **2011**.

2. Speidel, M.; Nau, R.; Arnold, F.; Schlager, H. and Stohl, A. (2007) Sulfur dioxide measurements in the lower, middle and upper troposphere: Deployment of an aircraft-based chemical ionization mass spectrometer with permanent in-flight calibration. *Atmospheric Environment* **2007***, 41, 2427–2437.*

Paper 3

Topi Rönkkö, Liisa Pirjola, Leonidas Ntziachristos, Juha Heikkilä, Panu Karjalainen, Risto Hillamo and Jorma Keskinen. Vehicle Engines Produce Exhaust Nanoparticles Even When Not Fueled. *Environmental Science & Technology*, 2014, 48, 2043–2050, doi: 10.1021/es405687m.

Vehicle Engines Produce Exhaust Nanoparticles Even When Not Fueled

Topi Rönkkö,[†,*] Liisa Pirjola,[‡] Leonidas Ntziachristos,[§] Juha Heikkilä,[†,⊥] Panu Karjalainen,[†] Risto Hillamo,[‖] and Jorma Keskinen[†]

[†]Aerosol Physics Laboratory, Department of Physics, Tampere University of Technology, P.O. Box 599, Tampere FIN-33720, Finland
[‡]Department of Technology, Metropolia University of Applied Sciences, P.O. Box 4000, Helsinki FIN-00180, Finland
[§]Laboratory of Applied Thermodynamics, Aristotle University Thessaloniki, P.O. Box 458, Thessaloniki GR 54124, Greece
[‖]Finnish Meteorological Institute, Air Quality Research, Erik Palmenin aukio 1, Helsinki FIN-00101, Finland

ABSTRACT: Vehicle engines produce submicrometer exhaust particles affecting air quality, especially in urban environments. In on-road exhaust studies with a heavy duty diesel vehicle and in laboratory studies with two gasoline-fueled passenger cars, we found that as much as 20−30% of the number of exhaust particles larger than 3 nm may be formed during engine braking conditions—that is, during decelerations and downhill driving while the engine is not fueled. Particles appeared at size ranges extending even below 7 nm and at high number concentrations. Their small size and nonvolatility, coupled with the observation that these particles contain lube-oil-derived metals zinc, phosphorus, and calcium, are suggestive of health risks at least similar to those of exhaust particles observed before. The particles' characteristics indicate that their emissions can be reduced using exhaust after-treatment devices, although these devices have not been mandated for all relevant vehicle types. Altogether, our findings enhance the understanding of the formation vehicle emissions and allow for improved protection of human health in proximity to traffic.
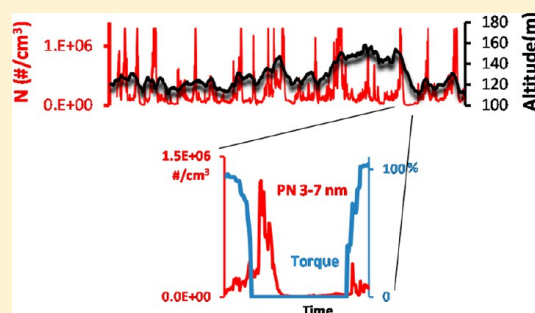
INTRODUCTION

Vehicles and engines produce submicrometer exhaust particles, affecting air quality and human exposure to particulate pollution, especially in urban environments.[1,2] Due to their small size, reaching only a few nanometers, these particles penetrate deep into the alveolar region[3] and induce health effects through interactions at the cellular or subcellular level.[4,5] Diesel exhaust particles have been reported to be either solid carbonaceous agglomerates formed during combustion by incomplete fuel burning—comprising the so-called "soot mode" or "accumulation mode"—or mostly semivolatile formed by nucleation and condensation of semivolatile material during exhaust dilution in atmosphere—the so-called "nucleation mode".[6−9] The mean diameters of soot particles are typically 40−100 nm. Nucleation mode particles, typically between 3 and 30 nm in diameter, consist mainly of semivolatile components, such as water, sulphuric compounds, and hydrocarbons,[6,8,10−12] but may contain also nonvolatile compounds.[13−15] The volatility of nucleation mode particles has been observed to be an indicator of the particle formation mechanism meaning that the volatile nucleation mode particles, typically observed at high engine load, seem to be formed via the nucleation of sulfuric species in the cooling dilution process of exhaust,[16,17] while the nucleation mode particles with a nonvolatile core seem to be initially formed in cylinder conditions and only the growth of the particles, driven by

sulfuric and hydrocarbon compounds, takes place during the cooling dilution of exhaust.[14,15,17] The concentration and relative importance of each mode significantly depends on the engine and exhaust aftertreatment technology,[15] operation and environmental conditions,[21] and fuel and lubricant oil properties,[18,19,22−24] The lubricant oil originated metals contribute significantly to the ash components,[1,25,26] of exhaust particulate matter and seem to also affect the processes such as oxidation of soot.[27] The increase in the sulfur level of lubricant increases the emissions of nucleation particles at high load, particularly if the engine is equipped with oxidative exhaust aftertreatment.[22,23,28] Instead, without exhaust after-treatment the hydrocarbons originating from lubricant oil may have a significant role in the formation of volatile diesel exhaust particulate matter; e.g., Sakurai et al.[13] have reported that more than 95% of the volatile components of both diesel exhaust nanoparticles and larger particles is composed of unburned lubricating oil.

The exhaust particle number concentrations of gasoline vehicles are typically lower than diesel exhaust particle concentrations. However, the general need to enhance the fuel economy has led to the use of direct fuel-injection

techniques also in gasoline vehicles. This change has increased particle emissions of these vehicles. As in diesel exhaust, the particle number emitted by gasoline direct injection (GDI) vehicles is dominated by ultrafine particles, the particle size distribution is often bimodal, and the particles consist mainly of elemental carbon.[24,29−32] In general, GDI technology is replacing port fuel injection (PFI) technology as the major fuel injection strategy and solution for gasoline engines. Current estimations hold that in North America, GDI vehicles could cover up to 60% of the light-duty vehicle fleet by 2016.[33]

In addition to technological parameters, changing driving conditions also affect particle emissions. In emissions legislation, this has been taken into account by including transient driving cycles in emission standards. As a result, the number of exhaust studies focusing on emissions at transient conditions has increased.[34] However, specific data for detailed driving conditions have remained limited because the regulated quantity is the particulate mass or number integrated over the test cycle. In general, it has been observed that during transient cycles, the particle size distributions have two modes,[35] and the highest particle emissions occur under heavy acceleration.[35−37] Transient driving conditions can affect both the nucleation mode particles and the soot particles.[38] Increased emissions of nucleation particles, affected by fuel sulfur content and exhaust dilution and thus proposed to be formed by sulfuric compounds, has been observed at deceleration as well.[38] As at steady state tests, the particle emissions during transient cycles has been observed to be affected by vehicle technologies like exhaust after-treatment[35] and fuel type.[34,35,38]

This work focuses on the observation that engines emit a high number of exhaust particles at engine braking conditions—that is, during decelerations and downhill driving. In practice, "engine braking" refers to the driver's lifting of the gas (accelerator) pedal and keeping the gear on, and it is typically used to enhance fuel economy or simply to limit or decrease a vehicle's speed during downhill driving or deceleration. With direct injection engines, the fuel consumption during engine braking is zero. This study consists of three experiments: one experiment conducted with a heavy-duty diesel truck at on-road conditions, and two conducted with gasoline direct injection (GDI) passenger cars at chassis dynamometer. Special attention is given in this study to the characteristics of particles and emission formation.

■ EXPERIMENTAL SECTION

The study consists of three separate experiments, as outlined below.

Experiment 1. Real-world measurements of heavy duty diesel truck emissions were performed under real driving conditions on the normal transportation route of a truck. Due to the continuously changing driving conditions, the data of certain driving parameters (engine speed, engine torque, pedal position, exhaust temperature, and pressure) were collected with a time resolution of 1 s. The location and speed of the vehicle were measured and saved using the GPS system. The truck (emission level Euro II) used diesel fuel fulfilling the fuel standard EN590:2009 and having fuel sulfur content less than 10 ppm. The lubricant oil was high quality SAE 10W-40 suitable for long oil change intervals, which fulfilled the requirements of truck manufacturer. The truck was not equipped with exhaust after-treatment systems.

Particle concentrations of the exhaust plume were measured by chasing the truck with a trailer by the mobile laboratory

vehicle.[39,40] The distance between truck and laboratory vehicle was kept in 12 ± 2 m. An aerosol sample taken directly from the exhaust plume had a 1.6 s exhaust residence time in the atmosphere at a speed of 80 km/h. This is considered sufficient for aerosol processes to achieve a relatively stable condition.[41] The probe to sample the exhaust plume aerosol located in the front bumper of the laboratory vehicle. Particle size distributions were measured by Electrical Low Pressure Impactor (ELPI, Dekati, Inc.) [42] equipped with a filter stage [43] and an additional impactor stage,[44] and by two scanning mobility particle sizers (SMPS).[45] One SMPS was equipped with a DMA 3085 and a CPC 3025 (nano-SMPS, TSI Inc.) and the other with a DMA 3071 and a CPC 3775 (SMPS, TSI Inc.). The measurement range of the ELPI was 7 nm to 6.6 μm, the nano-SMPS and the SMPS had measurement ranges of 3−60 nm and 10−400 nm, respectively. A CPC 3025 (TSI Inc.), used after a passive aerosol diluter (with a dilution ratio of 13), was used to monitor the total number concentration of particles larger than 3 nm in diameter. Particle volatility was studied using a thermodenuder where the aerosol was first heated up to 265 °C in order to evaporate volatile particle compounds and after that, gradually cooled in the denuder where the evaporated compounds were collected onto the activated charcoal. Particle losses in the thermodenuder were corrected according to Heikkilä et al.[46] In addition to particle measurements, gaseous NO_x, CO, and CO_2 and relative wind speed and direction, temperature, and relative humidity were also measured. The GPS unit was used to save velocity and position of the laboratory vehicle. During the measurement, the ambient air temperature and relative humidity were 5−15 °C and 57−92%, respectively.

Studies were conducted on Highway 4 in Finland between the cities of Oulu and Jyväskylä so that one test run was approximately 350 km. Near Jyväskylä the test consisted mainly of uphill and downhill driving conditions while near Oulu, the route was relatively flat. The vehicle speed was near 80 km/h during most of the measurement time. The engine load varied greatly, depending mainly on the altitude profile; during uphill driving, the engine torque was typically at maximum and during downhill driving, it was zero, meaning engine braking conditions. In total, more than 30% of the time, the engine was at maximum or minimum torque. Here "torque" refers to torque produced by the engine; negative torque caused by the inertia of the truck was not measured. In order to minimize the effects of other traffic on the results, the measurements were performed in the late evening and night. Thus, the number of oncoming vehicles averaged 28 per hour only during the 4.5-h test (46% heavy duty and 54% light duty vehicles).

Experiment 2. The second experiment was conducted using a light-duty vehicle chassis dynamometer. The test vehicle was a new gasoline direct injection (GDI) passenger car (model year 2011, displacement 2.0 dm^3), equipped with a three-way catalyst to control carbon monoxide (CO), hydrocarbon (HC), and NO_x emissions. On the basis of the on-board diagnostics (OBD) data, the vehicle ran at stoichiometric conditions at all operating ranges except directly after starting. The fuel was gasoline with ethanol content below 10%. Experiments were conducted during the standardized NEDC (New European Driving Cycle) consisting of accelerations, short steady state driving conditions, decelerations (conducted during engine braking), and idling conditions. All of the measurements were performed with a warmed-up engine (at least one NEDC cycle was driven just before the tests reported here).
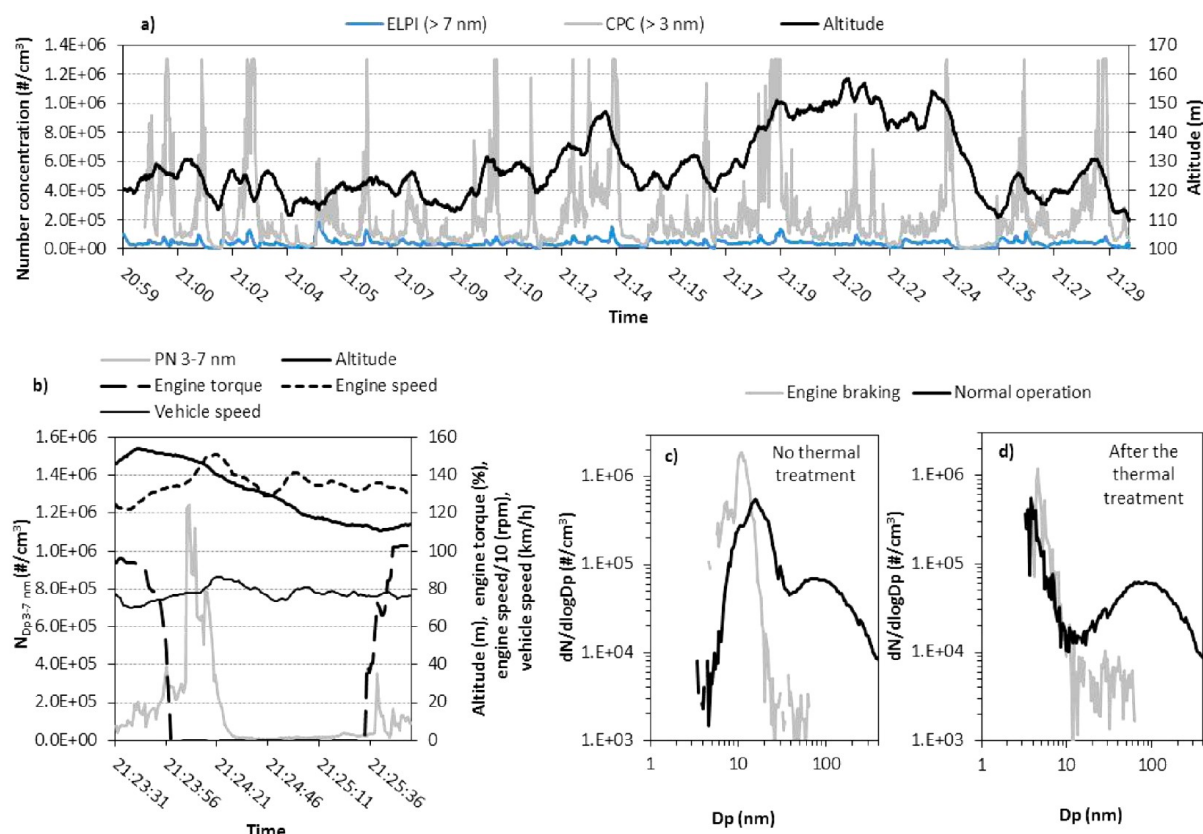
Figure 1. Particle concentrations and size distributions in the exhaust plume of heavy duty diesel truck. (a) Particle concentrations measured by an ELPI ($D_p > 7$ nm) and a CPC ($D_p > 3$ nm) at variable road gradients. (b) Engine operation, altitude profile, and concentration of particles in the 3–7 nm size range (PN 3–7 nm) during downhill driving. (c) Particle size distributions measured by SMPSs at engine braking conditions and at "normal" operation. (d) Similar to (c), but conducted after the thermal treatment of the aerosol in a thermodenuder. Note that size distributions in parts (c) and (d) are indicative because of low time resolution of SMPS instruments.

Exhaust aerosol was sampled from two different locations of the exhaust pipe: in the engine bay right after the exhaust manifold and after the whole exhaust pipe (including three-way catalyst) and transfer line. The sampling was conducted using a partial flow dilution system[42] consisting of a porous tube type diluter (PTD), an aging chamber, and an ejector type diluter. In the porous tube diluter, the dilution air temperature was 30 °C, the dilution ratio was adjusted to 12, and the dilution air's relative humidity was below 10%. A similar sampling system has been used in several other engine and vehicle exhaust studies,[14−17,20−22,41,46,47] mainly because it has been observed to mimic the real-world particle formation and growth processes.[21,41] Particle measurements were conducted by similar instruments to those used in experiment 1: particle size distributions were measured using the ELPI, total concentration of particles larger than 5 nm in diameter was measured by a CPC 3775 (TSI Inc.) and particle volatility was studied using a thermodenuder. Total dilution ratio of the sampled exhaust was determined using CO_2 concentrations of diluted and undiluted (raw) exhaust. Particle concentrations presented below have been corrected by those dilution ratio values.

Experiment 3. In the third experiment, the test vehicle was again a modern GDI passenger car (model year 2011, displacement 1.8 dm^3) equipped with a three-way catalyst and fueled with gasoline containing 10% ethanol. The experiment was conducted at a chassis dynamometer. In

addition to the NEDC, particle measurements were also conducted during three steady state driving modes (speed 80 km/h; fifth gear; wheel power: 5, 10, and 20 kW). Exhaust was sampled after the whole exhaust pipe using the same sampling system used in experiment 2. Particle number, size distributions, and volatility were studied using the ELPI, the CPC 3025 (counting particles larger than 3 nm), two SMPSs with different particle size ranges (during steady state driving only), and the thermodenuder. In addition to these online measurements, the exhaust particles were sampled onto the grids for microscopy studies. These particle samples were studied later using the transmission electron microscopy (TEM) and energy dispersive spectrometry (EDS) methods. Particles were collected onto the grids separately from the NEDC driving cycle and during the steady-state driving modes.

■ RESULTS

On-road exhaust particle studies with the heavy-duty diesel truck with a trailer were made on Highway 4 between Oulu and Jyväskylä. Figure 1a shows a typical driving condition dependent exhaust particle number concentration recording over a half an hour driving sequence in a relatively hilly part of a test route near Jyväskylä. Interestingly, with only few exceptions, the highest concentration peaks (frequently exceeding the maximum measuring range of the CPC after passive dilution) were observed during downhill driving. The peaks were repetitive, appearing throughout the downhill sections of
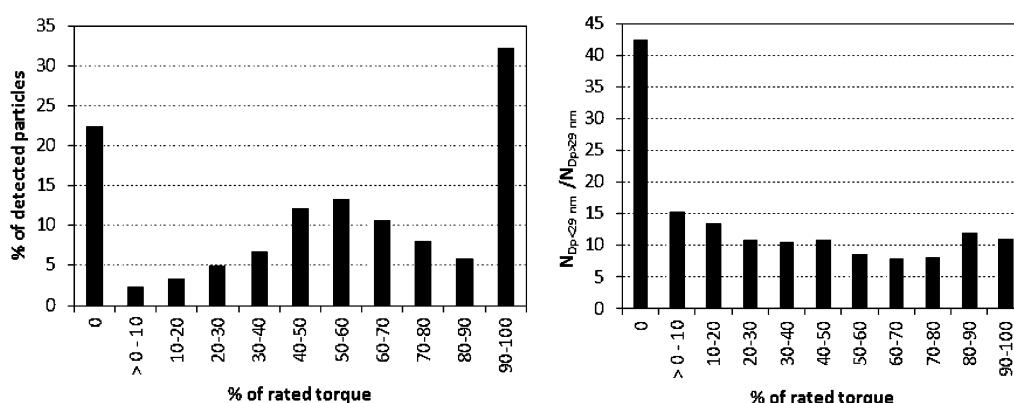
Figure 2. Fractions of particles detected by CPC ($D_p > 3$ nm) (left) and the ratio of particle number of small ($D_p < 29$ nm) and large particles ($D_p > 29$ nm) (B) at different torque conditions of heavy duty diesel truck. The data cover the entire test route. The concentration of large particles ($N_{Dp>29\ nm}$) was determined from the particle size distributions measured by ELPI. The concentration of small particles ($N_{Dp<29\ nm}$) was determined by subtracting $N_{Dp>29\ nm}$ from the total particle concentration measured by CPC.

the driving sequence. The CPC consistently measured higher number concentrations than the ELPI. Given the different size ranges of the two instruments (CPC and ELPI count particles larger than 3 and 7 nm, respectively) this suggests that the high particle concentrations during downhill driving (engine braking) were dominated by particles sized below 7 nm. In comparison, when the same instrumentation was used for the vehicle emitting only soot mode particles (larger particles), the particle concentrations measured by the CPC and the ELPI were at the same level.

Figure 1b focuses on one period of moderate downhill driving, wherein speed control was achieved by engine braking without activating the wheel brakes. As a result, the engine maintained a normal speed, but the torque produced by the engine was practically zeroed. The particle concentration in the 3−7 nm size range, estimated as the difference between the CPC and ELPI recordings, reached high levels directly after the engine torque dropped to zero. Size distribution measurements confirmed the small size of particles formed during engine braking (Figure 1c). Practically no soot mode (> 50 nm) was observed during engine braking, while the concentration of particles below 10 nm exceeded the typical concentrations for normal operation. It should be noted that in normal operation, the particle size distribution consisted of soot mode and nucleation mode, as is expected based on other studies conducted with heavy duty diesel engine and vehicles without exhaust after-treatment.[14] "Normal operation" here refers to driving a flat part of the test route at medium torque conditions; mean values and standard deviations for vehicle speed, engine speed, and engine torque were 78 ± 10 km/h, 1430 ± 85 rpm, and 50 ± 31%, respectively. Also, it should be noted that during the engine braking period shown in Figure 1b, the particle concentration remained high approximately 30 s, and after that, decreased to the level of ambient air. The reason for this behavior was not possible to solve in this study, but in principle, the behavior may indicate that the formation of engine braking particles depends on temperatures of engine oil or combustion chamber. Both of those decrease during engine braking, especially if engine braking takes place after the driving at high torque conditions, like in Figure 1b.

Thermal treatment for the exhaust aerosol, made by the thermodenuder, had very limited impact on the soot mode of particles formed in normal operation and significantly decreased the size of the nucleation mode particles (the geometric mean diameter decreased from 10 to 4 nm) (Figure 1d). In contrast, the same thermal treatment had a limited impact on particles formed during engine braking. Thus, the results indicate that the particles emitted during engine braking were nonvolatile at 265 °C, the operating temperature of the thermodenuder. It should be noted that, because of other traffic, the results include much higher uncertainty compared to on-road measurements in closed areas. However, measurements were made in the late evening and night, when other traffic was at a minimum. Also, the background concentrations, measured occasionally by a laboratory vehicle in front of the test truck, were low; e.g., the particle concentrations measured by the ELPI and NO_x concentrations in the background aerosol were typically below 2000 #/cm^3 and 0.01 ppm, respectively.

The contribution of these particles formed unconventionally during engine braking to total emissions was significant. In the first experiment with the heavy duty diesel truck the total number of detected particles was distributed rather in proportion to the time spent by the engine in each torque class (Figure 2); 22% of detected particles were observed during engine braking (0% of rated torque), which covered 16% of measurement time, and 32% were detected at full load conditions (>90% of rated torque), which the engine was in 22% of the time. However, the contribution of engine braking to nanometer-sized particles differed from the other driving conditions when the particle size was considered; at engine braking, the small particle (here $D_p < 29$ nm) concentration was 42 times higher than the large particle ($D_p > 29$ nm) concentration, while during other driving conditions, the ratio of small and large particle concentrations was around 10. A particle size of 29 nm was chosen here to separate the concentrations of smaller and larger particles because it is the cut size of the first impactor stage of ELPI and thus is carefully calibrated, however, this size lies between the particle modes in the vehicle's normal operation (see Figure 1c). It should be noted that the numbers presented in Figure 2 are for the entire measurement period. On the basis of Figure 1a, it is clear that when the analysis is focused on hilly periods only, the role of engine braking becomes much more emphasized.

Engine braking particles were also observed in experiments 2 and 3, conducted with modern GDI vehicles, when following the European statutory driving cycle. The New European

Driving Cycle (NEDC) used in the experiments consists of periods of constant speed as well as idling, accelerations, and decelerations. In experiment 2, the continuous exhaust samples were studied in real time using two alternative sampling points: one in the engine bay directly downstream of the exhaust manifold, and one at the end of the tailpipe. Repetitively high concentrations of particles were observed during engine braking in decelerations, when the sampling was conducted directly downstream of the exhaust manifold (Figure 3). The mean
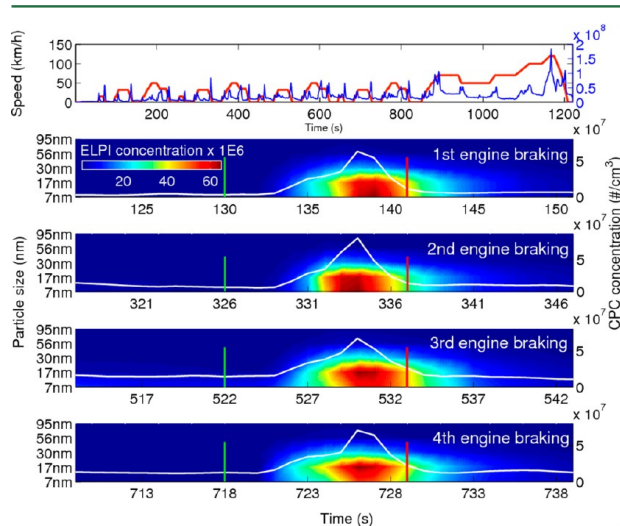

Figure 3. Top graph: Gasoline direct injection (GDI) vehicle speed and exhaust particle concentration over the New European Driving Cycle (NEDC). Lower graphs: Exhaust particle size distributions measured by ELPI (color map) and particle concentration measured by CPC (white line) during individual engine braking conditions (speed change from 32 km/h to 0 km/h). The starting point of engine braking is marked by a vertical green line, and the end point is marked by a vertical red line. The exhaust sample was taken from the exhaust manifold.

diameter of these particles varied from less than 10 nm to slightly larger than 20 nm, depending on the deceleration pattern (Figure 4). When sampled downstream of the complete exhaust line including the three-way catalyst, the concentration of particles was lower, and the mean particle size larger, probably due to the strongly size-dependent diffusional particle losses (Figure 5). Alternative measurements at the exhaust manifold and tailpipe outlet positions led to an additional interesting observation: Due to the decreased exhaust flow rate, particles formed during engine braking appeared in the tailpipe outlet when the engine had already reached idle (Figure 5). In the second experiment, with a modern GDI passenger car for which exhaust was measured at the tailpipe outlet position trough the whole NEDC, 23−29% of all emitted particles, in number, were observed during engine braking.

In experiment 3, GDI vehicle exhaust particle samples were collected and then analyzed using the transmission electron microscopy (TEM) method for shape, and by energy dispersive spectrometry (EDS) to find their elemental composition (Figure 6). Two distinct particle types were observed for samples collected over the whole NEDC. First, we found that 10−20% of collected particles, counted from TEM images, were nearly spherical, often including small enclosures. These particles included oxygen, zinc, phosphorus, and calcium. Zinc, phosphorus, and calcium can be found in engine oil but not in
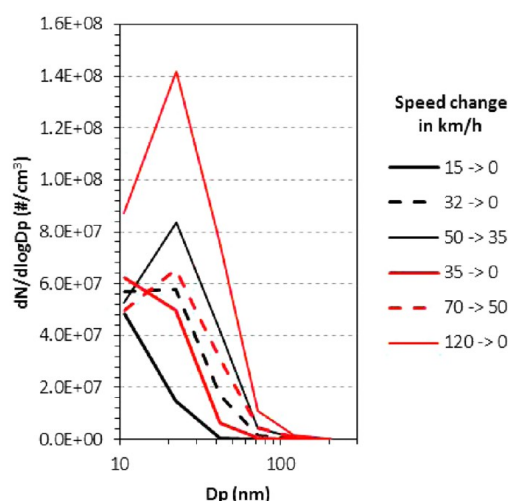

Figure 4. Exhaust particle size distributions of the GDI passenger car during engine braking, measured using an ELPI after the exhaust sampling from the exhaust manifold. Legend shows the change of wheel speed in km/h.

gasoline. Second, we identified soot particles with a typical agglomerated structure, consisting of elemental carbon but also oxygen, zinc, phosphorus, and calcium. When the particle sample was taken during steady state driving, agglomerated particles contained carbon, but not any metals. Thus, the studies indicate that engine braking particles, emitted during transient driving cycles, are associated with engine oil.

■ DISCUSSION

Engine braking is widely used in deceleration and to prevent vehicle acceleration in downhill driving. The clear and widely known benefit of engine braking is its effect on fuel consumption; for the engines with direct fuel injection technology, the fuel consumption during the engine braking is zero. The use of engine braking also decreases the wearing of wheel brakes. In principle, during engine braking, the inertia of a moving vehicle maintains the rotation of a crankshaft, and thus, the movement of pistons, without fuel combustion. The magnitude of engine's intake air-flow depends on the engine technology and design. In gasoline engines, the intake air flow is typically restricted by the throttles and/or valves. In diesel engines, in general, the resistance for the intake air flow is lower, and the braking effect can be weaker. Also, the engine speed affects the effectiveness of engine braking. However, during engine braking, the engine's intake air goes to the cylinder, where it is compressed to elevated pressures, its temperature raises, and, finally, it is exhausted to the atmosphere.

In this study, we observed that both the heavy-duty diesel vehicles and the modern gasoline-fueled passenger cars can emit substantially high emissions of exhaust particles also during engine braking condition. Both the characteristics of these particles and the mechanism by which they form seem to differ significantly from those of soot and nucleation particles. For the first time, we observed these new exhaust nanoparticles by following a heavy duty diesel truck under real-world conditions. The truck, powered by a Euro II engine without exhaust after-treatment, operated on its daily route when the driving pattern, road conditions, and vehicle loading were typical of a normal scheduled day. Thus, the emissions of these
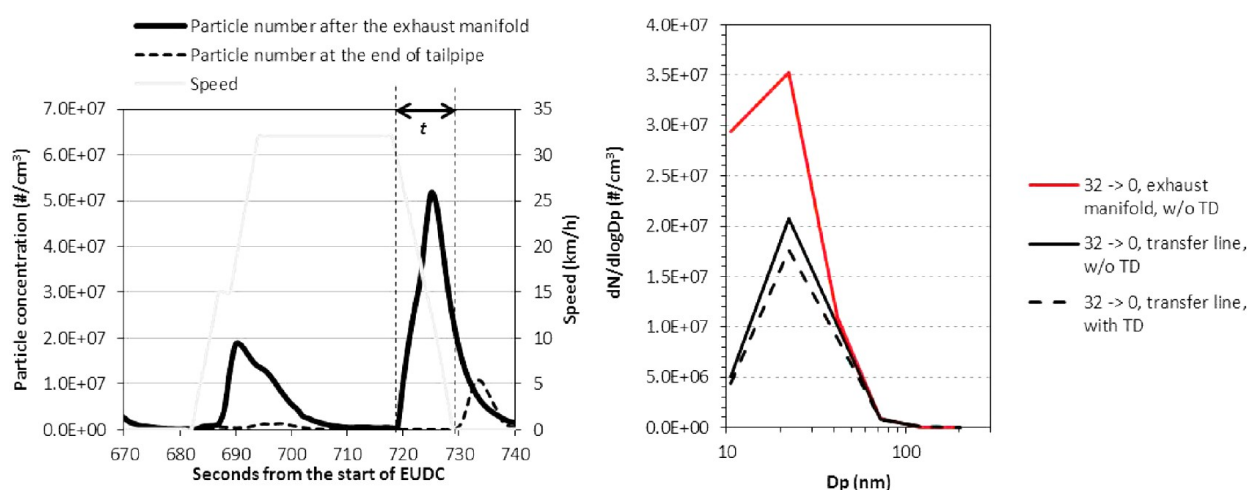
Figure 5. Instantaneous particle concentrations for the GDI vehicle exhaust when the sampling was conducted from the exhaust manifold and the entire tailpipe system. The data are shown for one period of the NEDC (left). Particle size distributions measured using the ELPI during highest particle concentrations of the fourth deceleration from 32 km/h to idle (same like in Figure 3) (right). The distribution drawn by a red line was measured after sampling from the exhaust manifold, and the other was measured after the sampling from the exhaust transfer line (exhaust went through the exhaust manifold, three way catalyst, exhaust pipe, and part of the transfer line before the sampling). The dashed line shows the distribution measured after the thermodenuder (TD) treatment of exhaust aerosol.
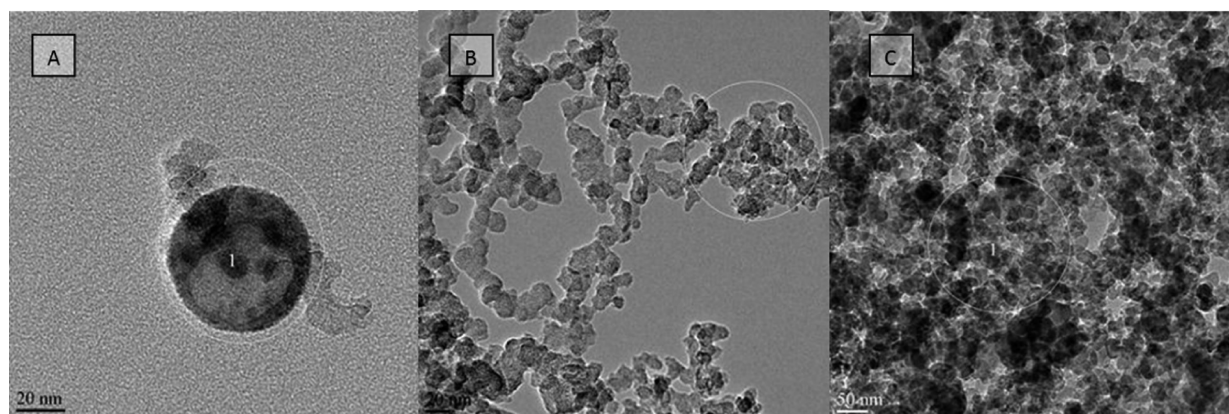

Figure 6. Transmission electron microscope (TEM) images of particles collected from an exhaust aerosol sample of a GDI passenger car. (a) A spherical O−Zn−P−Ca-rich particle with enclosures, sampled during the NEDC cycle. (b) Soot-like C−O−Zn−P−Ca-rich agglomerated particles sampled during the NEDC cycle. (c) Heavily loaded particle sample taken during steady-state driving. No elements such as Zn, P, and Ca were found. The circles show the focus of EDS (energy dispersive spectrometry) for elementary analyses.

engine braking particles were part of the real particle emissions of the truck. Because similar particles were observed in the exhaust of modern GDI passenger cars, it is obvious that the emissions are not characteristics of one vehicle or technology type only. Also, because of increased use of direct fuel injection technologies in gasoline-fueled vehicles not equipped with particle filtration systems, the exhaust particle emission during engine braking will remain a problem in the future.

In principle, the lubricant oil or some compounds within it can end up in the cylinder by spouting through the piston ring gap,[48] due to their evaporation from the cylinder liner, see e.g., refs 26 and 49 or via the crankcase ventilation system, which conducts the crankcase vapors into the engine's intake air.[50] The lubricant oil consumption has been reported to depend on driving conditions, especially transients.[51] Thus, it seems evident that the direct origin of these particles is not the combustion of fuel, but rather, the engine oil or some compounds within it. Because the observed particles are not

formed by direct combustion, they may contain chemical compounds similar to those of the engine oil. Although we only observed metal compounds, it is possible that these particles also contain hydrocarbon compounds from the engine oil. Because of their origin, in principle, no correlation between the emissions of these engine braking particles and CO_2 is expected. It is therefore possible that emission factors, typically determined by measuring particles and carbon dioxide concentrations simultaneously in an urban environment and using these quantities to calculate particles per unit of fuel combusted, are at least partly failed. This is, however, dependent for example on the location of urban air measurement station in relation to traffic routes. Also, our chassis dynamometer studies indicate that the high particle concentrations that are in reality caused by deceleration and engine braking are in some studies erroneously associated with idling.

The particle number in the urban atmosphere has been frequently observed to be dominated by nanoparticles.

Typically, nanoparticle concentrations are highest near traffic (e.g., near highways). Although in several countries, high-quality fuel is in use, and new vehicles are typically equipped with modern emissions reduction technologies, vehicles still represent one of the most significant particulate pollution sources in the urban environment. Particles with similar physical characteristics as those in this study have been found in urban environments with high human populations.[52,53] Our study indicates that these particles are emitted in short time bursts, causing extremely high and instantaneous increases of particle concentrations. In addition to downhill driving, these particles may be emitted while navigating locales with a frequent presence of people, such as when decelerating at crossroads, traffic lights with pedestrian crossings, or bus stops. Particularly in urban environments, this can lead to significant human exposure of these particle emissions.

The contribution of nanoparticles emitted during engine braking to total particle number emissions can be highly significant - in our tests 20–30%. However, these particles have not been taken into account in emission regulations and in the assessment of associated health risks. For example, in the case of gasoline vehicles and off-road engines, standards controlling these emissions have not yet been established, and the proper emission reduction technologies have not yet been applied. However, our study indicates that the particles were non-volatile, formed before the catalyst, and originating from engine oil. Thus, the results indicate that the emissions of engine braking particles can be reduced using exhaust particle filtration systems. Additionally, another potential but less direct way to reduce the emissions of these particles may be the modification of engine oil characteristics, such as metal content or viscosity. From an emissions control perspective, the problem remains for those older vehicle types that are not equipped with particle filters and possibly for new vehicle technologies for which particle filters have not been mandated, such as gasoline direct injection (GDI) vehicles.

■ AUTHOR INFORMATION

Corresponding Author
*Phone +358-40-1981019; fax: +358-3-31153015; e-mail: topi.ronkko@tut.fi.

Present Address
[⊥]Wärtsilä Finland Oy, Järvikatu 2–4,Vaasa FIN-65200, Finland.

Notes
The authors declare no competing financial interest.

■ REFERENCES

(1) Kittelson, D.; Watts, W.; Johnson, J. Nanoparticle emissions on Minnesota highways. *Atmos. Environ.* **2004**, *38*, 9−19.

(2) Virtanen, A.; Rönkkö, T.; Kannosto, J.; Ristimäki, J.; Mäkelä, J.; Keskinen, J.; Pakkanen, T.; Hillamo, R.; Pirjola, L.; Hämeri, K. Winter and summer time size distributions and densities of traffic related aerosol particles at a busy highway in Helsinki. *Atmos. Chem. Phys.* **2006**, *6*, 2411−2421.

(3) Alföldy, B.; Giechaskiel, B.; Hofmann, W.; Drossinos, Y. Size-distribution dependent lung deposition of diesel exhaust particles. *J. Aerosol Sci.* **2009**, *40*, 652−663.

(4) Oberdörster, G.; Oberdörster, E.; Oberdörster, J. Nanotoxology: An emerging discipline evolving from studies of ultrafine particles. *Environ. Health Perspect.* **2005**, *113*, 823−839.

(5) Paur, H.; Cassee, F.; Teeguarden, J.; Fissan, H.; Diabate, S.; Aufderheide, M.; Kreyling, W.; Hänninen, O.; Kasper, G.; Riediker, M.; Rothen-Rutishauser, B.; Schmid, O. In-vitro cell exposure studies for the assessment of nanoparticle toxicity in the lung—A dialog between aerosol science and biology. *J. Aerosol Sci.* **2011**, *42*, 668−692.

(6) Kittelson, D. Engines and nanoparticles: A review. *J. Aerosol Sci.* **1998**, *29*, 575−588.

(7) Harris, S.; Maricq, M. Signature size distributions for diesel and gasoline engine exhaust particulate matter. *J. Aerosol Sci.* **2001**, *32*, 749−764.

(8) Shi, J.; Harrison, R. Investigation of ultrafine particle formation during diesel exhaust dilution. *Environ. Sci. Technol.* **1999**, *33*, 3730−3736.

(9) Seigneur, C. Current understanding of ultrafine particulate matter emitted from mobile sources. *J. Air Waste Manage. Assoc.* **2009**, *59*, 3−17.

(10) Shi, J. P.; Khan, A. A.; Harrison, R. M. Measurements of ultrafine particle concentration and size distribution in the urban atmosphere. *Sci. Total Environ.* **1999**, *235*, 51−64.

(11) Tobias, H.; Beving, D.; Ziemann, P.; Sakurai, H.; Zuk, M.; McMurry, P.; Zarling, D.; Watylonis, R.; Kittelson, D. Chemical analysis of diesel engine nanoparticles using a nano-DMA/thermal desorption particle beam mass spectrometer. *Environ. Sci. Technol.* **2001**, *35*, 2233−2243.

(12) Schneider, J.; Hock, N.; Weimer, S.; Borrmann, S.; Kirchner, U.; Vogt, R.; Scheer, V. Nucleation particles in diesel exhaust: Composition inferred from in situ mass spectrometer analysis. *Environ. Sci. Technol.* **2005**, *39*, 6153−6161.

(13) Sakurai, H.; Tobias, H.; Park, K.; Zarling, D.; Docherty, K.; Kittelson, D.; McMurry, P.; Ziemann, P. On-line measurements of diesel nanoparticle composition and volatility. *Atmos. Environ.* **2003**, *37*, 1199−1210.

(14) Rönkkö, T.; Virtanen, A.; Kannosto, J.; Keskinen, J.; Lappi, M.; Pirjola, L. Nucleation mode particles with a nonvolatile core in the exhaust of a heavy duty diesel vehicle. *Environ. Sci. Technol.* **2007**, *41*, 6384−6389.

(15) Lähde, T.; Rönkkö, T.; Virtanen, A.; Schuck, T.; Pirjola, L.; Hämeri, K.; Kulmala, M.; Arnold, F.; Rothe, D.; Keskinen, J. Heavy duty diesel engine exhaust aerosol particle and ion measurements. *Environ. Sci. Technol.* **2009**, *43*, 163−168.

(16) Arnold, F.; Pirjola, L.; Rönkkö, T.; Reichl, U.; Schlager, H.; Lähde, T.; Heikkilä, J.; Keskinen, J. First on-line measurements of sulphuric acid gas in modern heavy duty diesel engine exhaust: Implications for nanoparticle formation. *Environ. Sci. Technol.* **2012**, *46*, 11227−11234.

(17) Rönkkö, T.; Lähde, T.; Heikkilä, J.; Pirjola, L.; Bauschke, U.; Arnold, F.; Schlager, H.; Rothe, D.; Yli-Ojanperä, J.; Keskinen, J. Effects of gaseous sulphuric acid on diesel exhaust nanoparticle formation and characteristics. *Environ. Sci. Technol.* **2013**, *47* (20), 11882−11889, DOI: 10.1021/es402354y.

(18) Maricq, M.; Chase, R.; Xu, N.; Laing, P. The effects of the catalytic converter and fuel sulfur level on motor vehicle particulate matter emissions: Light duty diesel vehicles. *Environ. Sci. Technol.* **2002**, *36*, 283−289.

(19) Holmén, B.; Ayala, A. Ultrafine PM emissions from natural gas, oxidation-catalyst diesel, and particle-trap diesel heavy-duty transit buses. *Environ. Sci. Technol.* **2002**, *36*, 5041−5050.

(20) Vaaraslahti, K.; Virtanen, A.; Ristimäki, J.; Keskinen, J. Nucleation mode formation in heavy-duty diesel exhaust with and without a particulate filter. *Environ. Sci. Technol.* **2004**, *38*, 4884−4890.

(21) Rönkkö, T.; Virtanen, A.; Vaaraslahti, K.; Keskinen, J.; Pirjola, L.; Lappi, M. Effect of dilution conditions and driving parameters on nucleation mode particles in diesel exhaust: laboratory and on-road study. *Atmos. Environ.* **2006**, *40*, 2893−2901.

(22) Vaaraslahti, K.; Keskinen, J.; Giechaskiel, B.; Solla, A.; Murtonen, T.; Vesala, H. Effect of lubricant on the formation of heavy-duty diesel exhaust particles. *Environ. Sci. Technol.* **2005**, *39*, 8497−8504.

(23) Kittelson, D.; Watts, W.; Johnson, J.; Thorne, C.; Higham, C.; Payne, M.; Goodier, S.; Warrens, C.; Preston, H.; Zink, U.; Pickles, D.; Goersmann, C.; Twigg, M.; Walker, A.; Boddy, R. Effect of fuel and lube oil sulfur on the performance of a diesel exhaust gas continuously regenerating trap. *Environ. Sci. Technol.* **2008**, *42*, 9276−9282.

(24) Maricq, M.; Szente, J.; Jahr, K. The impact of ethanol fuel blends on PM emissions from a light-duty GDI vehicle. *Aerosol Sci. Technol.* **2012**, *46*, 576−583.

(25) Givens, W.; Buck, W.; Jackson, A.; Kaldor, A.; Hertzberg, A.; Moehrmann, W.; Mueller-Lunz, S.; Pelz, N.; Wenninger, G. Lube formulation effects on transfer of elements to exhaust after-treatment system components. *SAE Tech. Pap. Ser.* **2003**, No. 2003-01-3109.

(26) Tornehed, P.; Olofsson, U. Lubricant ash particles in diesel engine exhaust. Literature review and modelling study. *Proc. Inst. Mech. Eng., D: J. Auto. Eng.* **2011**, *225*, 1055−1066.

(27) Jung, H.; Kittelson, D. B.; Zachariah, M. R. The influence of engine lubricating oil on diesel nanoparticle emissions and kinetics of oxidation. *SAE Tech. Pap. Ser.* **2003**, No. 2003-01-3179.

(28) Hall, D.; Dickens, C. The effect of sulphur-free diesel fuel on the measurement of the number and size distribution of particles emitted from a heavy-duty diesel engine equipped with a catalysed particulate filter. *SAE Tech. Pap. Ser.* **2003**, No. 2003-01-3167.

(29) Barone, T.; Storey, J.; Youngquist, A.; Szybist, J. An analysis of direct-injection spark-ignition (DISI) soot morphology. *Atmos. Environ.* **2012**, *49*, 268−274.

(30) Sementa, P.; Vaglieco, B.; Catapano, F. Thermodynamic and optical characterizations of a high performance GDI engine operating in homogeneous and stratified charge mixture conditions fueled with gasoline and bio-ethanol. *Fuel* **2012**, *96*, 204−219.

(31) Sgro, L.; Sementa, P.; Vaglieco, B.; Rusciano, G.; D'Anna, A.; Minutolo, P. Investigating the origin of nuclei particles in GDI engine exhausts. *Combust. Flame* **2012**, *159*, 1687−1692.

(32) Maricq, M.; Podsiadlik, D.; Brehob, D.; Haghgooie, M. Particulate emissions from a direct-injection spark-ignition (DISI) engine. *SAE Tech. Pap. Ser.* **1999**. No. 1999−01−1530.

(33) California Air Resources Board. *Preliminary Discussion Paper -Proposed Amendments to California'S Low-Emission Vehicle Regulations—Particulate Matter Mass, Ultrafine Solid Particle Number, and Black Carbon Emissions," Workshop Report,* 2010.

(34) Giakoumis, E.; Rakopoulos, C.; Dimaratos, A.; Rakopoulos, D. 2012. Exhaust emissions of diesel engines operating under transient conditions with biodiesel fuel blends. *Prog. Energy Combust. Sci.* **2012**, *38*, 691−715.

(35) Wang, J.; Storey, J.; Domingo, N.; Huff, S.; Thomas, J.; West, B. Studies of diesel engine particle emissions during transient operations using an engine exhaust particle sizer. *Aerosol Sci. Technol.* **2006**, *40*, 1002−1015.

(36) Maricq, M.; Podsiadlik, D.; Chase, R. Examination of the size-resolved and transient nature of motor vehicle particle emissions. *Environ. Sci. Technol.* **1999**, *33*, 1618−1626.

(37) Maricq, M.; Podsiadlik, D.; Chase, R. Gasoline vehicle particle size distributions: comparison of steady state, FTP, and US06 measurements. *Environ. Sci. Technol.* **1999**, *33*, 2007−2015.

(38) Liu, Z.; Vasys, V.; Kittelson, D. Nuclei-mode particulate emissions and their response to fuel sulfur content and primary dilution during transient operations of old and modern diesel vehicles. *Environ. Sci. Technol.* **2007**, *41*, 6479−6483.

(39) Pirjola, L.; Parviainen, H.; Hussein, T.; Valli, A.; Hämeri, K.; Aalto, P.; Virtanen, A.; Keskinen, J.; Pakkanen, T.; Mäkelä, T.; Hillamo, R. "Sniffer"—A novel tool for chasing vehicles and measuring traffic pollutants. *Atmos. Environ.* **2004**, *38*, 3625−3635.

(40) Pirjola, L.; Paasonen, P.; Pfeiffer, D.; Hussein, T.; Hämeri, K..; Koskentalo, T.; Virtanen, A.; Rönkkö, T.; Keskinen, J.; Pakkanen, T. A.; Hillamo, R. Dispersion of particles and trace gases nearby a city highway: Mobile laboratory measurements in Finland. *Atmos. Environ.* **2006**, *40*, 867−879.

(41) Keskinen, J.; Rönkkö, T. Can real-world diesel exhaust particle size distribution be reproduced in the laboratory? A critical review. *J. Air Waste Manage. Assoc.* **2010**, *60*, 1245−1255.

(42) Keskinen, J.; Pietarinen, K.; Lehtimäki, M. Electrical low pressure impactor. *J. Aerosol Sci.* **1992**, *23*, 353−360.

(43) Marjamäki, M.; Ntziachristos, L.; Virtanen, A.; Ristimäki, J.; Keskinen, J.; Moisio, M.; Palonen, M.; Lappi, M. Electrical filter stage for the ELPI. *SAE Tech. Pap. Ser.* **2002**, No. 2002-01-0055.

(44) Yli-Ojanperä, J.; Kannosto, J.; Marjamäki, M.; Keskinen, J. Improving the nanoparticle resolution of the ELPI. *Aerosol Air Qual. Res.* **2010**, *10*, 360−366.

(45) Wang, S. C.; Flagan, R. C. Scanning electrical mobility spectrometer. *Aerosol Sci. Technol.* **1990**, *13*, 230−240.

(46) Heikkilä, J.; Rönkkö, T.; Lähde, T.; Lemmetty, M.; Arffman, A.; Virtanen, A.; Keskinen, J.; Pirjola, L.; Rothe, D. Effect of open channel filter on particle emissions of modern diesel engine. *J. Air Waste Manage. Assoc.* **2009**, *59*, 1148−1154.

(47) Ntziachristos, L.; Giechaskiel, B.; Pistikopoulos, P.; Samaras, Z.; Mathis, U.; Mohr, M.; Ristimäki, J.; Keskinen, J.; Mikkanen, P.; Casati, R.; Scheer, V.; Vogt, R. Performance evaluation of a novel sampling and measurement system for exhaust particle characterization. *SAE Tech. Pap. Ser.* **2004**, No. 2004-01-1439.

(48) Ito, A.; Tsuchihashi, K.; Nakamura, M. A study on the mechanism of engine oil consumption—Oil upwards transport via piston oil ring gap. *SAE Int.* **2011**, 2011-01-1402.

(49) Audette, W.; Wong, V. A model for estimating oil vaporization from the cylinder liner as a contributing mechanism to engine oil consumption. *SAE Tech. Pap. Ser.* **1999**, No.1999-01-1520.

(50) Froelund, K. Real-time steady-state measurement of PCV contribution to oil consumption on Ford 4.6 L SI-engine. *SAE Tech. Pap. Ser.* **2000**, 2000−01−2876.

(51) Froelund, K.; Menezes, L.; Johnson, H.; Rein, W. Real-time transient and steady-state measurement of oil consumption for several production SI-engines. *SAE Tech. Pap. Ser.* **2001**, 2001-01-1902.

(52) Okada, K.; Heintzenberg, J. Size distribution, state of mixture and morphology of urban aerosol particles at given electrical mobilities. *J. Aerosol Sci.* **2003**, *34*, 1539−1553.

(53) Barone, T.; Zhu, Y. The morphology of ultrafine particles on and near major freeways. *Atmos. Environ.* **2008**, *42*, 6749−6758.

Paper 4

Panu Karjalainen, Liisa Pirjola, Juha Heikkilä, Tero Lähde, Theodoros Tzamkiozis, Leonidas Ntziachristos, Jorma Keskinen and Topi Rönkkö. Exhaust particles of modern gasoline vehicles: A laboratory and an on-road study. *Atmospheric Environment*, 2014, 97, 262–270, doi: 10.1016/j.atmosenv.2014.08.025.

Exhaust particles of modern gasoline vehicles: a laboratory and an on-road study

Panu Karjalainen[1], Liisa Pirjola[2], Juha Heikkilä[1], Tero Lähde[2], Theodoros Tzamkiozis[3], Leonidas Ntziachristos[3], Jorma Keskinen[1] and Topi Rönkkö*[1]

[1]Aerosol Physics Laboratory, Department of Physics, Tampere University of Technology, Tampere, Finland
[2]Department of Technology, Metropolia University of Applied Sciences, Helsinki, Finland
[3]Laboratory of Applied Thermodynamics, Department of Mechanical Engineering, Aristotle University of Thessaloniki, Thessaloniki, Greece

Highlights

- Four types of exhaust particles were observed in the exhaust of GDI vehicles.
- Nonvolatile particle size distribution consisted of two modes.
- GDI vehicles emitted particles also during engine braking conditions.
- Semivolatile nucleation particles were in the exhaust at high load conditions.
- Particle emissions were in real-world qualitatively similar as in the laboratory.

Abstract

Vehicle technology development and upcoming particle emission limits have increased the need for detailed analyses of particle emissions of vehicles using gasoline direct injection (GDI) techniques. In this paper the particle emission characteristics of modern GDI passenger cars were studied in a laboratory and on the road, with the focus on exhaust particle number emissions, size distributions, volatility and morphology. Both during acceleration and steady conditions the number size distribution of nonvolatile exhaust particles consisted of two modes, one with mean particle size below 30 nm and the other with mean particle size approximately 70 nm. Results indicate that both of these particles modes consisted of soot but with different morphologies. Both in laboratory and on the road, significant emissions of exhaust particles were observed also during decelerations conducted by engine braking. These particles are most likely originating from lubricant oil ash components. The semivolatile nucleation particles were observed in the laboratory experiments at high engine load conditions. Thus, in general, the study indicates that a modern gasoline vehicle can emit four distinctive types of exhaust particles. The differences in particle characteristics and formation should be taken into account in the development of emission control strategies and technologies and, on the other hand, in the assessment of the impact of particle emissions on environment and human health.

Keywords: exhaust particles, gasoline direct injection, nucleation, soot, particle emissions

1. Introduction

In the development of gasoline passenger cars the increased attention on global warming and the greenhouse gas emissions has led to a widespread use of gasoline direct injection (GDI) engines (Alkidas 2007). In general, GDI technologies offer better fuel economy compared to port fuel technologies and thus lower emissions of CO_2. Also the use of alternative fuels is increasing, both in diesel and in gasoline vehicle fleets. New technologies most likely affect both the regulated emissions like NO_x, hydrocarbons and particulate mass, and unregulated emissions like the amount or characteristics of emitted nanoparticles. The changes in the emissions other than CO_2 can be either advantageous or harmful (see e.g. Heikkilä et al. (2009) and Lähde et al. (2011)). In the case of the GDI technology, the direct fuel injection can increase the risk for increased particulate emission due to incomplete fuel volatilization, partially fuel rich zones, and impingement of fuel to piston and cylinder surfaces (Maricq et al., 1999b; Bonandrini et al., 2012; Sementa et al., 2012).

Particle emissions of vehicles are restricted by emission standards which have significant variation depending on the country. In the US, since 2004 same standards have been applied to vehicles regardless of the fuel and thus the limits for the particulate mass emission have covered also the gasoline vehicles. In the European Union, a particulate mass emission limit for direct injection gasoline engines took effect in 2009 (Euro 5), and the first restrictions for particle number emissions will come into effect in 2014 (Euro 6). Thus, globally the particle emission limitations for gasoline vehicles are under strong development (Dieselnet, 2014). Especially the European particle number emission limit for GDI engines may enforce the vehicle industry to change their emission reduction technologies and methods.

The relative importance of particle emissions of gasoline vehicles has increased because of forthcoming particle emission regulations, and because port-fuel injection (PFI) has been widely replaced by GDI technologies. On the other hand, the significance of gasoline particle emissions is now higher because of low emission level of modern diesel passenger cars. The fraction of the GDI vehicle in vehicle fleet is forecasted to grow significantly during the next years (CARB, 2010). It is known that the GDI technologies offer lower fuel consumption and NO_x emission (Alkidas, 2007). However, the knowledge related to gasoline vehicle exhaust particles is not at the same level as the knowledge of diesel exhaust particles. The disadvantage of GDI technologies is an increase in particle number emission compared to PFI technology (Aakko and Nylund, 2003; Mohr et al., 2006; Braisher et al. 2010). If compared to diesel exhaust particle number concentrations, the GDI exhaust number concentrations are typically significantly lower than the concentration of diesel engine exhaust particles without a diesel particulate filter (DPF) but higher than concentrations with a DPF (Mathis et al., 2005). The study of Maricq et al. (2012), conducted for exhaust particles of a light-duty truck with a GDI engine, indicates that the particulate matter emission of a GDI engine is dominated by elemental carbon (EC) whereas organic carbon (OC) constitutes only a small fraction. Several studies (e.g. Maricq et al., 1999a; Harris and Maricq, 2000; Khalek et al., 2010) indicate that the GDI exhaust particles are (in number) mainly in particle sizes below 100 nm. In addition, the size distribution has been observed to be bi-modal (Barone et al., 2012; Sementa et al., 2012; Sgro et al., 2012; Maricq et al., 1999a). The mode of smaller particles (mean particle size between 10-20 nm) has previously been observed to consist of spherical amorphous carbon (Sgro et al., 2012; Barone et al., 2012) and to be partly charged indicating their formation at high temperatures (Sgro et al., 2012). Although the volatility characteristics of the smallest particles have not been inspected in all the previous studies,

some studies (e.g. Mathis et al., 2005; Li et al., 2013) indicate that the GDI exhaust can contain semivolatile nucleation particles too. In contrast to small amorphous carbon particles (Sgro et al., 2012), and in general, nonvolatile core particles formed during diesel combustion (e.g. Lähde et al., 2009), the entirely semivolatile nucleation mode is formed in the atmospheric dilution and cooling process of the diesel exhaust (Rönkkö et al., 2006; Lähde et al., 2009).

In this study the focus is on the physical characteristics and emissions of particles emitted by modern gasoline passenger cars. Results of particle number emission, size distribution, volatility and morphology are presented. Measurements were conducted not only on a chassis dynamometer in the laboratory but also on the road. On-road studies provide a real-world driving environment and make possible to gather information from real-world exhaust dilution and dispersion processes in the atmosphere. For instance, for diesel vehicles the exhaust nanoparticle concentrations have been reported to be affected by sampling and dilution parameters used in the laboratory study (e.g. Rönkkö et al., 2006). Thus, to get comprehensive and real information on exhaust particles also real-world studies are required. Also, real-world studies produce the most relevant information from the viewpoint of human exposure on particle emission. It should be noted that in the future also the vehicle emission legislation may shift towards the real-world measurements, e.g. due to the requirements for portable emission measurement systems.

2. Experimental

2.1. Experimental procedure on chassis dynamometer

The test vehicle was a modern gasoline passenger car made in 2011 (vehicle 1). The GDI engine of the test vehicle (1.8 l displacement) was turbocharged and used fuel stratified injection below about 3000 rpm. In the stratified mode, the global average air to fuel ratio is stoichiometric but due to stratified operation there are local rich and lean zones in the combustion chamber. The exhaust aftertreatment was performed with a three-way catalytic converter (TWC). The engine ran with low sulfur (< 10 mg/kg) 95-octane gasoline-ethanol blend fuel where ethanol concentration was below 10%. The lubricant oil was viscosity grade 5W-30 which contained phosphorus, sulfur, calcium and zinc, 900 mg/kg, 2780 mg/kg, 3200 mg/kg and 920 mg/kg, respectively.

Experimental routine consisted of test cycles and different engine load steady points controlled by the chassis roll resistance. Before the test series, the vehicle was warmed up during a New European Driving Cycle (NEDC). During this warm-up run the emissions were also measured. The NEDC test cycle was repeated in total eight times. Selected steady-state tests were driven at the wheel speed of 80 km/h in fifth gear and at wheel powers 5 kW, 10 kW and 20 kW, controlled by the chassis roll brake.

The exhaust gas sample was extracted from an exhaust transfer tube from a sampling point that located 2 m after the tailpipe end. Exhaust dilution was conducted using a partial exhaust flow dilution system (Ntziachristos et al., 2004) consisting of a porous tube diluter, a short ageing chamber and a secondary diluter. The dilution system has been observed to mimic relatively well the real-world cooling and dilution processes, especially from the viewpoint of exhaust nanoparticle formation (Rönkkö et al., 2006; Keskinen and Rönkkö, 2010). The primary dilution ratios of the

porous tube diluter and secondary diluter (Dekati Diluter) were approximately 12 and 4.5, respectively. Both the primary dilution ratio and the total dilution ratio (~50) were calculated based on the CO_2 concentrations of the raw exhaust and diluted exhaust. After the secondary dilution the diluted exhaust sample was at room temperature of about 25°C.

Particles were measured with an EEPS (Engine exhaust particle sizer, model 3090, TSI Inc.), an UCPC (Ultrafine condensation particle counter, TSI Inc. model 3025) and an ELPI (Electrical low pressure impactor, Dekati Oy). The ELPI was used with a filter stage (Marjamäki et al., 2002) and an additional impactor stage for nanoparticles (Yli-Ojanperä et al., 2010). In order to study particle morphology and elemental composition, the exhaust particles were collected from the diluted sample on holey-carbon grids (Agar Scientific) by a flow-through sampler where flow of 1 l/min was used. The collected particles were then analyzed by shape with a Transmission electron microscopy (TEM) and by elemental composition with an energy dispersive spectrometry (EDS). During half of the measurements (4 NEDCs), a thermodenuder (TD) with low nanoparticle losses was employed in order to estimate particle volatility characteristics with the UCPC and ELPI. In the TD, the continuous exhaust sample was first heated up to 265 °C, and after that, conducted through the denuder part in order to decrease the concentration of volatilized compounds. The data was corrected for the nanoparticle losses in the TD which vary between 32% and 50% for mobility sizes 10 and 4.5 nm, respectively (Heikkilä et al., 2009). More information of the instruments and experimental setup is reported in the supplementary material.

2.2. Experimental procedure on road

The gasoline engine (1.8 l displacement) of the test vehicle in on-road experiments (vehicle 2) was also turbocharged. However, the engine was newer generation with differences in the fuel injection system compared to the engine used in the laboratory tests. The engine adopts a combination of GDI and port fuel injection (PFI) technologies, in order to reduce the soot emissions. Under low load conditions only the PFI is used. In stratified GDI operation, the fuel is injected during both intake and compression strokes. Also this engine operated under global stoichiometric combustion conditions. Due major differences in the fuel injection compared to vehicle 1, smaller particle emissions were expected. The fuel and lubricant used were from exactly the same batches as in the laboratory experiments.

On-road tests consisted of controlled acceleration/deceleration routines (Table 1) and constant speed chasing tests. Experiments were performed in Alastaro (Finland) in a low-traffic road section far away from highly populated areas. Thus, the rural background particle concentrations were low, 2000-3000 1/cm^3. Before the test series, the vehicle was driven around 200 km at typical highway/freeway speeds of 80-120 km/h. The experiments were performed under sunny and dry conditions (temperature 23-24 $^{\circ}$C, wind speed 1-2 m/s, RH 40-60%).

The test vehicle was chased with the "Sniffer" mobile laboratory van (Supplementary Information; Pirjola et al., 2004; Rönkkö et al., 2006). The inlet probe located 0.5 m from ground level above the front bumper of the van. The chasing distance between the car and van was kept at around 12 m, although during accelerations and decelerations the constant distance was difficult to maintain exactly. The particle number concentrations and size distributions of the exhaust plume were measured with similar instruments as in the laboratory study: a UCPC, a UCPC after the TD, an ELPI and an EEPS.**3. Results**

3.1. Laboratory study of particle emissions

Time-resolved particle emissions were determined from measured exhaust particle concentrations by taking into account the simultaneous exhaust flow mass rate. Four NEDCs were measured without the TD and four NEDCs with the TD upstream of the ELPI and UCPC. The EEPS was always used without the TD. Averaged temporal particle emissions (particles per second, 1/s) with standard deviations are shown in Figure 1 for the whole NEDC. Results for the UCPC (a), the ELPI (b) and the EEPS (c) are shown separately. The emissions for particles larger than 23 nm in diameter (d) and the particulate mass emissions (e) are shown too, both calculated from the size distribution data measured using the EEPS. Mass emission was calculated for particles in the size range of 5.6-560 nm assuming particle density of 1 g/cm^3. Overall, instruments showed a very good repeatability between the NEDCs with an exception that the standard deviation was relatively high during the last 100 seconds of the NEDC. In general, particle emissions depended a lot on the driving condition; e.g. at the end of idle modes the concentration level was low, in the particle size range covered by the ELPI and the EEPS even near zero if the detection limits of the instruments are taken into account, while during accelerations the particle number emission increased to high values, at first accelerations even larger than 10^{12} 1/s. It should be noted that the particle emissions increased again also under deceleration conditions, especially when the speed decreased from 120 km/h to 0 km/h at the end of the test cycle but also at decelerations starting from lower speeds. These emissions can be seen in particle sizes larger than 23 nm (Figure 1d) as well as in smaller particles. The decelerations were conducted by engine braking, i.e. in conditions where the fuel was not injected into the cylinders.

In addition to time-resolved emissions, we determined the particle number emission factors (1/km) particulate mass (µg/km) for the Urban driving cycle (UDC) and Extra-urban driving cycle (EUDC) as well as for the whole NEDC. These can be seen in Table 2. In general, the total particle number emission factors were smaller during the UDC compared to the EUDC when the semivolatile particles were included in the numbers, i.e. the measurement was conducted without the TD. When looking at the nonvolatile particles (TD) the situation was reversed; the emissions were higher during the UDC than the EUDC. Thus, when the results are studied from the viewpoint of mileage, the measurement shows that the semivolatile particles are emitted mainly during the EUDC of the NEDC (higher speeds) whereas the UDC contributes more on the nonvolatile particle emissions. This can also be seen from Figure 1; the TD treatment did not affect significantly the particles during the first 1100 s of the NEDC. Instead, the particle emissions measured by the ELPI and the UCPC were decreased strongly by the TD treatment when the vehicle speed was over 100 km/h. The similar effect was seen also in the following deceleration and idle. At highest speeds the particle emissions measured by the UCPC without the TD treatment were higher than the concentrations measured by the ELPI and the EEPS which indicates that significant fraction of the emitted particles was 2.5-6 nm in diameter. Also, the emission of these small and semivolatile particles depended on the driving history; this was seen e.g. when the particle emissions over the EUDC were studied from an NEDC to another. During the first EUDC the particle emission measured by the UCPC without the TD was 3.0·10^{13} 1/km, in the following EUDCs 2.3·10^{13} 1/km, 5.0·10^{12} 1/km and 4.5·10^{12} 1/km. The emission of these small semivolatile particles was related to the situation of high exhaust gas temperature (above 700 °C in the catalyst). Because also the driving history affected the emissions, the formation of these particles seems to be caused by release of semivolatile compounds from the aftertreatment system, engine or exhaust line surfaces.

The emission of particles larger than 23 nm, obtained from the EEPS data, was higher during the UDC compared to the EUDC. The overall emission of these particles was about 2.5×10^{12} 1/km. In perspective of the European legislation, the upcoming Euro 6 level for GDI vehicle particle number will be at start 6×10^{12} 1/km and after three years 6×10^{11}. So the emission level of the tested vehicle is somewhere between these limits. However, one must keep in mind that the official measurement protocol differs from the measurement method here.Figure 2 shows the raw exhaust particle number size distributions (a) and size-segregated emissions (b). The particle size distributions were bi-modal during acceleration and steady speed conditions; the geometric mean diameter (GMD) of the smaller particle mode was ~10 nm while for the larger mode the GMD was ~70 nm, according to the EEPS data. During accelerations, i.e. when the engine was most heavily loaded, the concentrations of larger particles were typically higher than concentrations in the smaller particle mode. Instead, under deceleration conditions and following idle, the particles were generally smaller than 20 nm in diameter, and only one particle mode existed. The largest concentrations of sub-20 nm particles were observed during deceleration from 120 km/h to 0 km/h. Note here that the changes in the exhaust temperature and mass flow cause changes in the residence time of exhaust in the vehicles tailpipe system within a transient cycle (Rönkkö et al., 2014). Thus, the small particles measured under idle conditions were most likely emitted from the engine during deceleration. Also, it should be noted that the real contribution of particle emissions during deceleration was smaller than indicated based on the concentration results shown in the Figure 2a. For instance, during the last deceleration from 120 km/h to 0 km/h the concentrations of sub-20 nm particles were very high (Figure 2a), but when exhaust mass flow is taken into account and the results are looked at emission point of view (Figure 2b), their role diminishes. Similar trend is seen in decelerations from lower speeds also. In order to confirm the observations from transient driving, we measured the size distributions also at steady state driving conditions (speed 80 km/h, wheel powers 5 kW, 10 kW and 20 kW), with and without the TD. These can be seen in Figure 3. We can conclude that the TD treatment (at 265 °C) did not cause any significant change in the size or number of the exhaust particles in the particle size range measured by the ELPI. However, there was a very significant decrease in the concentration measured by the CPC during the 20 kW driving mode when the sample was passed through the TD (not plotted). In that case the majority of particles vanished in the TD treatment indicating that particles below 6 nm were semivolatile.

3.2. Particle morphology, laboratory study

The TEM images of collected particles are shown in Figure 4. Two clearly distinct particle types were observed for samples collected over the whole NEDC. Firstly, around 10-20% of collected particles were nearly spherical (Figure 4a-b,d), often containing internal structure of lighter and darker areas. The size of those particles varied from 10 nm to even larger than 200 nm. The EDS analyses indicated that these particles were composed of at least oxygen, zinc, phosphorous and calcium where the metals are compounds of engine oil but not of fuel. Thus in general, the results are in line with our previous study (Rönkkö et al., 2014), which indicated that under transient driving conditions or, more detailed, under engine braking conditions gasoline vehicles can emit particles consisting of the lubricant oil originating compounds. Related to that, Figure 2 shows that the particles are emitted during acceleration and steady speed conditions (during combustion) but also during engine braking when the fuel is not injected into the combustion chamber.

The second particle type was agglomerated soot consisting of elemental carbon but also oxygen, zinc, phosphorous and calcium. Several soot particles included spherical darker parts similar to individual "lube oil originated" particles mentioned above. It should be noted that also very small nearly spherical soot-like particles were observed (Figure 4b), possibly giving explanation for the bi-modal size distributions during acceleration and steady state driving. However, the accumulated particles can agglomerate also on the grid which prevents the direct comparison of number of collected particles with particle size distributions.

3.3. Particle emissions in the on-road study

The on-road study of particle emissions of the vehicle 2 was conducted at circumstances with very low particle concentrations in ambient air. Measurements were made in order to see the effects of on-road driving conditions and exhaust dilution on particle emissions but also to verify what are the particle concentrations and characteristics in the real exhaust plume. Because of the differences in technology between the vehicles 1 and 2, the exact and quantitative comparison to the laboratory results is not meaningful. On the qualitative manner, results largely confirmed many findings of the laboratory study.

The on-road study consisted of steady speed (low load) tests and transient acceleration/deceleration routines. During constant speeds, the total particle concentrations in the exhaust plume were at the background concentration level ($\sim$2000-3000 1/cm^3) indicating very low particle emissions. Instead, in the transient tests the particle emissions were significant both in accelerations and decelerations. This can be seen in Figure 5 where the exhaust plume CO_2 concentration, total particle number concentrations measured by a UCPC (TSI model 3776), nonvolatile particle number concentrations (downstream the TD) measured by a UCPC (another TSI model 3776), and vehicle speed for the second gear test between 30 km/h and 70 km/h are shown.

The highest particle concentrations were observed during accelerations where the total number concentrations of the exhaust plume reached the level of 40000-50000 1/cm^3, which is about 20-fold compared to the background aerosol. During accelerations, particle plume concentration followed well the trends of CO_2 concentrations. Instead, small but distinguishable exhaust plume concentration peaks (particle concentration between 3000-5000 1/cm^3) associated with the start of deceleration (engine braking) did not follow the concentration of CO_2. Because CO_2 can be used as a tracer for combustion originated particles, the result shows that those particles emitted during engine braking are not originated from combustion. To give a rough estimation for exhaust emission factors by estimating the dilution ratio from CO_2 concentrations of diluted sample and raw exhaust during 70 km/h constant speed and taking account the exhaust flow rates, the vehicle-out emission factors were during the deceleration and acceleration 3.1×10^{10} 1/s and 7.7×10^{11} 1/s, respectively. In any case, the on-road study showed that the emission of engine braking particles is a real-world phenomenon for gasoline vehicles affecting human exposure to particles and, in general, air quality. Comparison of exhaust plume particle concentrations at acceleration-deceleration routines are shown in Figure 6. All the repetitions of experiments (Table 1) were analyzed. The concentrations presented here are the average maximum concentrations reached during acceleration/deceleration, measured by the UCPC. The error bars indicate the standard deviation of maximum concentrations. It can be seen that the increased engine torque and lower engine speed increased the particle number concentration in the exhaust plume; when accelerated from 30 km/h to 70 km/h the

concentrations were larger in 3rd gear than in 2nd gear. Also, the particle emissions during engine braking were higher when the deceleration started at higher engine rpm compared to lower rpm situations. Finally, although the engine braking increases the total particle number emission of the studied vehicle, it should be noted that the total emission was dominated by particles emitted during acceleration conditions.

The UCPC measurement showed clearly that the particle concentrations increased during the decelerations but, however, the concentrations were too low and/or the size of emitted particles was too small for the size distribution measurements. Instead, during accelerations the size distribution measurement was possible. Results of maximum concentrations of accelerations from 30 to 90 km/h are shown in Figure 7. Like in the laboratory study, the particle number size distribution of real-world size distribution was dominated by ultrafine particles. The mean size of the emitted particles was approximately 20 nm for the ELPI. In addition, the bi-modality of particle size distributions was observed at certain acceleration but, however, not as clearly as in the laboratory experiments (Figures 2 and 3).

4. Summary and discussion

The study shows that the gasoline fuelled vehicle exhaust contains particles with very different concentration, size, morphology and chemical composition. Driving conditions were observed to have very significant effect on these particles, not only on the concentrations but also on the characteristics of the particles. The real-world study conducted on the road shows that the observations are relevant also from the viewpoint of the real emissions of GDI vehicles. It should be noted that, overall, the GDI technologies are diverse, even more diverse than PFI or diesel, with multiple degrees of freedom in choosing the operation parameters. Differences in technologies and operation parameter choices and as well as in drivers' behaviors can lead to different emission profiles than reported here which should be taken into account in the further use of the results.

In the laboratory part of the study, particle size distribution during the combustion of fuel (accelerations, steady state) consisted of two distinctive nonvolatile particle modes with the mean mobility diameters of ~10 nm and ~70 nm, respectively. In the on-road measurements this bi-modality was not as clear. In the laboratory, bi-modal size distributions were also measured under steady speed conditions for vehicle 1 while they were absent under steady speed conditions in the on-road experiments of vehicle 2. We suggest that these particles were soot similarly as diesel soot but with a difference that the soot was now divided into two distinctive modes. Also our results related to particle morphology, gathered from TEM analyses, support that. Note that the number-weighted particle concentrations of the modes were in this study at similar level which usually is not the case in diesel exhaust between the nucleation and soot mode particles. In diesel exhaust the nucleation mode tends to dominate the particle number concentrations when observed (e.g. Heikkilä et al 2009). Also, in diesel exhaust the differences between the mean diameters of particles in different nonvolatile modes have been reported to be larger (e.g. Lähde et al., 2011). Also Xe et al. (2012) and Barone et al., (2012) have observed that gasoline vehicle exhaust particle size distributions can be bi-modal. Barone et al. (2012) have reported that the smaller particles may consist solely of carbonaceous primary spheres whereas the larger particles are agglomerates.

Based on the NEDC tests, the particle emissions during deceleration conducted by engine braking are repeatable and systematic. In addition, results indicate that these particles consist of both

nonvolatile and semivolatile compounds (see Figure 1). The on-road part of this study shows that the emission of these particles is a real-world phenomenon. Also, the oil-originated compounds found from the TEM samples and the on-road observation that the emissions of these particles do not follow the CO_2 concentration of the exhaust, indicate that the particles are not originated from fuel combustion, but instead, from lubricant oil. The mechanisms how the lubricant oil compounds can end up to exhaust are discussed e.g. in Rönkkö et al. (2014). However, it should be kept in mind that other sources cannot be surely ruled out and the particle composition can be affected also e.g. by compounds releasing from engine or exhaust system (see e.g. Karjalainen et al. 2014). Compared to the particles emitted during acceleration, both the laboratory and on-road studies indicate that during deceleration the particles are smaller in diameter. These particles inevitably increase the particle number emissions during transient test cycles and in real-world driving but for the vehicles studied here, the total emissions were about an order of magnitude lower than the concentration of particles emitted during acceleration. The on-road study shows that for these emissions the particle emission factor calculation with respect to CO_2 fails because of simultaneous zero CO_2 emissions. This should be taken into account e.g. in the source appointment studies conducted in the vicinity of traffic. Also, the study indicates that the emissions of lubricant oil originated particles are strongly linked with certain driving conditions, possibly affecting their spatial existence in the urban environment.

During the high speed part of the NEDC and 20 kW steady loading, semivolatile particles were observed in the laboratory experiments. The number emission of these particles varied from an NEDC to another, indicating the strong role of driving history. Due to the volatility and small particle size, the chemical composition of these particles cannot be solved within this study. However, the results are relatively similar than previously reported for diesel exhaust where semivolatile particles, typically smaller than 20 nm, are found under high load conditions. In diesel exhaust, the formation of semivolatile nanoparticles is strongly linked to exhaust gaseous sulfuric acid concentration (Arnold et al., 2012; Rönkkö et al., 2013), or at least, to fuel sulfur content (Karjalainen et al., 2014). The effect of driving history seems to be linked with the storage and release of compounds in the tailpipe system; components such as gaseous sulphuric acid, SO_3 or heavy organics can be stored on engine, tailpipe or catalyst surfaces. These components may later get released when temperature is increased causing formation of new particles in the exhaust dilution and cooling process (Gieschaskiel et al., 2007; Karjalainen et al., 2014). It should be noted here, according to authors' knowledge, that similar particle formation has not been reported for gasoline vehicles before. In this study, the semivolatile particle mode was not observed during the on-road tests where the maximum vehicle speed was 90 km/h and the engine loading was relatively low. If higher engine loading and thus higher exhaust temperatures are achieved in on-road testing e.g. driving on a freeway or uphill, also semivolatile nucleation mode formation is expected.

The upcoming legislation limit for particle number will enforce modifications for technologies related to GDI engines. Based on this study a combination of PFI and GDI technologies can be advantageous when the solid particle number is considered. The legislation will focus on solid particles larger than 23 nm in diameter. This study indicates that a major share of solid particles in the modern gasoline vehicle exhaust can be below this particle size limit, and during high engine load, vehicles can emit also small semivolatile particles.

Corresponding Author*

Topi Rönkkö
Aerosol Physics Laboratory, Department of Physics, Tampere University of Technology
P.O.Box 692, FI-33101 Tampere, FINLAND
E-mail: topi.ronkko@tut.fi, Tel.: +358445861404, Fax: +358331153015

References

Aakko, P.; Nylund, N. Particle Emissions at Moderate and Cold Temperatures Using Different Fuels. *SAE Technical Paper* **2003**, 2003-01-3285.

Alkidas, A. Combustion advancements in gasoline engines. *Energy conversion and Management* **2007**, 48, 2751-2761.

Arnold, F.; Pirjola, L.; Rönkkö, T.; Reischl, U.; Schlager, H.; Lähde, T.; Heikkilä, J.; Keskinen, J. First Online Measurements of Sulfuric Acid Gas in Modern Heavy-Duty Diesel Engine Exhaust: Implications for Nanoparticle Formation. *Environmental Science and Technology* **2012**, 46, 11227-11234.

Barone, T.; Storey, J.; Youngquist, A.; Szybist, J. An analysis of direct-injection spark-ignition (DISI) soot morphology. *Atmospheric Environment* **2012**, 49, 268-274.

Bonandrini, G.; Di Gioia, R.; Papaleo, D.; Venturoli, L. Numerical Study on Multiple Injection Strategies in DISI Engines for Particulate Emission Control. *SAE Technical Paper* **2012**, 2012-01-0400.

Braisher, M.; Stone, R.; Price, P. Particle Number Emissions from a Range of European Vehicles. *SAE Technical Paper* **2010**, 2010-01-0786.

California Air Resources Board (CARB). Preliminary Discussion Paper – Proposed Amendments to California's Low-Emission Vehicle Regulations – Particulate Matter Mass, Ultra fi ne Solid Particle Number, and Black Carbon Emissions. Workshop Report **2010**.

Dieselnet, www.dieselnet.com, information retrieved 14.1.2014.

Giechaskiel, B.; Ntziachristos, L.; Samaras, Z.; Casati, R.; Scheer, V.; Vogt, R. Effect of Speed and Speed-Transition on the Formation of Nucleation Mode Particles from a Light Duty Diesel Vehicle, *SAE Technical Paper Series* **2007**, 2007-01-1110.

Harris, S.; Maricq, M. Signature size distributions for diesel and gasoline engine exhaust particulate matter. *Journal of Aerosol Science* **2001**, 32, 6, 749-764.

Heikkilä, J.; Rönkkö, T.; Lähde, T.; Lemmetty, M.; Arffman, A.; Virtanen, A.; Keskinen, J.; Pirjola, L.; Rothe, D. Effect of open channel filter on particle emissions of modern diesel engine. *Journal of the Air & Waste Management Association* **2009**, 59, 10, 1148.

Karjalainen, P.; Rönkkö, T.; Pirjola, L.; Heikkilä, J.; Happonen, M.; Arnold, F.; Rothe, D.; Bielaczyc, P. and Keskinen, J. Role of storage and release of sulphur compounds in diesel exhaust nucleation mode particle formation. *Environmental Science and Technology* **2014**, 48, 2336-2343.

Keskinen, J.; Rönkkö, T. Can Real-World Diesel Exhaust Particle Size Distribution be Reproduced in the Laboratory? A Critical Review. *Journal of the Air & Waste Management Association* **2010**, 60, 1245-1255.

Khalek, I.; Bougher, T.; Jetter, J. Particle emissions from a 2009 Gasoline Direct Injection Engine Using Different Commercially Available Fuels. *SAE International Journal of Fuels and Lubricants* **2010**, 3, 2, 2010-01-2117.

Li, T.; Chen, X.; Yan, Z. Comparison of fine particles emissions of light-duty gasoline vehicles from chassis dynamometer tests and on-road measurements. *Atmospheric Environment* **2013**, 68, 82-91.

Lähde, T.; Rönkkö, T.; Virtanen, A.; Schuck, T. J.; Pirjola, L.; Hämeri, K.; Kulmala, M.; Arnold, F.; Rothe, D.; Keskinen, J. Heavy Duty Diesel Engine Exhaust Aerosol Particle and Ion Measurements. *Environmental Science and Technology* **2009**, 43, 163-168.

Lähde, T.; Rönkkö, T.; Happonen M.; Söderström, C., Virtanen, A.; Solla, A.; Kytö, M.; Rothe, D and Keskinen, J. Effect of Fuel Injection Pressure on a Heavy-Duty Diesel Engine Nonvolatile Particle Emission. *Environmental Science & Technology* **2011**, 45, 2504-2509.

Maricq, M.; Podsiadlik, D.; Brehob, D.; Haghgooie, M. Particulate Emissions from a Direct-Injection Spark-Ignition (DISI) Engine. *SAE Technical Paper Series* **1999**, 1999-01-1530.

Maricq, M. M.; Podsiadlik, D. H.; Chase, R. E. Examination of the size-resolved and transient nature of motor vehicle particle emissions. *Environmental Science & Technology* **1999**, 33, 1618-1626.

Maricq, M.; Szente, J.; Jahr, K. The Impact of Ethanol Fuel Blends on PM Emissions from a Light-Duty GDI Vehicle. *Aerosol Science and Technology* **2012**, 46, 5, 576-583.

Marjamäki, M.; Ntziachristos, L.; Virtanen, A.; Ristimäki, J.; Keskinen, J.; Moisio, M.; Palonen, M.; Lappi, M. Electrical Filter Stage for the ELPI. *SAE Technical Paper Series* **2002**, 2002-01-0055.

Mathis, U., Mohr, M., Forss, A. Comprehensive particle characterization of modern gasoline and diesel passenger cars at low ambient temperatures. *Atmospheric Environment* **2005**, 39, 1, 107-117.

Mohr, M.; Forss, A; Lehmann, U. Particle Emissions from Diesel Passenger Cars Equipped with a Particle Trap in Comparison to Other Technologies. *Environmental Science and Technology* **2006**, 40, 2375-2383.

Ntziachristos, L.; Giechaskiel, B.; Pistikopoulos, P.; Samaras, Z.; Mathis, U.; Mohr, M.; Ristimäki, J.; Keskinen, J.; Mikkanen, P.; Casati, R.; Scheer, V.; Vogt, R. Performance Evaluation of a Novel

Sampling and Measurement System for Exhaust Particle Characterization. *SAE Technical Paper Series* **2004**, 2004-01-1439.

Pirjola, L.; Parviainen, H.; Hussein, T.; Valli, A.; Hämeri, K.; Aalto, P.; Virtanen, A.; Keskinen, J.; Pakkanen, T.A.; Mäkelä, T.; Hillamo, R.E. "Sniffer" — a novel tool for chasing vehicles and measuring traffic pollutants. *Atmospheric Environment* **2004**, 38, 3625-3635.

Rönkkö, T.; Virtanen, A.; Vaaraslahti, K.; Keskinen, J.; Pirjola, L.; Lappi, M. Effect of dilution conditions and driving parameters on nucleation mode particles in diesel exhaust: laboratory and on-road study. *Atmospheric Environment* **2006**, 40, 2893-2901.

Rönkkö, T.; Lähde, T.; Heikkilä, J.; Pirjola, L.; Bauschke, U.; Arnold, F.; Schlager, H.; Rothe, D.; Yli-Ojanperä, J.; Keskinen, J. Effects of Gaseous Sulphuric Acid on Diesel Exhaust Nanoparticle Formation and Characteristics. *Environmental Science and Technology* **2013**, 47, 11882-11889.

Rönkkö, T.; Pirjola, L.; Ntziachristos, L.; Heikkilä, J.; Karjalainen, P.; Hillamo, R.; Keskinen, J. Vehicle engines produce nanoparticles even when not fuelled. *Environmental Science & Technology* **2014**, 48, 2043-2050.

Sementa, P.; Vaglieco, B.; Catapano, F. Thermodynamic and optical characterizations of a high performance GDI engine operating in homogeneous and stratified charge mixture conditions fueled with gasoline and bio-ethanol. *Fuel* **2012**, 96, 204-219.

Sgro, L.; Sementa, P.; Vaglieco, B.; Rusciano, G.; D'Anna, A.; Minutolo, P. Investigating the origin of nuclei particles in GDI engine exhausts. *Combustion on Flame* **2012**, 159, 1687-1692.

Xe, H.; Ratcliff, M.; Zigler, B. Effects of Gasoline Direct Injection Engine Operating Parameters on Particle Number Emissions. *Energy & fuels* **2012**, 26, 2014-2027.

Yli-Ojanperä, J.; Kannosto, J.; Marjamäki, M.; Keskinen, J. Improving the nanoparticle resolution of the ELPI. *Aerosol and Air Quality Research* **2010**, 10, 4, 360-366.
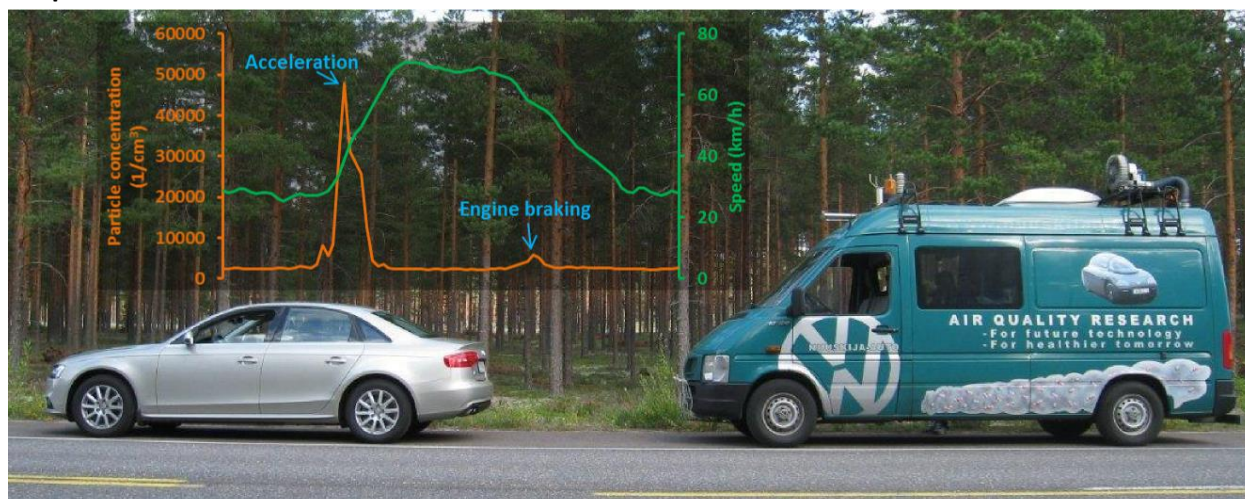
Graphical abstract

Table 1. Acceleration/deceleration test routines in the on-road experiments with the amount of repetitions.

Mode	Speed range	Gear	Repetitions
Acceleration	20-50 km/h	1st	12
Deceleration	50-20 km/h	1st	12
Acceleration	30-70 km/h	2nd	16
Deceleration	70-30 km/h	2nd	14
Acceleration	30-70 km/h	3rd	15
Deceleration	70-30 km/h	3rd	12
Acceleration	30-90 km/h	2nd	5
Deceleration	90-30 km/h	2nd	4

Table 2. Total particle number emission factors (1/km) for UDC, EUDC and NEDC, measured using the UCPC, ELPI and the EEPS. Emission factors for particle number > 23 nm in diameter (EEPS, > 23 nm) and for particulate mass (EEPS, mass) were calculated from the EEPS data. TD indicates the measurement with the thermodenuder.

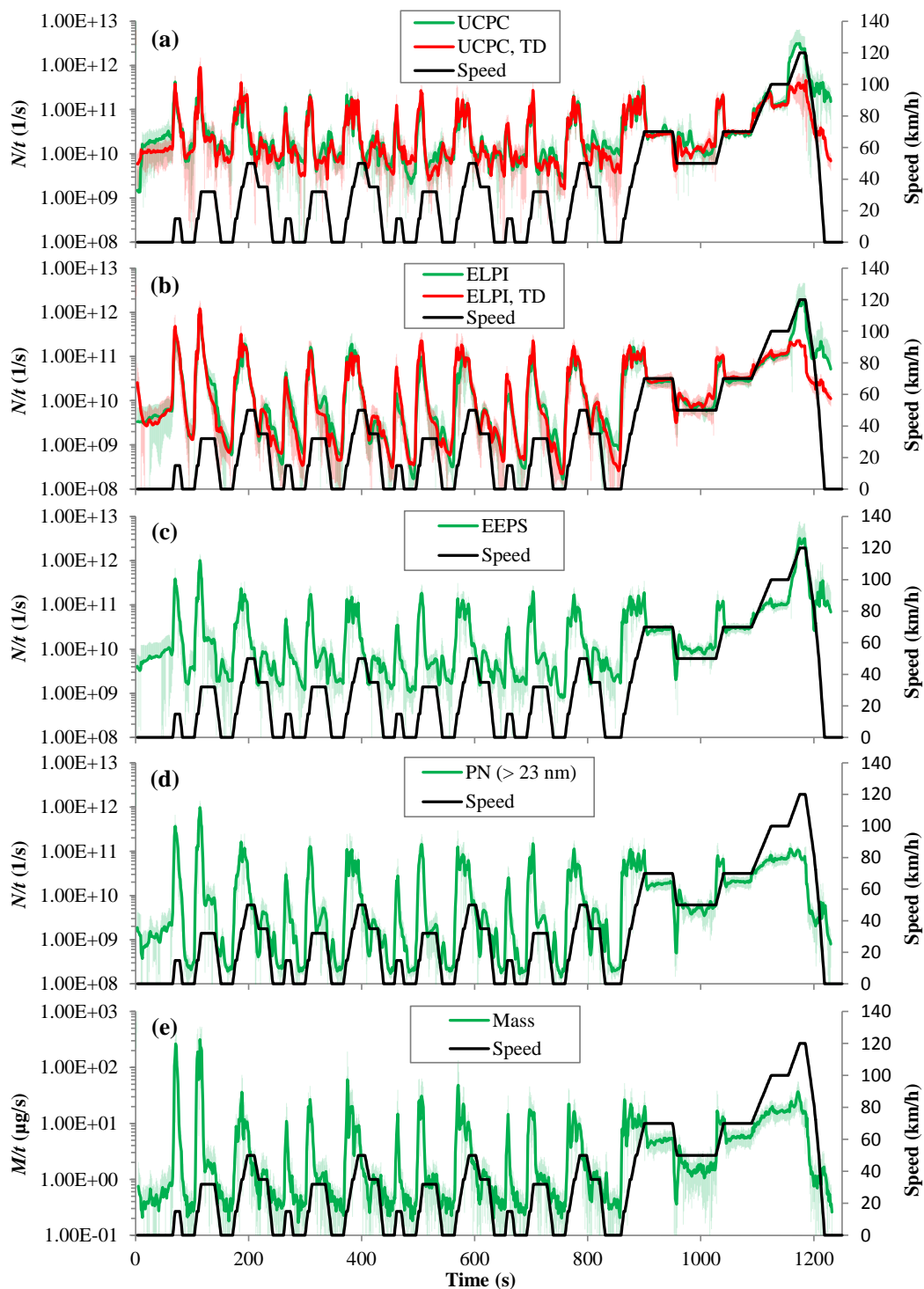| Instrument	UDC	EUDC	NEDC
UCPC (1/km)	6.87E+12	1.55E+13	1.23E+13
UCPC (1/km), TD	7.33E+12	4.58E+12	5.60E+12
ELPI (1/km)	5.64E+12	7.36E+12	6.73E+12
ELPI (1/km), TD	6.84E+12	3.23E+12	4.56E+12
EEPS (1/km)	5.54E+12	1.04E+13	8.58E+12
EEPS, > 23 nm (1/km)	3.92E+12	1.75E+12	2.55E+12
EEPS, mass (µg/km)	4.36E+02	1.29E+03	7.51E+02

Figure 1. Time series of particle emissions over the NEDC cycles for (**a**) particle number measured with the UCPC (w & w/o TD), (**b**) number with the ELPI (w & w/o TD), (**c**) number with the EEPS (only w/o TD), (**d**) number of particles over 23 nm calculated from the size distributions measured by the EEPS and (**e**) particulate mass, calculated also from the EEPS data. "Shadowed" area indicates the standard deviation.
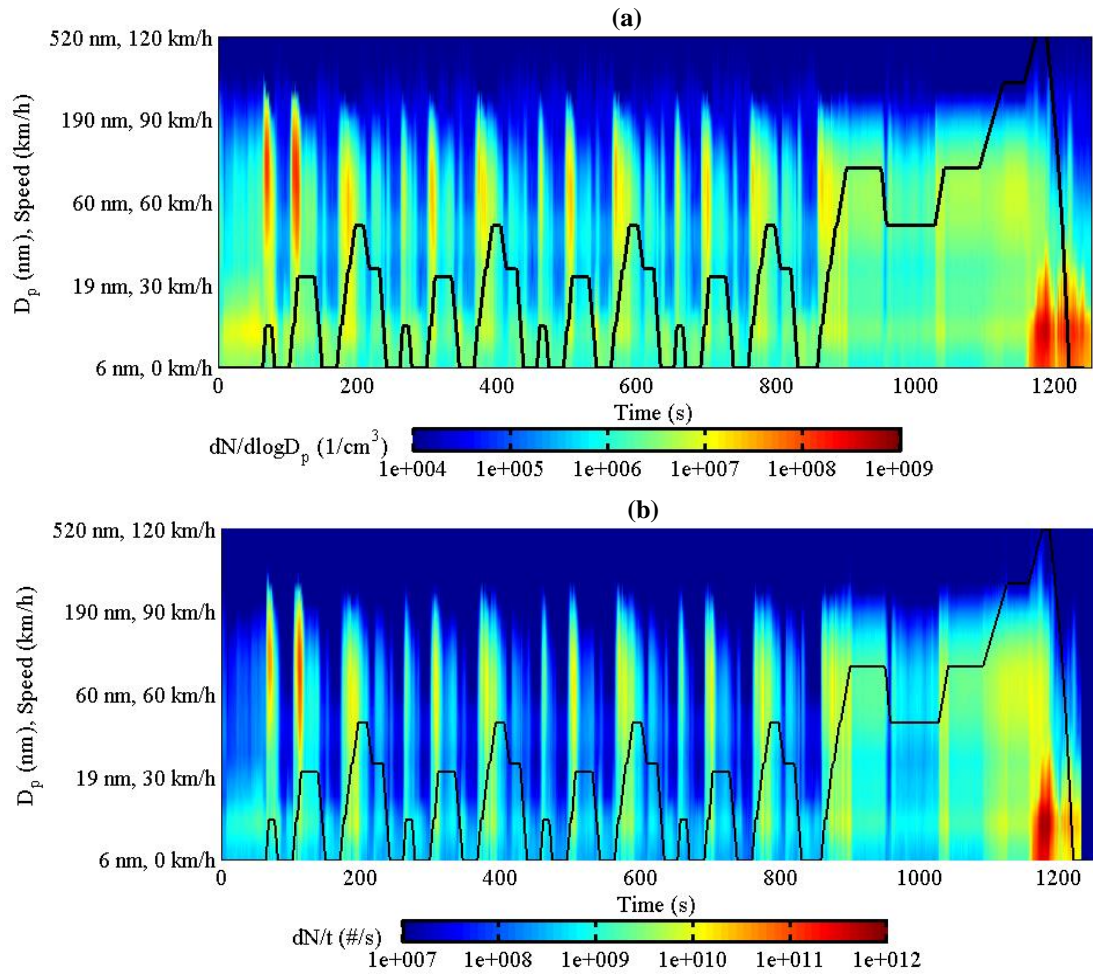
Figure 2. Mean particle size distributions measured by the EEPS during the NEDC (8 repetitions) cycle in terms of (a) dilution ratio corrected particle concentrations (dN/dlogD_p) and (b) particle emissions per second (dN/t). Black line shows the wheel speed profile.
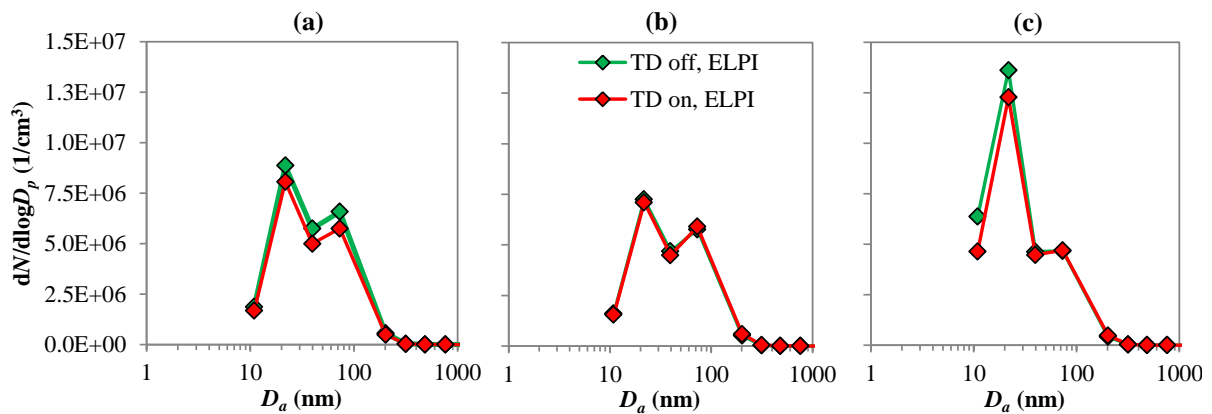
Figure 3. Effect of thermodenuder treatment (TD at 265 °C) on the exhaust particle size distributions measured by the ELPI at steady state driving modes: (**a**) 5 kW, (**b**) 10 kW and (**c**) 20 kW.
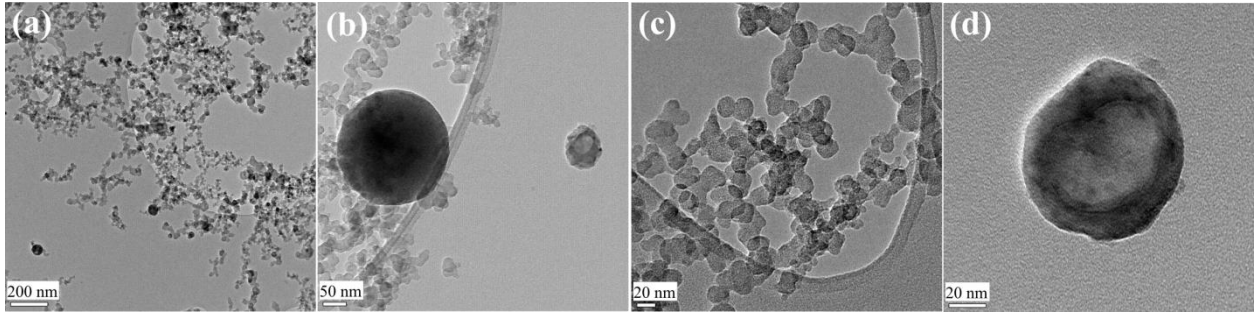
Figure 4. TEM images of collected exhaust particles during the NEDC cycle with various magnifications.
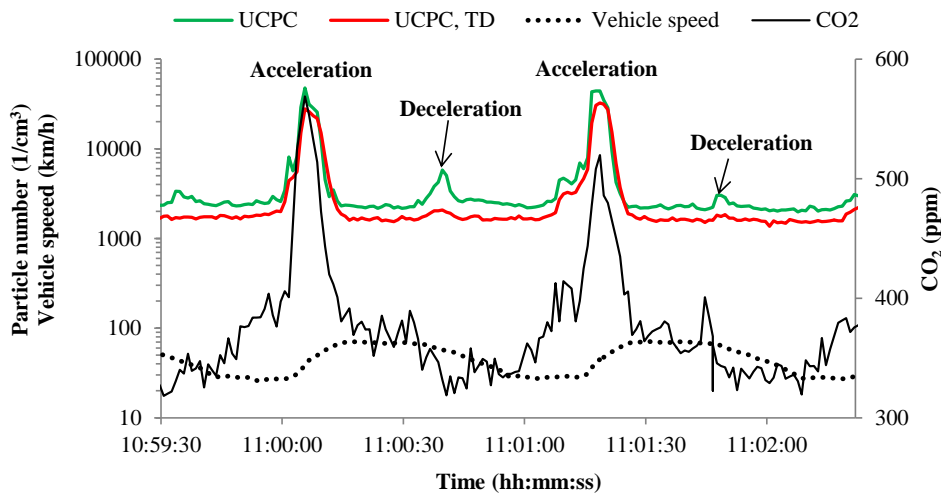

Figure 5. Total particle number (UCPC), nonvolatile particle number (UCPC, TD) and CO_2 concentrations in the exhaust plume of vehicle 2 during the acceleration and deceleration routine between 30 km/h and 70 km/h (2nd gear).
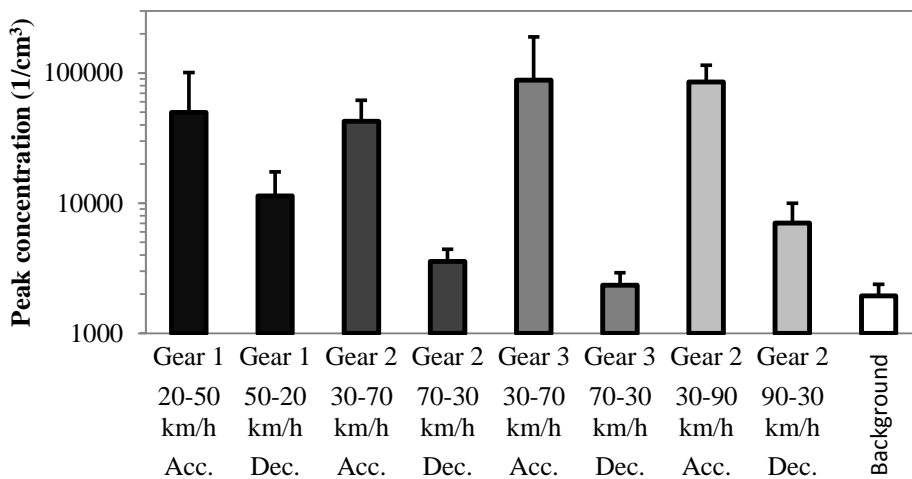

Figure 6. Exhaust plume total particle concentrations (UCPC measurement) during accelerations and decelerations in the on-road experiment. Error bars indicate the standard deviation (only mean+stdev) of mean concentrations between several consecutive tests. Also, the background aerosol concentration is shown.
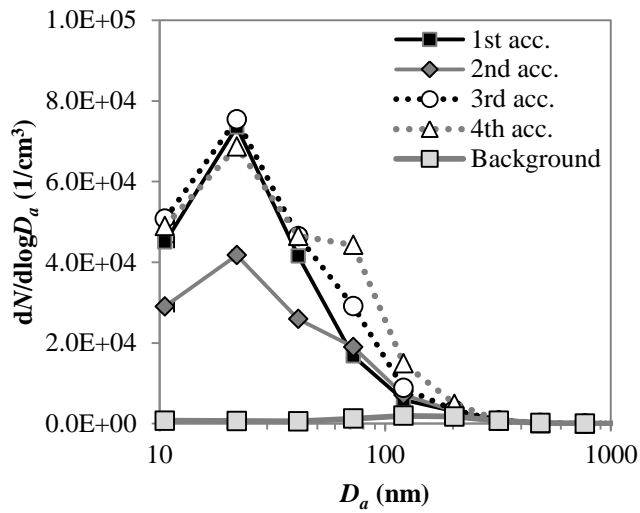
Figure 7. Particle number size distributions (ELPI measurement) during the repetitions of acceleration tests from 30 km/h to 90 km/h. Background particle size distribution was measured a few minutes after the test on the same test road.

Supplementary information

Exhaust particles of modern gasoline vehicles: a laboratory and an on-road study

Panu Karjalainen[1], Liisa Pirjola[2], Juha Heikkilä[1], Tero Lähde[2], Theodoros Tzamkiozis[3], Leonidas Ntziachristos[3], Jorma Keskinen[1] and Topi Rönkkö*[1]

[1]Aerosol Physics Laboratory, Department of Physics, Tampere University of Technology, Tampere, Finland
[2]Department of Technology, Metropolia University of Applied Sciences, Helsinki, Finland
[3]Laboratory of Applied Thermodynamics, Department of Mechanical Engineering, Aristotle University of Thessaloniki, Thessaloniki, Greece

Laboratory tests

In the engine laboratory test, the exhaust gas sample was extracted from an exhaust transfer tube from a sampling point that located 2 m after the tailpipe end. A schematic of the sampling setup is shown in Figure S1. Exhaust dilution was conducted using a partial exhaust flow dilution system (Ntziachristos et al., 2004) consisting of a porous tube diluter, a short ageing chamber and a secondary diluter. The dilution system has been observed to mimic relatively well the real-world cooling and dilution processes, especially from the viewpoint of exhaust nucleation particle formation (Rönkkö et al., 2006; Keskinen and Rönkkö, 2010). The primary dilution ratio of the porous tube diluter was set to 12, calculated from the CO_2 concentrations of the exhaust gas and the diluted exhaust gas. The secondary dilution was performed with an ejector diluter (Dekati Diluter) where the dilution ratio was about 4.5. However, the exact total dilution ratio (~50) was calculated based on the CO_2 concentrations of the raw exhaust and diluted exhaust.

Exhaust particles were measured with aerosol instruments suitable for transient and steady measurements of aerosol particle size distributions and number concentrations – an EEPS (Engine exhaust particle sizer, model 3090, TSI Inc.), an UCPC (Ultrafine condensation particle counter, TSI Inc. model 3025) and an ELPI (Electrical low pressure impactor, Dekati Oy) were used. The raw exhaust particle size concentrations (or formation potential for semivolatile particles) were determined by multiplying the measured concentrations with total dilution ratio. The particle emissions were determined by multiplying the raw exhaust concentrations with the exhaust flow rate.

The EEPS (Johnson et al., 2004) from TSI Inc. measures particles according to mobility diameter in the size range 5.6–560 nm. The measurement is performed by charging particles with a unipolar corona charger and classifying charger particles with an electric field. Current signal is then transformed by complex algorithms into a 32-bin particle size distribution. The instrument is capable of measuring the particles with frequency of 10 Hz, however in these tests 1 Hz data acquisition rate was sufficient. The sample flow is 10 l/min.

The UCPC from TSI Inc. (model 3025) is a condensation particle counter with a small cut size (~2.5 nm). Thu, the instrument basically measures particle concentration ($1/cm^3$) of particles larger than 2.5 nm. In the instrument, particles are grown by butanol vapor to a much larger particle size ~10 µm. After the condensation process individual particles are optically counted which enables the determination of particle concentration when the sample flow is known. The sample flow used in the experiment was 1.5 l/min.

The ELPI (from Dekati Oy) used was a modified version of the commercial Classic ELPI with a filter stage (Marjamäki et al., 2002) and an additional impactor stage for nanoparticles (Yli-Ojanperä et al., 2010). The

measurement is carried out by unipolar charging of the particles, and later on, collecting the charged particle into different stages of a cascade impactor. Thus the size classification is based on the aerodynamic diameter of the particles. The particle size distribution is obtained by knowing the sample flow, particle charge and penetration efficiency as well as the measured current in each stage. The sample flow of the ELPI is 10 l/min.

In order to study particle morphology and elemental composition, the exhaust particles were collected from the diluted sample on holey-carbon grids (Agar Scientific) by a flow-through sampler where flow of 1 l/min was used. In the sampler, the flow is forced through porous holey-carbon grids so that particles are collected by diffusion, inertial impaction or interception on the substrate. The grids containing collected particles were then analyzed by shape with a transmission electron microscopy (TEM, Jeol JEM-2010) and by elemental composition with an energy dispersive X-ray spectrometry (EDS Noran Vantage with Si(Li) detector, Thermo Scientific). Mostly qualitative analysis was performed to the TEM and EDS results.

During half of the measurements (4 NEDCs), a thermodenuder (TD) with low nanoparticle losses (Rönkkö et al., 2011) was employed in order to estimate particle volatility characteristics with the UCPC and ELPI. In the TD, the continuous exhaust sample was first heated up temperature of 265 °C, and after that, conducted through the denuder part in order to decrease the concentration of volatilized compounds. The nonvolatile particle loss correction was performed according to the curve presented by Heikkilä et al., 2009.
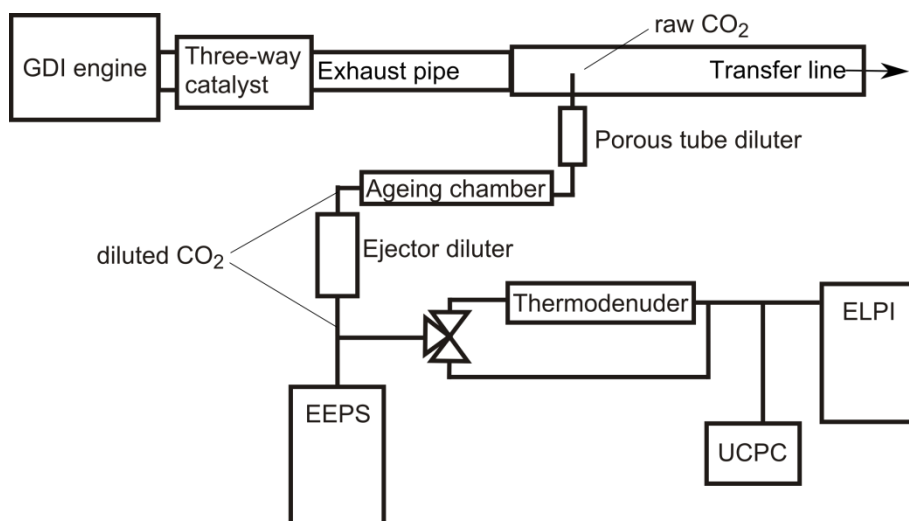

Figure S1. Sampling setup in the laboratory tests

On-road tests

The test vehicle was chased with the "Sniffer" mobile laboratory van (Pirjola et al., 2004; Rönkkö et al., 2006) (Figure S2). The inlet probe located 0.5 m from ground level above the front bumper of the van. The chasing distance between the car and van was kept at around 12 m, although during accelerations and decelerations the constant distance was difficult to maintain exactly. The particle number concentrations and size distributions of the exhaust plume were measured with similar instruments as in the laboratory study: two UCPCs (both model 3776), the ELPI and the EEPS.

On-road tests were performed in Alastaro (Finland) in a low-traffic road section (Figure S3) far away from highly populated areas. Test conditions were ideal; the rural background particle concentrations were low (2000–3000 $1/cm^3$), and the weather was sunny (temperature 23–24 ^{o}C and wind speed 1–2 m/s).
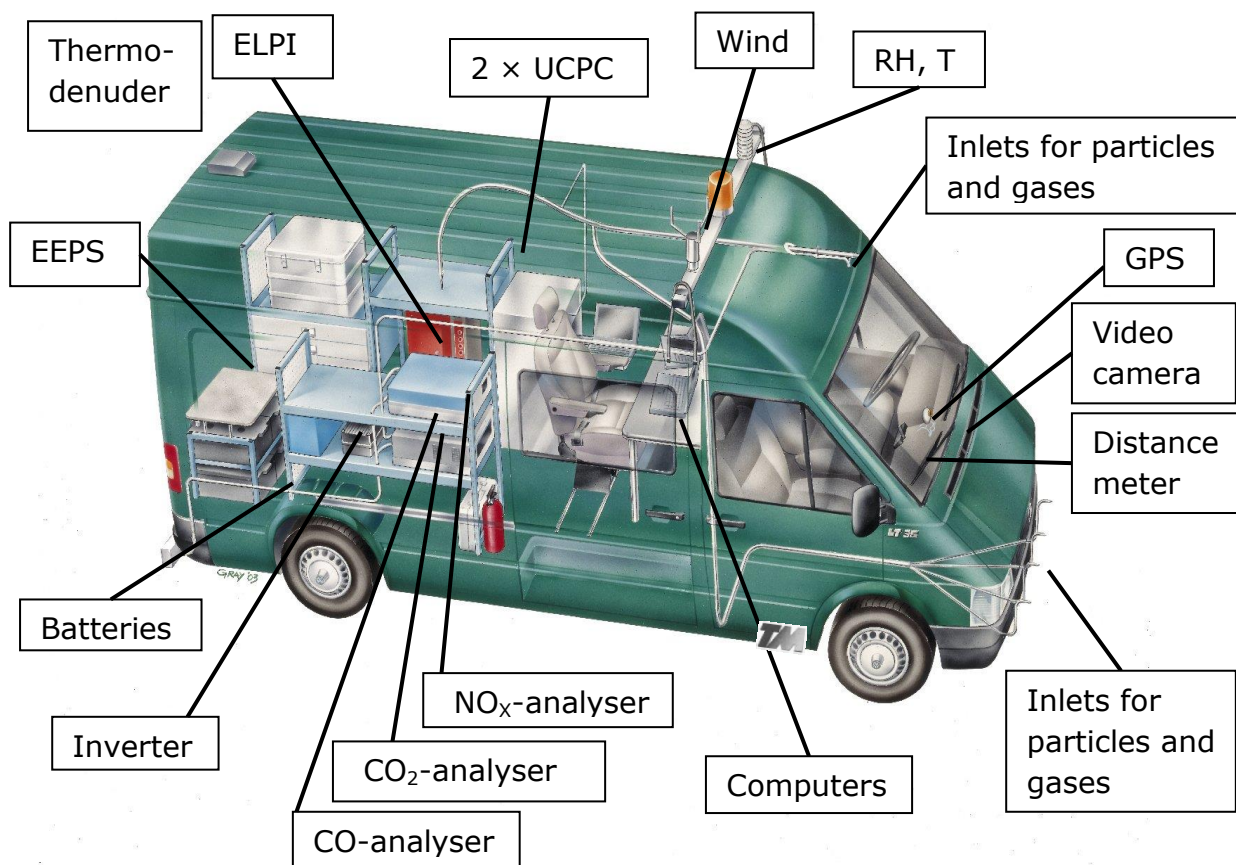
Thermo-denuder

ELPI

2 × UCPC

Wind

RH, T

Inlets for particles and gases

EEPS

GPS

Video camera

Distance meter

Batteries

Inverter

NO_X-analyser

CO_2-analyser

CO-analyser

Computers

Inlets for particles and gases

Figure S2. Sampling setup in the on-road tests
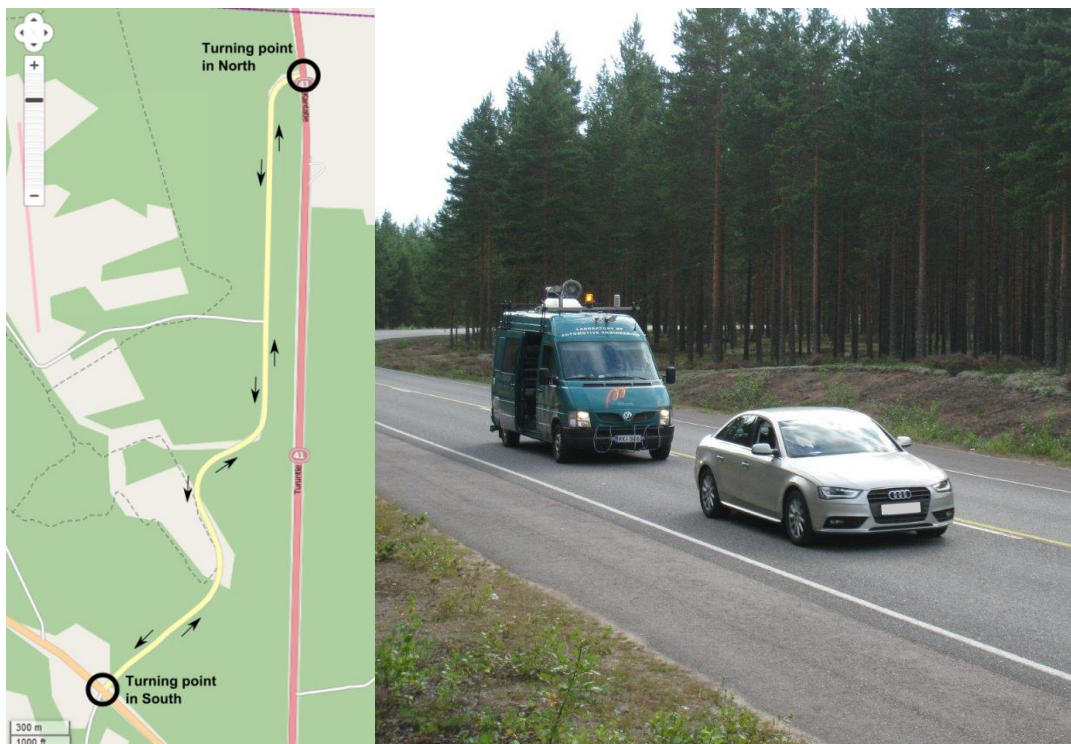
Figure S3. Map of the route in the chasing study (left) ($^{©}$OpenStreetMap contributors, CC BY-SA, see http://www.openstreetmap.org/) and a photo of the chase (right). The experiments were executed back and forth on the test road (yellow color in figure) between the turning points in North and South.

References

Heikkilä, J.; Rönkkö, T.; Lähde, T.; Lemmetty, M.; Arffman, A.; Virtanen, A.; Keskinen, J.; Pirjola, L.; Rothe, D. Effect of open channel filter on particle emissions of modern diesel engine. *Journal of the Air & Waste Management Association* **2009**, 59 (10), 1148.

Johnson, T.; Caldow, R.; Pöcher, A.; Mirme, A.; Kittelson, D. A New Electrical Mobility Particle Sizer Spectrometer for Engine Exhaust Particle Measurements. *SAE Technical Paper* **2004**, 2004–01–1341.

Keskinen, J.; Rönkkö, T. Can Real-World Diesel Exhaust Particle Size Distribution be Reproduced in the Laboratory? A Critical Review. *Journal of the Air & Waste Management Association* **2010**, 60, 1245–1255.

Marjamäki, M.; Ntziachristos, L.; Virtanen, A.; Ristimäki, J.; Keskinen, J.; Moisio, M.; Palonen, M.; Lappi, M. Electrical Filter Stage for the ELPI. *SAE Technical Paper Series* **2002**, 2002–01–0055.

Ntziachristos, L.; Giechaskiel, B.; Pistikopoulos, P.; Samaras, Z.; Mathis, U.; Mohr, M.; Ristimäki, J.; Keskinen, J.; Mikkanen, P.; Casati, R.; Scheer, V.; Vogt, R. Performance Evaluation of a Novel Sampling and Measurement System for Exhaust Particle Characterization. *SAE Technical Paper Series* **2004**, 2004–01–1439.

Pirjola, L.; Parviainen, H.; Hussein, T.; Valli, A.; Hämeri, K.; Aalto, P.; Virtanen, A.; Keskinen, J.; Pakkanen, T.A.; Mäkelä, T.; Hillamo, R.E. "Sniffer" — a novel tool for chasing vehicles and measuring traffic pollutants. *Atmospheric Environment* **2004**, 38, 3625–3635.

Rönkkö, T.; Virtanen, A.; Vaaraslahti, K.; Keskinen, J.; Pirjola, L.; Lappi, M. Effect of dilution conditions and driving parameters on nucleation mode particles in diesel exhaust: laboratory and on-road study. *Atmospheric Environment* **2006**, 40, 2893–2901.

Rönkkö, T.; Arffman, A.; Lähde, T.; Karjalainen, P.; Heikkilä, J.; Pirjola, L.; Rothe, D.; Keskinen, J. Diesel exhaust nanoparticle volatility studies by a new thermodenuder with low solid nanoparticle losses, *15th ETH Conference on Combustion Generated Nanoparticles* **2011**.

Yli-Ojanperä, J.; Kannosto, J.; Marjamäki, M.; Keskinen, J. Improving the nanoparticle resolution of the ELPI. *Aerosol and Air Quality Research* **2010**, 10, 4, 360–366.